

## Authors' response to Hess-2018-395-RC2

(Hess-2018-395, by Bing-Qi Zhu et al., words in blue color)

*Author's response: The author's response should be structured in a clear and easy-to-follow sequence: (1) comments from referees/public, (2) author's response, and (3) author's changes in manuscript. Regarding author's changes, a marked-up manuscript version (track changes in Word, latexdiff in LaTeX) converted into a \*.pdf including the author's response must be submitted.*

(2) Hess-2018-395-RC2

Interactive comment on "Direct or indirect recharge on groundwater in the middle-latitude desert of Otindag, China?" by Bing-Qi Zhu et al.

Anonymous Referee #2.

Received and published: 21 November 2018.

The work consists in a hydrogeochemical and isotopical study to determine the origin of the groundwater in a sandy desert region of China, bordered by a flat steppe terrain and mountainous regions. The authors propose an accurate analysis of the isotopes and ion chemistries of different water samples including natural samples collected from precipitation, depression spring, shallow and deep aquifers, perpetual lakes and outflowing rivers. They conclude that the groundwater in this desert is possible to originate from remote mountain areas and that the linkage between the desert area and the mountain region is crucial. They use multiple environmental tracers, taking into account the topography, the geomorphology, the climate, the vegetation and the soil, the geology and the hydrology of the Otindag Desert and its surrounding areas. However, in my opinion, the methodology they use for the hydrogeochemical investigation/interpretation, the key of the study, is not innovative or firstly applied in this kind of problem. Moreover, the outcomes derived (basically) merely by isotopical investigation are not supported by any hydrogeological model. A proper model could take into account and quantify in an integrated scenario the complexity of interacting physical phenomena such as the flow and transport processes, the spreading the mixing and the diffusion of the investigated tracers and the variable (in time and space) recharge in such heterogenous domain. Therefore, I do not think this work is now prompt for publication in HESS.

Authors' response and author's changes in manuscript:

We thank the reviewer #2 very much for his/her help in reviewing and commenting on our manuscript. According to the basis of the above opinions, we have revised the original manuscript. First of all, we think that we need to explain to the reviewer 2 here about the question on the research method of this paper: (1) Up to now, no any earth scientist has done any research works on groundwater recharge and its sources in the Otindag Desert before, and our research work is the first and pioneering one; (2) because no any study work has been done for groundwater research in this extensive area before, therefore, our study have no any background information and data of predecessors (especially hydrogeological data) to refer to, so we use the traditional methods to carry out preliminary research; However, both the collection of samples, the acquisition of analytical data and the research results based on these works are the first achievements in this blank area, which are very valuable and also pioneering. Secondly, for the question about the hydrogeological model proposed by the reviewer 2, we have made key modifications to the discussion part of the paper, and systematically supplemented the relevant content in the revised manuscript. We show them here as the following:

4. 6. Speciation modeling and hydrogeological conceptual model

Speciation modeling. Selected results of speciation modeling are provided in Table 6. All samples are undersaturated with respect to calcite, aragonite, dolomite, halite and gypsum. The values of log PCO<sub>2</sub>, ranging between -4.77 and -1.45 in the samples from the sedimentary sandy aquifer, indicating that groundwater in the study area is not at equilibrium with atmospheric PCO<sub>2</sub>.

Based on the above analyses, a conceptual model of groundwater recharge was suggested to facilitate understanding of the hydrogeological conditions in the study area. Local and regional

modern precipitation is a negligible source. Quaternary unconsolidated sediments with large exposed area form the main aquifer in the study area. Groundwater is recharged by cold water from remote mountain areas, and it flows from east to west along the Solonker Suture Zone. Evaporation is a minor process during groundwater hydrogeochemical evolution. Mineral dissolution may contribute to groundwater salinization, because saturation indices of all minerals are less than zero, indicating that these minerals still can dissolve into groundwater. These clues mean that the origin of groundwater in the desert is mainly controlled by geological structures and processes. The tectonic settings are more important than climatic and topographical settings to explain the origin of groundwater in the desert.

In a view of orogenic belt of the global middle-latitude regions, various groundwater and hydrogeological case studies have established a link between geological perspectives and origin of groundwater flows. Tague and Grant (2004) identify, for instance, the dominant control of a young volcanic geological unit on the groundwater regime of the studied region in Oregon, this geological formation having an exceptionally high permeability. Pfister et al. (2017) show that bedrock permeability significantly influences the ratio between average summer and winter run-off of 16 investigated catchments in Luxembourg. For a selection of Swiss catchments, Naef et al. (2015) associate lower groundwater flow with slowly draining porous bedrock and low streamflow during dry periods for catchments dominated by Moraine deposits. Kaser and Hunkeler (2016) have shown that alluvial aquifers, even if they represent only a small portion of the catchment surface, can contribute significantly to the catchment groundwater outflow especially during low-flow periods. Alluvial aquifers can thus also be relevant for total catchment groundwater storage. Chen and Wang (2009) proposed that earthquake is a possible mechanism for groundwater releasing in the Qilian Mountains and discharging it in the Hexi Corridor. Carlier et al. (2018) statistically analyzed 22 catchments of the Swiss Plateau and Prealpes to establish relationships between streamflow indicators and various geological and hydrogeological properties of the bedrock and Quaternary deposits, along with meteorological, soil, land use, and topographical characteristics. The study shows that the geological characteristics dominate catchment response during high and low groundwater flow conditions.

These studies focused the influence of base/surrounding rock, topography, recharge source and permeability on groundwater flow in orogeny area. According to the hydrologically active bedrock hypothesis (Uchida et al. 2008) the bedrock is an active reservoir that significantly contributes to baseflow (Tague and Grant 2004; Andermann et al. 2012; Welch and Allen 2012; Birkel et al. 2014). The hydraulic conductivity of the bedrock controls storage processes (Hale et al. 2016; Pfister et al. 2017). Most importantly, the ratio of the hydraulic conductivity to recharge rates has been shown to be relevant for water table elevation (Gleeson and Manning 2008). Haitjema and Mitchell-Bruker (2005) propose a criterion based on the Dupuit-Forchheimer approximation combining this ratio with geometrical aquifer properties and topographical characteristics to determine whether the water table is controlled by the topography or the recharge. From the above review it can be seen that various studies have used spatially distributed, synthetic groundwater models to identify and explore how topography, recharge and/or bedrock permeability influence groundwater fluxes and flow patterns (e.g., Gleeson and Manning 2008; Welch et al. 2012; Welch and Allen 2012; Welch and Allen 2014).

These studies highlight the complex interplay of topography and hydrogeology on groundwater flow. They, however, mainly focus on the geology of the bedrock, no studies mentioned the important role of tectonic structure on the groundwater flow. Thus, based on this study in the Otindag Desert, we proposed a simple conceptual model of multiprocesses that constrain the mechanism of groundwater recharge in the desert, namely mountain water (M) – tectonic fault hydrology (T) – unconfined vadose zone with underlying buried fault (V) – groundwater formation and recharge (G), i.e. the MTVG mechanism. Although the model is still conceptual but not practical at present, it provides a new perspective into the origin and evolution of groundwater resources in the middle-latitude deserts of the arid Asia.

Thank the reviewers and the editor of HESS again for your help in dealing with our manuscript. We look forward to hearing from you at your earliest convenience.

Best regards,  
B.Q. Zhu  
25 Jan 2019

**Comments from previous Referee #1**  
(hess-2018-71)

Interactive comment on “Direct or indirect recharge on groundwater in the middle-latitude desert of Otindag, China?” by Bing-Qi Zhu and Xiao-Zong Ren, Anonymous Referee #1, Received and published: 22 May 2018.

The manuscript describes interesting results about the recharge mechanisms of arid zones in China, especially considering the importance of the topic. Despite the multidisciplinary approach, which is very useful in groundwater recharge studies, there are many weak points which have to be improved for a publication in HESS. The main points are listed below: 1) The datasets belong to sampling campaigns carried out in different moments (years) and seasons and for this reason in my opinion cannot be discussed together, without a clear distinction between the different phases. 2) A reconstruction of the piezometric morphology as well as a stratigraphy of the considered study areas should be reported. This could help also the discussion of the groundwater preferential pathways. 3) The organization of the paper is still at a draft level, since there is not a clear distinction between the results and discussion paragraphs. Many paragraphs need to be summarized and better explained. 4) The number of figures should be reduced (probably putting together some and deleting others). 5) The English is very poor and there are many typo errors. The reported delta notation is wrong. Due to the consideration of these main points the manuscript can be accepted only if major revision will be reported.

Interactive comment on Hydrol. Earth Syst. Sci. Discuss., <https://doi.org/10.5194/hess-2018-71>, 2018.

**The authors' responses to the comments from Referee #1**

Dear Dr/Professor Referee #1:

On behalf of my co-authors, we thank you very much for giving us an opportunity to revise our manuscript. We appreciate you very much for your positive and constructive comments and suggestions on our manuscript (hess-2018-71). We have studied your comments carefully and have made revision which marked in red in the revised manuscript. We tried our best to revise our manuscript according to the comments point by point. Attached please find the revised version, which we would like to submit for your kind consideration. Thank you and best regards.

1) The datasets belong to sampling campaigns carried out in different moments (years) and seasons and for this reason in my opinion cannot be discussed together, without a clear distinction between the different phases.

Our response: AGREE AND NO CHANGES MADE.

Firstly, we thank you very much for this comment from you and we truly agree this point that water samples collected in different moments (years) and seasons cannot be discussed together without a clear distinction between the different water phases. In fact, although we stated in the manuscript that our fieldwork had taken place during the summer season of 2011 and the spring season of 2012, we collected the natural water samples at the same time for the same phases in the study area. For example, (1) all the groundwater samples discussed in this paper were collected during the 2011 summer in five days in the Otindag Desert. For other natural water samples discussed in this study, the detailed sampling methods are as follow: (2) all the spring water samples and (3) the precipitation water sample (p1) discussed in this paper were also collected during the 2011 summer in five days in the study area, and (4) all the river water samples and (5) lake water samples were collected during the spring season of 2012 in three days in the study area. This is to say that the water samples within the same phase are discussed together in the paper.

2) A reconstruction of the piezometric morphology as well as a stratigraphy of the considered study areas should be reported. This could help also the discussion of the groundwater preferential pathways.

Our response: AGREE AND CHANGES MADE.

We thank you very much for this comment. And yes, according to this comment, we revised the manuscript and focused on reporting the geological (tectonic, lithological, sedimentological and structural), geomorphological, hydrogeological and stratigraphical settings of the study area. Please see the section 2 “Regional setting” of the revised manuscript in its pages 3-5 lines 103-189.

3) The organization of the paper is still at a draft level, since there is not a clear distinction between the results and discussion paragraphs. Many paragraphs need to be summarized and better explained.

Our response: AGREE AND CHANGES MADE.

We thank you very much for this comment. And yes, we have revised the manuscript accordingly. The structure and content of the paper has been thoroughly reorganized in the revised manuscript, especially for the results and discussion sections, to make the content and context of the paper being more logic, coherent and readable. And yes, almost all of the paragraphs in the paper are newly summarized and explained. The detailed changes can be easily observed in the revised manuscript by reading one of the two resubmitted MS-Word files with the “changes marked” version (in contrast, another version is “clear copy”).

4) The number of figures should be reduced (probably putting together some and deleting others).

Our response: AGREE AND CHANGES MADE.

We thank you very much for this comment. And yes, we have revised the manuscript accordingly. We reduced the number of figures in the revised manuscript by putting some figures together and deleting several figures. At last the revised manuscript has 11 figures compared with the original manuscript that including 15 figures. For example, the Figs. 5, 11, 13, 14a in the original manuscript are deleted in the revised manuscript, and the Figs. 7 and 8, the Figs. 10, 12 and 14a are combined, respectively. In addition, two newly-built figures are added into the revised manuscript according to the second comment from you (the detailed content of this comment can be seen above). The specific changes and the final results of these figures can be seen in the newly submitted revised manuscript.

5) The English is very poor and there are many typo errors. The reported delta notation is wrong.

Our response: AGREE AND CHANGES MADE.

We thank you very much for this comment. We are very sorry for our poor and incorrect English writing in the original manuscript. For the shortcomings of the English presentation and the grammatical edit in the first paper, we have checked and revised the whole manuscript carefully to avoid language errors, and finally we have got the help of a native English speaking professional to check and improve the English quality of the revised manuscript. We believe that the language is now acceptable for the publishing purpose.

In addition, the wrong use of the delta notation in the original manuscript, such as  $\delta^2\text{H}$ , has been corrected as “ $\delta\text{D}$ ” in the revised manuscript.

6) Due to the consideration of these main points the manuscript can be accepted only if major revision will be reported.

Our response: AGREE AND CHANGES MADE.

Special thanks to you for your good comments. We have tried our best to improve the manuscript and made specific changes in the revised manuscript according to the comments from you one by one. These changes will not influence the content and framework of the paper. And here we did not list the changes but marked in red in the revised paper. We hope that the correction will meet with approval. Once again, thank you very much for your comments and suggestions.

**Comments from previous Referee #2**  
(hess-2018-71)

Interactive comment on “Direct or indirect recharge on groundwater in the middle-latitude desert of Otindag, China?” by Bing-Qi Zhu and Xiao-Zong Ren, Anonymous Referee #2, Received and published: 6 June 2018.

Groundwater availability in arid and semi-arid regions is one of the key issues in hydrogeology and is becoming even more important because of the expected climate changes. Within this context, the contribution by Zhu and Ren provides an interesting analysis on the possible recharge supporting the availability of significant groundwater resources in the Otindag desert, north-eastern China. The analyses have been carried out using hydrogeochemical tracers and isotopic measurements on water samples collected from groundwater, surficial (river, lake, and spring) waters, and precipitation water, as well as in-situ records of temperature, pH, conductivity, and TDS concentration. The various steps implemented by the authors to reject possible hypotheses on the groundwater origin (e.g., water flowing from another nearby arid area, precipitation, paleo-water resources) are presented in detail and discussed. Zhu and Ren concludes that, based on the available evidences, the groundwater resources in this region are recharged by the leakage through the bed on incise rivers bounding the desert to the east and conveying downward the waters originated from the precipitation on Daxinganling Ranges. Hence, an “indirect” recharge is the main mechanism supporting the water availability in the study arid lands.

Two are the main weaknesses of this ms: 1) the chemical/isotopic investigations seem not supported by a (at least minimum) knowledge of the hydrogeological setting. This is likely one of the reasons why the analyses carried out by the authors are mainly able to exclude recharge mechanisms, but not definitely explain from where this water is originated. The last part of Section 5.5 provides a list of speculative mechanisms (lines 614-652): how the Xilamulun river can recharge the Dali lake when Fig. 15 shows that the bed of the former is less elevated than that of the latter? What support the “speculation” about the “flash floods” in the southern portion of the desert? How you only “theoretically estimate” the isotopic firm of the precipitation on the Yinshan Ranges? 2) the contribution is over-long. The introduction addresses the topic with a too-wide perspective, concepts are repeated, with verbose descriptions. There are also too many figures that can be fruitfully combined. The English form must be improved too. Moreover, the location of the study area is unclear: Fig 1a is obscure, the various portions of the desert are not provided in the maps shown in Figs. 1b and 2, a large part of the toponymy cited in the text is not added to the maps. Because of this, the ms need a major revision.

Interactive comment on Hydrol. Earth Syst. Sci. Discuss., <https://doi.org/10.5194/hess-2018-71>, 2018.

**The authors’ responses to the comments from Referee #2**

Dear Dr/Professor Referee #2:

On behalf of my co-authors, we thank you very much for giving us an opportunity to revise our manuscript. We appreciate you very much for your positive and constructive comments and suggestions on our manuscript (hess-2018-71). We have read your comments carefully and have made revision which marked in red in the revised manuscript. We tried our best to revise our manuscript according to your comments and suggestions one by one. Attached please find the revised version, which we would like to submit for your kind consideration. Thank you and best regards.

1) The chemical/isotopic investigations seem not supported by a (at least minimum) knowledge of the hydrogeological setting. This is likely one of the reasons why the analyses carried out by the authors are mainly able to exclude recharge mechanisms, but not definitely explain from where this water is originated. The last part of Section 5.5 provides a list of speculative mechanisms (lines 614-652): how the Xilamulun river can recharge the Dali lake when Fig. 15

shows that the bed of the former is less elevated than that of the latter? What support the “speculation” about the “flash floods” in the southern portion of the desert? How you only “theoretically estimate” the isotopic firm of the precipitation on the Yinshan Ranges?

Our response: AGREE AND CHANGES MADE.

We thank you very much for this comment. Yes, any chemical and isotopic investigations need to be supported by knowledge of the regional- and local-scale hydrogeological settings. According to this comment, we have added the specific information about the hydrogeological, geological (tectonic, lithological, sedimentological and structural), geomorphological, stratigraphical settings of the study area in the revised manuscript. Detailed changes and the added information can be seen from the section “2. Regional settings” and the section “4.5 remote water recharge on groundwater in the Otindag: mountains waters” in the revised manuscript (pages 3-5 lines 103-189 and pages 12-13 lines 442-484). Besides, two newly-built figures about the geological and hydrogeological maps of the study area are also provided as auxiliary instructions to illustrate the hydrogeological characteristics of the Otindag Desert in the revised manuscript. These figures are Figs. 2 and 3 in the revised manuscript. With the help of these newly-added materials we believe that we can definitely and logically explain from where the groundwater in the Otindag is originated.

About the Fig. 15 in the original manuscript (at present it is Fig. 11 in the revised manuscript) and the question “how the Xilamulun river can recharge the Dali lake when Fig. 15 shows that the bed of the former is less elevated than that of the latter?”, our explanation is that: actually, the elevation of the Xilamulun river channel is not lower than the Dali lake. The recent elevation of the Dali Lake is 1,226 m above sea level (Xiao et al., 2008, J Paleolimnol, 40, 519-528). The elevations of the river samples collected from the Xilamulun River in this study ranges between 1360 and 1374 m (Table 1). The real elevation data (measured by handheld GPS in the field) for the river samples l1, l2, l3, l4, l5, l6 in this study are 1368 m, 1368m, 1365 m, 1366 m, 1360 m and 1374 m (Table 1), respectively. Thus, the elevation of the Xilamulun river channel is about 140 m higher than that of the Dali Lake. In Fig. 15 (Fig. 11 in the revised manuscript), it shows the variation of the topographical elevation along the section S1 (see Fig. 1b) from the upstream of the Dali Lake to the location site of the spring water samples s2. It does not show the elevations of the river samples from the Xilamulun River. Strictly speaking, however, this sketch map (Fig. 15) is likely to cause misunderstanding if we think about the river water but not the spring water. So we specially stated that “Note that no river water samples are shown in this figure” in the figure caption of Fig. 11 in the revised manuscript.

About the question “What support the “speculation” about the “flash floods” in the southern portion of the desert?”, we have added specific information about the hydrological settings of the flash floods derived from the Yinshan Piedmont in the section “2. Regional settings” in the revised manuscript (see page 5 lines 158-189).

About the question “How you only “theoretically estimate” the isotopic firm of the precipitation on the Yinshan Ranges?”, we use the words “theoretically estimate” because we have not obtained the precipitation water samples from the Yinshan Mountains in this study. Thus the isotopic firm of the precipitation on the Yinshan Ranges is calculated based on the altitude effect of mountain temperature on stable isotopes fractionation in the original manuscript. It is thus a theoretical estimation. In order to avoid ambiguity, we deleted the discussion of this “theoretically estimation” in the revised manuscript.

2) The contribution is over-long. The introduction addresses the topic with a too-wide perspective, concepts are repeated, with verbose descriptions. There are also too many figures that can be fruitfully combined. The English form must be improved too.

Our response: AGREE AND CHANGES MADE.

We thank you very much for this comment. Yes, according to the comment that “the contribution is over-long”, we have rewritten the manuscript and made an intensive compression on the length of the paper. At present the number of text words in the revised manuscript has been greatly decreased compared with the original manuscript.

According to the comment that “The introduction addresses the topic with a too-wide

perspective, concepts are repeated, with verbose descriptions”, we have rewritten the introduction section of the manuscript to make the topic being specific and not being too broad in its perspective. We tried our best to avoid repeat and verbose descriptions in the revised manuscript whatever on the concept or the context of this section. The detailed changes can be seen in pages 1-3 lines 32-101 in the revised manuscript.

According to the comment that “There are also too many figures that can be fruitfully combined”, we reduced the number of figures in the revised manuscript by putting some figures together and deleting several figures. At last the revised manuscript has 11 figures compared with the original manuscript that including 15 figures. For example, the Figs. 5, 11, 13, 14a in the original manuscript are deleted in the revised manuscript, and the Figs. 7 and 8, the Figs. 10, 12 and 14a are combined, respectively. In addition, two newly-built figures are added into the revised manuscript according to the first comment from you (the detailed content of this comment can be seen above). The specific changes and the final results of these figures can be seen in the newly submitted revised manuscript.

About the comment that “The English form must be improved too”, we are very sorry for our poor and incorrect English writing in the original manuscript. For the shortcomings of the English presentation and the grammatical edit in the first paper, we have checked and revised the whole manuscript carefully to avoid language errors, and finally we have got the help of a native English speaking professional to check and improve the English quality of the revised manuscript. We believe that the language is now acceptable for the publishing purpose.

Moreover, the location of the study area is unclear: Fig 1a is obscure, the various portions of the desert are not provided in the maps shown in Figs. 1b and 2, a large part of the toponymy cited in the text is not added to the maps.

Our response: AGREE AND CHANGES MADE.

We thank you very much for this comment. According to this comment, we have revised the Fig. 1a and 1b and Fig. 2 (now it is Fig. 4 in the revised manuscript) to make them clear and make sure that the various portions of the Otindag Desert are provided in the corresponding maps. We tried our best to add each of the toponymy cited in the text to be included in these maps. The specific changes and the final results of these figures can be seen in the newly submitted revised manuscript (Figs. 1-4).

Finally, we want to say that special thanks to you for your good comments. We have tried our best to improve the manuscript and made specific changes in the revised manuscript according to the comments from you one by one. These changes will not influence the content and framework of the paper. And here we did not list the changes but marked in red in the revised paper. We hope that the correction will meet with approval. Once again, thank you very much for your comments and suggestions.

1 | **Potential source of groundwater**~~Direct or indirect recharge on groundwater~~ in the  
2 | **middle-latitude desert of Otindag, China?**

3 | Bing-Qi Zhu<sup>1\*</sup>, Xiao-Zong Ren<sup>2</sup>, Patrick Rioual<sup>3</sup>

4 | <sup>1</sup>KLWCRES, IGSNRR, CAS, Beijing, China

5 | <sup>2</sup>SGS, TYNU, Jinzhong, China

6 | <sup>3</sup>KLCGE, IGGCAS, Beijing, China

7 | *Correspondence to:* Bing-Qi Zhu (zhubingqi@sina.com)

8 | **Abstract.** The Otindag Desert in the middle-latitude desert zone of northern  
9 | Hemisphere (NH) is essential to livestock-economy and ecoenvironment of northern  
10 | China. Many areas in this zone are unexpectedly rich with groundwater resources  
11 | although they have been under arid or hyper-arid climate ~~for a long time.~~  
12 | Widespread fresh groundwater deep to 60 m was found at the eastern part of the  
13 | Otindag Desert. The occurrence of this massive fresh groundwater raises doubts on  
14 | the long-lasting hypothesis in academic circles that regional atmospheric  
15 | precipitation or palaeowater, ~~namely the direct recharge,~~ is the source of water in  
16 | the middle-latitude desert aquifers of northern China. Understanding of the recharge  
17 | sources of this fresh groundwater is important in evaluating the feasibility of  
18 | groundwater exploitation and utilization. In this study we conducted  
19 | hydrogeochemical and isotopical analyses to assess possible origin and recharge of  
20 | these groundwaters. The analytical results indicate that the fresh groundwater is  
21 | neither originated from regional atmospheric precipitation derived from the Asian  
22 | Summer Monsoon system, nor from palaeowater that formed during the last glacial  
23 | period. These findings suggest that the groundwater in this desert is possible to  
24 | originate from remote mountain areas via the faults of the Solonker Suture zone,  
25 | ~~including the Daxing'Anlin and Yinshan Mountains.~~ In addition, it is concluded that  
26 | the hydrogeological linkage between desert aquifers and mountain systems through  
27 | the suture zone is crucial to the hydrological functioning of the Otindag aquifer. This  
28 | suggests that the modern indirect recharge mechanism, instead of the direct  
29 | recharge and the palaeo-water recharge, is the most significant for  
30 | groundwater recharge in the Otindag Desert. This study provides a new perspective  
31 | into the origin and evolution of groundwater resources in the middle-latitude desert  
32 | zone of HA.

33 |  
34 | **Keywords:** fresh groundwater recharge; atmospheric precipitation; direct recharge;  
35 | indirect recharge; palaeowater recharge; fault hydrology; middle-latitude desert;  
36 | Otindag Desert.

37 |  
38 | **1. Introduction**

39 | The deficit of rainfall occurs globally in semi-arid to arid regions. It is usually  
40 | made up by extracting groundwater to supply the needs of a growing population and  
41 | a higher standard of living. Many areas in the middle-latitude desert zone of  
42 | northern China such as the Badanjilin Desert, the Mu US sandy Land and the Hobq  
43 | Desert (Chen et al., 2012a; Chen et al., 2012b), are unexpectedly rich with large  
44 | groundwater resources although they have been under arid or hyper-arid climate for

45 a long time (Sun et al., 2010). How these groundwaters originated and how they are  
46 recharged in these deserts are thus fundamental scientific questions. Until now,  
47 however, no consensus has been achieved in academic circles.

48 The Otindag Desert is one of the largest sandy lands located at the monsoon  
49 margin of northern China and is the geographical centre of the northeastern Asian  
50 Continent (Fig. 1), which can be regarded as a significant repository of information  
51 relating to the groundwater recharge in the arid Inner Asia. At present, the eastern  
52 Otindag is also a typical case for its unexpected groundwater resources, because  
53 there is abundant groundwater in this desert land and even rivers originate there due  
54 to the spillover of spring water, such as the tributaries of Xilamulun River in its north  
55 and the Shandian River in its south (Fig. 1). Climatically, the monsoon margin of  
56 northern China refers to a strip along the present East Asian Summer Monsoon  
57 (EASM) limits and is considered to be sensitive to climate change (Wang and Feng,  
58 2013). Geologically, the Otindag Desert lies in a tectonic depression of the central  
59 Solonker suture zone with a few faults stretching east and west (Fig. 2), with its  
60 northern margin along a fault marked by a series of lake basins. Thus, the large-scale  
61 hydrogeological conditions of the Otindag Desert belong to a fault zone under the  
62 influence of the EASM climate.

63 Until now, however, whether the climate or other factors affected the  
64 groundwater recharge in the Otindag is still not known. Little data about the  
65 groundwater and its origin is available in the literature, and knowledge and reliable  
66 data on various hydrogeological characteristics of the desert such as the catchment  
67 extent, input/output, the hysteretic hydraulic functions, the transient hydraulic  
68 conditions, in-homogeneities, and on transfer functions to overcome scale problems  
69 are also missing. Under such conditions, conventional methods such as water  
70 balance and hydraulic methods sometimes fail in determining groundwater recharge,  
71 particularly in extreme environments (arid, semi-arid, or cold) (Drever, 1997).  
72 Because pristine aquatic conditions may significantly differ from managed conditions  
73 in arid environment, and thus groundwater recharge is not a fixed number, but may  
74 vary with the boundary conditions of the recharge system (Seiler and Gat, 2007).

75 Groundwater recharge can be broadly classified into two categories: the direct  
76 recharge by native water resources and the indirect recharge by external water  
77 resources (Herczeg and Leaney, 2011). Water infiltration of atmospheric precipitation  
78 through the unsaturated zone to the groundwater is hydrologically defined as the  
79 direct recharge, and the indirect recharge is defined as recharge from mappable  
80 features such as rivers, canals, lakes and originates from remote areas (Scanlon et al.,  
81 2006; Healy, 2010). It is well known that groundwater recharge can be influenced by  
82 environmental factors, including climate change, underlying soil and geology, land  
83 cover and the growth in human population that affects withdrawal and economic  
84 development (Zhu et al., 2015, 2017). Among these environmental factors, climate  
85 and land cover largely determine precipitation and evapotranspiration, whereas the  
86 underlying soil and geology dictate whether a water surplus (precipitation minus  
87 evapotranspiration) can be transmitted and stored in the subsurface (Doll, 2008,  
88 2009; Giordano, 2009).

89 For some earth scientists, the direct recharge is thought to be very important  
90 for groundwaters in the wide desert lands of north China due to the lack of surface  
91 runoffs (Yang et al., 2010; Yang and Williams, 2003; Zhao et al., 2017). They argued

92 that although the amount of atmospheric precipitation is small, the vast catchment  
93 area in the desert region could concentrate the rainfall into large inland basins,  
94 creating an aquifer with large storage capacity and great thickness. However, some  
95 hydrologists estimated by the chloride mass balance method that the direct recharge  
96 was 1.4 mm/year, which represents approximately only 1.7% of the mean annual  
97 precipitation in a cold large desert (Badanjilin) in northern China (Gates et al., 2008).  
98 A similar estimation of 1 mm/year was given for Gobi deserts from the Hexi Corridor  
99 to the Inner Mongolia Plateau in northwestern China (Ma et al., 2008). Consequently,  
100 they thought that heavy potential evaporation and little precipitation make it difficult  
101 for direct recharge to meet the supply of groundwater in these desert areas. Thus,  
102 the indirect recharge is considered to be an important mechanism for groundwater  
103 recharge in these desert areas. For example, Zhao et al. (2012) suggested that little  
104 precipitation had recharged into groundwaters in the Badain Jaran Desert. Chen et al.  
105 (2004) argued that the groundwaters in the Badanjilin Desert were recharged by  
106 palaeo-glacial melt water through faults and deep carbonate layers far away from the  
107 local desert. Many studies also suggested that palaeowaters stored in an aquifer  
108 during wetter climate periods could recharge to groundwater under certain  
109 conditions in arid lands (Edmunds et al., 2006; Ma and Edmunds, 2006). Other kinds  
110 of indirect recharge, such as mountain front recharge from adjacent mountain blocks,  
111 are also proposed to offer an important inflow to aquifers within arid to semiarid  
112 catchments (Blasch and Bryson, 2007).

113 In this paper, we focus to answer the question that whether groundwater  
114 recharge in Otindag is mainly direct or indirect, using hydrochemical and isotopic  
115 indicators as tracers to offer a valuable support for identifying the contributions of  
116 precipitation recharge on groundwater, since these indicators reflect the  
117 composition of water molecules and are sensitive to physical processes such as  
118 mixing and evaporation (Sultan et al., 2000; Guendouz et al., 2003; Petrides et al.,  
119 2006; Scanlon et al., 2006; Zhu et al., 2007, 2008; Jobbágy et al., 2011). The detailed  
120 objectives are: (1) to recognize the major sources of groundwater in the area, and (2)  
121 to identify the key mechanism of groundwater recharge in the desert.

122

## 123 **2. Regional settings**

124 Geographical location. The Otindag Desert lies between latitudes 42° and 44°N  
125 and longitudes 112° and 118° E (Fig. 1). It is an east part of the great middle-latitude  
126 desert zone between northwestern and northeastern China which extends from the  
127 Taklamakan Desert in northwestern China to the Kelqin Desert in northeastern China,  
128 near the west coast of the Pacific Ocean. The desert has an area of approximately  
129 21,400 square kilometers located in the eastern Inner Mongolia and at the monsoon  
130 margin of northern China (Fig. 1). It is the fourth largest sandy lands in China (Yang et  
131 al., 2012) and is bordered by a flat steppe terrain of Dali Basin to the north, the  
132 Yinshan Mountains and mountainous loess landscape to the south, and the the  
133 Greater Khingan (Daxing'Anling) Mountains to the east (Fig. 1). The Otindag Desert is  
134 essential to livestock-economy and ecoenvironment of northern China. Settlements  
135 in this desert are constrained to oases to frequent springs, groundwater with high  
136 level and areas where cultivation and irrigation are feasible. Some herdsmen live a  
137 precarious life by grazing livestock in the desert.

138 Topography and geomorphology. The relief in the Otindag Desert is varied with

139 a combination of extensive dune fields and rugged piedmonts and mountains along  
140 the eastern and southern rims. In the east, the Daxing'Anling Mountains has an  
141 average elevation ranging from 1,100 to 1,400 m and extend from the Heilong River  
142 Valley into the upper reach valleys of the Xilumulun River from northeast to  
143 southwest, with a gradual increase in height northwards from about 180 m near  
144 Huma to Huanggangliang, where the highest mountaintop reach 2,029 m. In the  
145 south and southeast, the Yinshan Mountains decline gradually near Duolun and  
146 Zhenglanqi, and in some areas leave wide alluvial plains. The terrain of the Otindag  
147 Desert is less rough and elevations decrease from ca. 1300 m in the southeast to ca.  
148 1000 m in the northwest. Over the greater part of this desert the ground cover  
149 consists of fixed and semi-fixed sandy dunes, with a few mobile dunes in area of little  
150 vegetation. The dominated dune types are represented from parabolic to barchans,  
151 linear and grid-formed types, ranging from a few meters to over 40 m in height (Zhu  
152 et al., 1980; Yang et al., 2008).

153 Climate, vegetation and soil. The climate of the Otindag Desert was not uniform  
154 in geological period, with much sand movement, occasional rainy years, and several  
155 wetter intervals during the Holocene (Yang et al., 2015; Tian et al., 2017). At present  
156 the whole desert belongs to the arid and semi-arid temperate zone, with a mean  
157 annual temperature of 2 °C in the north and 4°C in the south (Liu and Yang, 2013). At  
158 the regional scale, the climate of the desert is typically controlled by the East Asian  
159 Monsoon system, characterized by a warm summer, with precipitation transported  
160 by the EASM, and by a cold and dry winter under the influence of the East Asian  
161 Winter Monsoon (EAWM). The rainfall in the desert exhibits a wide variation in space  
162 and time. Influence of the EASM changes from southeast to northwest in the desert,  
163 varying with the distance increase from the Pacific Ocean and leading to the mean  
164 annual rainfall decreasing from ~450 mm in the southeast to ~150 mm in the  
165 northwest (Yang et al., 2013). The spatial inequality of rainfall makes a great impact  
166 on the availability of near-surface moisture, consequently on the distribution of  
167 vegetation, soil and the animal husbandry potential of local communities. The major  
168 soil type is the grey desert soil in the west and changes to the sierozems and  
169 chernozem or chestnut soil in the east. Through the desert, vegetation is sparse in  
170 the west and relatively abundant in the east. The native vegetation is scrub  
171 woodland in the east and is steppe in the west, showing a natural characteristic of  
172 the temperate desert or semi-desert. It is greatly affected by temperature, rainfall  
173 and elevation in the growing season due to the scarcity of surface runoff.

174 Geology. The Otindag Desert is located in a tectonic depression of the Solonker  
175 Suture Zone (Jian et al., 2010) bounded by the Northern Early to Mid-Paleozoic  
176 Orogen Zone and the Hatug Uul Block to the north, the Southern Early to  
177 Mid-Paleozoic Orogen Zone and the North China Craton system to the south (Fig. 2).  
178 A few faults such as the Xar Moron Fault and Chifeng-Bayan Obo Fault stretch east  
179 and west, with its northern margin along the Solonker Suture Zone marked by a  
180 series of lake basins (Figs. 1 and 2). The tectonostratigraphic units and overall  
181 structural trends are mainly oriented NE–SW (Fig. 2), which may be interpreted as  
182 resulting from overall compressive stresses oriented principally in the NW–SE  
183 quadrants during orogenesis (Jian et al., 2010; Zhang et al., 2015). Diverse rock types  
184 from unlithified and lithified clastic sediments through to carbonate, crystalline, and  
185 volcanic rocks are distributed in and around the Otindag Desert (Zhang et al., 2015)

186 (Figs. 2 and 3). Tertiary and Quaternary sandstones and mudstones are the common  
187 basement rocks under the dunes of the Otindag, and extensive volcanic basalts  
188 forming flat terrains are to the north (Zhu et al., 1980; Li et al., 1995).

189 Hydrology and hydrogeology. The Otindag Desert originated during the Late  
190 Quaternary (Yang et al., 2015) and various alluvial fans formed at the margins of this  
191 desert during the early to middle Holocene. These are composed of conglomerate  
192 and sand deposits, where major periodic streams or wadis debouched into the  
193 Otindag. At present two rivers run through the eastern margin of the Otindag Desert,  
194 i.e. the Xilamulun River in the north and the Shandian River and its two tributaries,  
195 the Shepi River and Tuligen River in the south. Both stem from the eastern and  
196 southeastern parts of the Otindag (Fig. 1). The Xilamulun River, 380 km in length and  
197  $32.54 \times 10^3 \text{ km}^2$  in area, is a neighboring river both to the northeastern Otindag and  
198 the southeastern Dali Basin, the northern catchment of the Otindag Desert. The  
199 Xilamulun River flows to the east and finally goes into the Xiliao River, with an annual  
200 mean runoff of  $6.58 \times 10^8 \text{ m}^3$  (Wu et al., 2014). The Shandian River is the upper  
201 reach of the Luan River, with a length of 254 km and a catchment area of  $4.11 \times 10^3$   
202  $\text{km}^2$  (Yao et al., 2013). Spotted salt crusts can extensively develop on land surface  
203 due to the high rate of evaporation. Sabkhas and salt pans often form in areas  
204 surrounding the flat shorelines of some lakes in the Otindag. During rainy season,  
205 some rain and floodwaters (generally coming from the Yinshan piedmonts) are  
206 retained in low-lying areas, which may temporarily recharge shallow aquifers. Under  
207 storm conditions, fast-flowing floods often form in some wadi channels with rich soil  
208 due to the occasional short, heavy rainstorms.

209 Groundwater resources in the Otindag Desert and its surrounding areas depend  
210 on several kinds of aquifers with different water-bearing formations and units (Fig. 3).  
211 Coarse- to fine-grained sedimentary rocks, magmatic rocks and metamorphic rocks of  
212 the Inner Mongolia-Daxing'Anling Orogenic Belt (Zhang et al., 2015) form the major  
213 regional aquifer unit (Fig. 3). They are composed mainly of alluvial sediments  
214 (mid-Permian Zhesi Formation), melange (Solonker suture zone), A-type granite  
215 (early Permian), bimodal volcanic rocks with sedimentary intercalations (early  
216 Permian Dashizhai Formation), diorite-quartz diorite-granodiorite rocks  
217 (Carboniferous-Permian) and metamorphic complex (predominantly gneiss, early  
218 Paleozoic) (Fig. 2). The aquifer is generally unconfined in dune fields of the Otindag  
219 Desert, unconfined to semi-confined in the Yinshan Mountains' piedmont, and  
220 semi-confined to confined in the Daxing'Anling uplands (Fig. 3). Water-level  
221 measurement in June 2010 indicated that the general depth of unconfined  
222 groundwater level ranges between 10 to 70 m in the Otindag Desert (Fig. 3). Local  
223 granular aquifers in the central desert are composed of coarse fluvial, lacustrine and  
224 aeolian sediments, but their extent and thickness vary throughout the watershed  
225 (Zhu et al., 1980; Li et al., 1995). The generally coarse-grained texture of the  
226 unconsolidated rock formations provides primary porosity in terms of groundwater  
227 flow in the desert.

228

### 229 3. Methods

230 The isotopes and ion chemistries of different water samples in the Otindag  
231 Desert, including natural samples collected from local and regional precipitation,  
232 depression springs, shallow and deep aquifers, perpetual lakes and outflowing rivers,

233 are analyzed here and discussed. Relationships between the study area and the  
234 regional prevailing EASM climate, the dominant topographical, geological (tectonic)  
235 and hydrogeological conditions, are also explored and interpreted, using multiple  
236 graphs and diagrams. Fieldworks took place during the summer season of 2011 and  
237 the spring season of 2012. Water samples were mainly retrieved from shallow and  
238 deep wells located over a wide area in dune fields of the study regions. The detailed  
239 locations of the sampling sites are shown in Fig. 4.

240 In this study, we designed two groups of parameters to characterize the  
241 physiochemistry of each water sample. One is the field-measured parameters and  
242 another is the lab-measured parameters. The former includes those parameters that  
243 will change in a shorter period of time when they are not directly measured in the  
244 field, such as the total dissolved solid (TDS, mg/L), electrical conductivity (EC in  
245 micro-Siemens per centimeter or  $\mu\text{S}/\text{cm}$ ), hydrogen-ion concentration (pH) and  
246 temperature ( $^{\circ}\text{C}$ ). The analysis for major cations ( $\text{F}^{-}$ ,  $\text{Cl}^{-}$ ,  $\text{NO}_2^{-}$ ,  $\text{NO}_3^{-}$ ,  $\text{SO}_4^{2-}$ ,  $\text{HCO}_3^{-}$ ,  
247  $\text{CO}_3^{2-}$  and  $\text{H}_2\text{PO}_4^{-}$ ) and anions ( $\text{Li}^{+}$ ,  $\text{Na}^{+}$ ,  $\text{NH}_4^{+}$ ,  $\text{K}^{+}$ ,  $\text{Mg}^{2+}$  and  $\text{Ca}^{2+}$ ) are determined for all  
248 of the water samples collected. Contents of stable ( $^2\text{H}$  and  $^{18}\text{O}$ ) and radioactive  
249 isotopes ( $^3\text{H}$ ) in the rain and groundwater samples are precisely measured. The  
250 analytical data of the physiochemical parameters and the stable and radioactive  
251 isotopes of the water samples collected in this study are listed in Tables 1, 2 and 3,  
252 respectively.

253

## 254 4. Results and Discussions

255

### 256 4. 1. Hydrochemical characteristics of natural waters

257 The natural water samples collected in this study are generally neutral to slightly  
258 alkaline, with the pH values varying between 6.26 and 9.44 (except the precipitation  
259 sample p1, 4.61) (Table 1) and a median value of 7.27. The TDS values range between  
260 67 and 660 mg/L (average 211 mg/L) (Table 1), all belonging to fresh water (TDS <  
261 1000 mg/L) in the salination classification of natural water (Meybeck, 2004). The  
262 variations in ion concentrations of the major cations and anions in the studied water  
263 samples were displayed in a fingerprint diagram with a semi-logarithm y-axis (Fig. 5).  
264 The rain water sample is the most depleted in ions among these samples. The  
265 groundwater samples have the highest concentrations of cations and anions and the  
266 lake, river and spring waters had intermediate values. The calcium concentration is  
267 the highest among cations in almost all of the water samples, and the  $\text{HCO}_3^{-} + \text{CO}_3^{2-}$   
268 concentration (bicarbonate + carbonate, alkalinity) is the highest among anions in  
269 most of the water samples. For several groundwater samples (g3, g4, g5, g6 and g11),  
270 spring sample (s1) and precipitation sample (p1), they have higher  $\text{SO}_4^{2-}$   
271 concentrations than alkalinity (Fig. 5).

272 Two chemically distinct water types are recognized for the studied waters via a  
273 Piper diagram (Fig. 6), calcium bicarbonate and calcium sulphate. No Chloride-type  
274 and sodium-type waters occur in the study area (Fig. 6). It has been reported that the  
275 global groundwater tends to evolve chemically towards the composition of seawater  
276 (Chebotarev, 1955), and this evolution is associated with regional changes in  
277 dominant anions but not cations. This general evolution of groundwater can be  
278 illustrated as a anion evolution line (Freeze and Cherry, 1979):  $\text{HCO}_3^{-} \rightarrow \text{HCO}_3^{-} + \text{SO}_4^{2-}$   
279  $\rightarrow \text{SO}_4^{2-} + \text{HCO}_3^{-} \rightarrow \text{SO}_4^{2-} + \text{Cl}^{-} \rightarrow \text{Cl}^{-} + \text{SO}_4^{2-} \rightarrow \text{Cl}^{-}$ , which travels along the flow paths

280 and increasing ages. It can be deduced from this line that bicarbonate water is the  
281 early product of groundwater evolution with low salinity , renewable water resources  
282 or low residence time, while sulfate waters is the intermediate or advanced product  
283 of groundwater evolution with higher salinity passing through gypsum and anhydrite  
284 aquifers (Clark, 2015). The distribution pattern of water chemical types occurred in  
285 the study area indicates a primary stage of groundwater evolution in the Otindag  
286 Desert.

287 The  $\delta D$  values of the groundwater samples collected in this study varied from  
288  $-63.42\text{‰}$  to  $-75.92\text{‰}$  (Table 3), with an average  $-69.53\text{‰}$ . The  $\delta^{18}O$  values ranged  
289 between  $-8.64\text{‰}$  and  $-11.26\text{‰}$  (Table 3), with an average  $-10.17\text{‰}$ . The spring water  
290 samples were relatively concentrated in  $\delta D$  and  $\delta^{18}O$  and were greatly similar to  
291 those of the groundwater samples (Fig. 7). The  $\delta D$  and  $\delta^{18}O$  values in the river water  
292 samples were slightly more variable and were also similar to those of the  
293 groundwater (Fig. 7). The lake water samples were enriched in  $\delta D$  and  $\delta^{18}O$  by  
294 comparison to the groundwater samples (Fig. 6). The precipitation sample p1 was  
295 also enriched in  $\delta D$  and  $\delta^{18}O$  by comparison to the groundwater samples (Fig. 7). The  
296 content of radioactive isotope of tritium ( $^3H$ ) measured in seven well groundwater  
297 samples with 6-60 m depth ranged from 1.86 to 24.35 TU (Table 3), with an average  
298 14.95 TU, higher than the mean tritium concentration (9.8 TU) of groundwater in the  
299 Vienna Basin, Austria (Stolp et al., 2010), the seat of the International Atomic Energy  
300 Agency (IAEA).

301 If we plot the relationships between oxygen and hydrogen isotopes of  
302 groundwater, spring, river and lake water samples, we observed that most of the  
303 data points fell on a straight line that can be expressed by a regression equation:  $\delta D$   
304  $= 4.09\delta^{18}O - 28.31$  ( $R^2=0.93$ ,  $n=24$ ) (EL1 in Fig. 7). This local groundwater line (LGWL)  
305 is different from the Global Meteoric Water Line (GMWL,  $\delta D = 8\delta^{18}O + 10$ ) and the  
306 Mediterranean Meteoric Water Line (MMWL,  $\delta D = 8\delta^{18}O + 20$ ) estimated by Craig  
307 (1961), but it is similar to the local groundwater lines established for other deserts in  
308 northern China and central Asia with a same slope but different Y-intercepts, such as  
309  $\delta D = 4.17\delta^{18}O - 31.3$  for the Badanjilin Desert (Jin et al., 2018),  $\delta D = 4.8\delta^{18}O - 15.2$   
310 for the Ejina Desert in China (Wang et al., 2013), and  $\delta D = 4.26\delta^{18}O + 9.23$  for the  
311 Rub Al Khal Desert in the United Arab Emirates (Rizk and El-Etr, 1997). The data  
312 points are scattered for the lake water samples (Fig. 7) in the Otindag, suggesting  
313 that the lake waters are affected by evaporation, but the other waters in the desert  
314 are not so.

315

#### 316 | 4. 2. **Summer pP**precipitation recharge on groundwater in the Otindag

317 In order to compare the isotopic signals between groundwater and precipitation  
318 at a regional scale, the isotopic analysis of precipitation from similar areas surrounding  
319 | the study area, such as Baotou, were incorporated with local data of **summer**  
320 precipitation (p1) in this study (Fig. 7). The Baotou station is the nearest long-term  
321 station to the Otindag Desert and was monitored for the isotopic composition of  
322 rainfall for the period 1986-2001 within the International Atomic Energy Agency  
323 Global Network of Isotopes in Precipitation (IAEA-GNIP) database. The stable isotope  
324 data from Baotou was used to represent the regional background of stable isotopic  
325 | compositions of the present-day **summer** meteoric water, especially in the westward  
326 inland areas of the Otindag Desert (Fig. 1). In addition, stable isotope data of the

327 | Tianjin station was also used to represent the regional background of [summer](#)  
328 | precipitation in the eastern coastal areas of the Otindag Desert (Fig. 1).

329 | Based on the isotopic data from the Baotou station, the local meteoric water  
330 | lines can be statistically expressed as the isotopic regression equation of  $\delta D =$   
331 |  $6.36\delta^{18}O - 5.21$  (LMWL-B). It can also be expressed as  $\delta D = 6.57\delta^{18}O + 0.31$  (LMWL-T),  
332 | based on the data from the Tianjin station (Fig. 7). The precipitation sample p1  
333 | collected in this study fell onto the GMWL (Fig. 7). It also showed similar  $\delta D$  and  $\delta^{18}O$   
334 | values to those of the precipitation collected in the GNIP stations of Baotou and  
335 | Tianjin (Fig. 7).

336 | Compared to the [summer](#) precipitation data from the GNIP stations and from  
337 | the local [summer](#) precipitation (p1), the groundwater, spring, and river water  
338 | samples were evidently depleted in heavy stable isotopes in the Otindag (Fig. 7).  
339 | Except for the lake water samples, most of the groundwater, river water and spring  
340 | water samples in the Otindag fall on or lay between the LMWL-B and the LMWL-T  
341 | lines, and are located at the lower left area of the precipitation points (Fig. 7).

342 | Because the isotopic evolution of  $\delta D$  and  $\delta^{18}O$  in water illustrated in the Craig  
343 | line represents a one-way and irreversible process, the water bodies distributed at  
344 | the upper right area of the Craig line can not be recharge sources for the water  
345 | bodies distributed at the lower left area of the line. Such results indicate that the  
346 | groundwater, river water and spring water in the Otindag are not recharged by the  
347 | regional precipitation, namely no significant modern direct recharge has taken place  
348 | for groundwater in the Otindag.

349 | Dogramaci et al. (2012) documented that only intense and remarkable rainfall  
350 | events  $>20$  mm could recharge groundwater in the semi-arid Hamersley Basin of  
351 | northwest Australia, while the rainfall events  $<20$  mm had limited influences on  
352 | groundwater recharge. Chen et al. (2014) described that rainfall events  $\leq 5$  mm in the  
353 | [summer](#) arid and semi-arid region of northern China would be evaporated into the  
354 | atmosphere rapidly before it is infiltrated into the groundwater system. Based on the  
355 | analysis on the data records from two meteorological stations around the Otindag,  
356 | i.e. the Duolun and Xilinhaote stations (see Fig. 1a), we observed that [summer](#) rainfall  
357 | events  $>20$  mm on average only occur 2.5-3.4 times per year (Table 4). In some years  
358 | (e.g. from 2005 to 2007 at the Xilinhaote Station), no [summer](#) rainfall events  $>20$  mm  
359 | even occurred. It further indicated the limited contribution of regional [summer](#)  
360 | precipitation on groundwater recharge in the Otindag.

361 | In addition to groundwater, the river and spring water samples from the Otindag  
362 | also deviated from the local precipitation in the Craig diagram (Fig. 7). These water  
363 | samples came from the Xilamulun, Shepi and Tuligen rivers. They shared the same  
364 | evaporation line (EL1) with the groundwater and lake water samples (Fig. 7).  
365 | Generally speaking, natural waters that have a same recharge source are distributed  
366 | on a same line of evaporation in the  $\delta^2$  and  $\delta^{18}O$  diagram (Chen et al., 2012b). This  
367 | indicates that the recharge sources of groundwater, river water, spring water and lake  
368 | water in the Otindag are genetically associated each other and differ from the local  
369 | precipitation.

370 |

### 371 | **4. 3. Winter precipitation and palaeowater recharge on groundwater in the Otindag**

372 | Since the groundwater samples in the Otindag are depleted in their  $\delta D$  and  $\delta^{18}O$   
373 | values even more than those of the local rainfall (Fig. 7), they must be sourced from

374 other waters characterized by similar or more depleted signals in their stable  
375 isotopes compositions. Due to the temperature effect (such as evaporation) on  
376 isotopic fractionation, only the waters issued from colder environments can be more  
377 depleted in their  $\delta D$  and  $\delta^{18}O$  values even more than those of the local rainfall.

378 Because the Otindag Desert is under the control of the EASM climate (Fig. 1),  
379 the local rainfall in the desert is mainly sourced from summer precipitation. This can  
380 also be illustrated by the seasonal distributions in annual mean precipitation (Fig.8a),  
381 in annual mean air temperature (Fig. 8b) and in annual mean water vapor pressure  
382 (Fig. 8c) over the last forty years at the two surrounding GNIP weather stations in  
383 Baotou and Tianjin. The seasonal distributions of stable isotopes in the two stations  
384 (Fig. 8d-e) show that the summer rainfall is evidently positive in its signals of  $\delta D$  and  
385  $\delta^{18}O$  by comparison with those of the winter rainfall, further suggesting that the  
386 waters issued from cold environments can be more depleted in their  $\delta D$  and  $\delta^{18}O$   
387 values than those of the summer rainfall. Thus we speculate that groundwater in the  
388 Otindag can be potentially derived from (1) modern precipitation in winter, (2)  
389 palaeowater formed in the past glacial period, or (3) remote/mountain waters that  
390 emanate in colder and wetter conditions.

391 The annual mean values of  $\delta D$  and  $\delta^{18}O$  over the last forty years are more  
392 depleted in winter precipitation than in summer precipitation at the Baotou and  
393 Tianjin stations (Fig. 8d-e). This isotopic signal qualifies the regional winter  
394 precipitation to be a potential source of groundwaters in the Otindag. However, the  
395 precipitation amounts and the water vapor pressures (effective moisture) in winter  
396 months are much lower than those in the summer months at both the Baotou and  
397 Tianjin stations (Fig. 8a and 8c). It indicates that the winter seasons in these regions  
398 are relatively colder and drier but not colder and wetter. A colder-wetter winter  
399 season is a necessary condition for winter precipitation to be a water source for the  
400 formation of groundwater under a summer monsoon climate. This is because the  
401 bigger amounts of summer precipitation will easily remove or weaken the depleted  
402 isotopic signals of winter precipitation in groundwater. In this regard, modern winter  
403 precipitation is unlikely to be an important source of groundwater in the Otindag.

404 As to the palaeowaters formed in colder and wetter periods such as the last  
405 glacial, it has been proposed to be a potential water source for groundwaters in the  
406 wide arid lands of the world. The depleted signals of stable isotopes ( $\delta D$  and  $\delta^{18}O$ ) in  
407 groundwater have been recognized in global arid and semi-arid regions, such as the  
408 Sinai Desert in Egypt (Gat and Issar, 1974), Israel (Gat, 1983), South Australia (Love et  
409 al., 1994, 2000), northern China (Ma et al., 2010), Saudi Arabia (Bazuhaier and Wood,  
410 1996) and North Africa (Guendouz et al., 2003). These signals are very often  
411 explained as palaeo-groundwater that recharged by precipitation during past wetter  
412 and colder periods (Love et al., 1994, 2000; Herczeg and Leaney, 2011).

413 Here we use the tritium data as an environmental tracer to estimate the  
414 groundwater age in the Otindag. The tritium data at the GNIP stations of the Baotou  
415 and Tianjin are also referenced as the background values in precipitation of recent  
416 years. The residence time of groundwater in aquifer and the residual tritium of a  
417 water body can be calculated by  $N = N_0 e^{-\lambda t}$  (Yang and Williams, 2003). Where  $N$  =  
418 content of residual tritium in water sample,  $\lambda = 0.0565$ , the radioactive decay  
419 constant,  $N_0$  = content of tritium at the time of rainfall and  $t$  = years after  
420 precipitation. Based on this equation, the residual tritium was theoretically

421 calculated and the standard for tritium dating was established for seven groundwater  
422 samples in the Otindag Desert (Table 3). As a result, ages of 0-60 years were obtained  
423 for these groundwater samples (Table 5). This indicates that recent recharge took  
424 place several decades after the peak in global nuclear tests. We thus conclude that  
425 groundwater is generally not older than 70 years in the study area. It means that  
426 groundwater in the Otindag are not palaeowater recharged.

427 Both the modern summer and winter precipitation recharge and the  
428 palaeowater recharge can be refuted, indicating that direct recharge is not a major  
429 mechanism controlling the groundwater recharge in the Otindag.

430

#### 431 | **4. 4. External Remote-water recharge on groundwater in the Otindag: Dali Basin**

432 The third hypothesis that “remote/mountain waters emanate under colder and  
433 wetter conditions” is further considered here. In essence, it is an indirect recharge  
434 mechanism as water originates from remote areas (Healy, 2010; Herczeg and  
435 Leaney, 2011).

436 It is worth noting that the values of deuterium and oxygen-18 for groundwater  
437 in the north part of the study area are more depleted in  $\delta D$  and  $\delta^{18}O$  than those in  
438 the south part (Table 3). It suggests that the Otindag groundwater might be  
439 potentially recharged by water resources coming from the northern neighboring  
440 catchment, such as the Dali Basin.

441 Recently published data of  $\delta D$  and  $\delta^{18}O$  in groundwater, lake water, river water  
442 and spring water sampled from the Dali Basin (e.g., Chen et al., 2008; Zhen et al.,  
443 2014) were compiled in this study and were co-analyzed with the data from the  
444 Otindag. About 70 natural water samples from the Dali and Otindag with  $\delta D$  and  
445  $\delta^{18}O$  values are shown in a Craig diagram (Fig. 9). All of these samples fell on or lied  
446 near the evaporation line EL2 in the Craig diagram (Fig. 9), with a regression  
447 equation of  $\delta D = 4.81\delta^{18}O - 21.55$  and a high correlation coefficient ( $R^2=0.98$ ,  $n=70$ ).  
448 Compared to the groundwater samples in the Otindag, water samples from the  
449 groundwaters, rivers and springs from the Dali Basin are more depleted in  $\delta^{18}O$  and  
450  $\delta D$  (Fig. 9). Such results further indicate that, in terms of isotopic signature, the  
451 groundwater in the Otindag has a close relationship with the natural waters in the  
452 Dali Basin.

453 The similar signals of  $\delta D$  and  $\delta^{18}O$  between the groundwater in the Otindag and  
454 the river water in the Dali (Fig. 9) point towards the idea that the groundwater in the  
455 Otindag might be sourced from the river water in the Dali Basin, since the Dali has  
456 more depleted isotopic signals in water than the Otindag (Fig. 9). Considering the  
457 topographical gradient of elevations between the two regions, however, river water  
458 in the Dali Basin cannot flow into the eastern Otindag, because the terrain elevation  
459 of the Dali Basin is lower than that of the Otindag (Fig. 1). This is also the reason why  
460 the huge Dali Lake that lies in the Dali Basin has no equivalent in the Otindag (Fig. 1).  
461 If there is a hydraulic linkage between the two regions, water should flow from the  
462 Otindag into the the Dali, but not conversely.

463 In view of the hydraulic gradient, river water in the Dali Basin could not be a  
464 recharge source for groundwater in the Otindag. However, in view of the isotopic  
465 gradients, groundwater in the Otindag could not conversely be the source of river  
466 water in the Dali (Fig. 9). Thus, the similar isotopic signals between the river water in  
467 Dali and the groundwater in Otindag indicate that these waters might be recharged

468 from a common source.

469 Similar isotopic signals also occurred in the groundwaters between the Otindag  
470 and the Dali Basin (Fig. 9). In order to understand the linkage of groundwaters  
471 between the two regions, the potential movement of groundwater in the transition  
472 zone of the two regions need to be known. In this study, a groundwater-sampling  
473 project was designed in the field along a N-S section of a palaeo-channel located at  
474 the transition zone between the Dali and Otindag (Figs. 1, 2). The channel was  
475 named "PCSX" in this study, with its north part named "NPCSX" and the south part  
476 named "SPCSX".

477 The GPS elevation of the northernmost sampling site in the NPCSX (g11, about  
478 1317 m a.s.l.) was much lower than that of the southernmost site in the SPCSX (g1,  
479 1396 m a.s.l.) (Fig. 2 and Table 1). Regarding to the topographical gradient in the  
480 channel, there is a drop of about 80 m between the NPCSX and the SPCSX. Under  
481 such slope, the underground hydraulic gradient for groundwater flow can be roughly  
482 parallel with that of the surface water flow, namely that the groundwaterflow should  
483 move downwards from the SPCSX area into the NPCSX area. Thus we can speculate  
484 that groundwater in the NPCSX would have higher salinity than those in the SPCSX  
485 under such flowing direction. In order to verify this speculation, actual variations of  
486 water salinity (chloride and TDS) were detected along the PCSX section. The sampling  
487 site g1 was defined as the initial point and the distances between g1 and other  
488 sampling sites along the PCSX section were calculated, based on their GPS  
489 geographical coordinates measured in the field. The results are shown in Fig. 10a-b.  
490 It is clear that the variations of chloride and TDS concentrations in groundwater do  
491 not increase along the palaeo-channel from south to north (Fig. 10a-b). On the  
492 contrary, both the values of chloride and TDS are lower in the NPCSX area than those  
493 in the SPCSX area. Such kind of spatial variations in the chloride and TDS values  
494 contradict the speculated patterns abovementioned, suggesting that the hydraulic  
495 gradient of groundwater flowing path in this region is not controlled by the  
496 topographical gradient between the NPCSX and SPCSX areas.

497 Compared between the NPCSX and SPCSX regions, the stable isotopic values  
498 ( $\delta^{18}\text{O}$  and  $\delta\text{D}$ ) of groundwaters in the SPCSX region vary greatly with a large  
499 amplitude, while those in the NPCSX are relatively constant (Fig. 10c-d). The constant  
500 variations indicate that the recharge source of groundwater in the NPCSX is relatively  
501 unitary. The isotopic values in the SPCSX are much lighter than those in the NPCSX  
502 along the distance section from south to north (Fig. 10c-d). The heaviest values  
503 occurred in the sample g11 collected from the NPCSX (Fig. 10c-d), indicating a water  
504 being earlier recharged. The spring water sample s2, a representation of discharge  
505 water, is characterized by medium values of  $\delta\text{D}$  and  $\delta^{18}\text{O}$ . These results indicate that  
506 the groundwaters in the SPCSX area, with relatively enriched isotopic signals in  $\delta\text{D}$   
507 and  $\delta^{18}\text{O}$  by comparison with those in the NPCSX area, are composed of a mixture of  
508 the groundwaters in the NPCSX with other waters.

509 The tritium contents were broadly and positively related to the values of  
510 deuterium excess in the groundwater samples in the PCSX (Fig. 10e). For water that  
511 experiences an evaporation process, the d-excess value will increase in the  
512 evaporated water vapor, but will decrease in the residual water body (Dansgaard,  
513 1964; Merlivat and Jouzel, 1979). In this study, except for sample g11 (a sample very  
514 close to the riverhead area), the positive relationship between the tritium and the

515 deuterium excess generally shows that the d-excess values are higher in the  
516 groundwaters collected from the NPCSX, but are lower in those from the SPCSX (Fig.  
517 10e). This distribution pattern indicates that the groundwaters in the NPCSX are  
518 relatively younger and experienced a lower degree of evaporation than those in the  
519 SPCSX. The d-excess gradient, increasing from south to north in the PCSX, further  
520 suggests that groundwater does not flow from the SPCSX area to the NPCSX area,  
521 namely out of the topographical control.

522 Many studies (e.g., Boronina et al., 2005; Kazemi et al., 2006) have  
523 demonstrated that groundwater flows in the direction in which it gets older. In view  
524 of this point, groundwaters in the PCSX region should flow from the NPCSX area to  
525 the SPCSX area, in opposition to the S-N topographical gradient between the Otindag  
526 and Dali regions. Thus groundwater in the Dali are not the source of groundwater in  
527 the Otindag. The similar isotopic signals between groundwaters in the two regions  
528 indicate that these waters might be recharged from a common source in other place.  
529

#### 530 **4. 5. Remote-Wwater sourcesrecharge from remote areas foren groundwater in the** 531 **Otindag: mountains waters**

532 The discussions above revealed that both the groundwaters in the Otindag and  
533 DaliBasin might be recharged from a common source derived from another place.  
534 Considering the third hypothesis abovementioned that “remote/mountains waters  
535 emanate under colder and wetter conditions”, we propose that this “common source”  
536 of the two regions are from mountians areas surrounding the Otindag and Dali Basin.

537 There are two large permanent rivers and lots of small intermittent streams  
538 entering the Dali Basin (Xiao et al., 2008), including the Xilamulun River to the south  
539 and the Gongger River to the north, both of which are stemming from the Greater  
540 Khingan Mountains (Daxing’Anling Mountains in Chinese pinyin, 1,100-1,400 m above  
541 seal level) (Fig. 1). The Xilamulun River carries a large amount of water (about  
542  $6.58 \times 10^8 \text{ m}^3/\text{y}$ ) from the Daxing’Anling Mountains flowing through the east margins  
543 of the Dali and Otindag (Wu et al., 2014). This is an important clue linking natural  
544 waters between the Otindag and Dali Basin.

545 Variation in the elevation from the Dali Lake to the riverhead of the Xilamulun  
546 River can be clearly found along a land surface topographical section (Fig. 11). The  
547 channel of the Xilamulun River is located in the Xar Moron Fault (Fig. 1), which is a  
548 part of the Solonker Suture Zone (Eizenhöfer et al., 2014) or the  
549 Xilamulun-Changchun-Yanji plate suture zone (Sun et al., 2004) in the regional  
550 tectonical settings (Fig. 2). Outcrop observations indicate that fault zones commonly  
551 have a permeability structure suggesting they should act as complex conduit–barrier  
552 systems in which along-fault flow is encouraged and across-fault flow is impeded  
553 (Bense et al., 2013). Thus the hydraulic grediant of groundwater flow in the Eastern  
554 margins of the Otindag and Dali Basin must be controlled by the fault zone  
555 hydrogeology. This may be the reason why the hydraulic gradient of groundwater  
556 represented by the isotopic and hydrogeochemical gradients of groundwater samples  
557 in this study is not consistent with the local topographical gradient in the Otindag  
558 Desert. On the other hand, the regional aquifer is generally unconfined in dune fields  
559 of the Otindag Desert but semi-confined to confined in the Daxing’Anling uplands (Fig.  
560 3), thus the thick unconsolidated aquifers in the study area (Figs. 3 and 11) will be  
561 favourable conditions for groundwater storage and transportation along the Solonker

562 Suture Zone. When rivers stem from the Daxing'Anling Mountains and flow  
563 downward to the marginal areas of the Dali and Otindag, leakage water from these  
564 rivers can recharge the desert land through thick unconsolidated aquifers. A strong  
565 isotopic evidence is that the lake and river waters in the Dali Basin share the same  
566 evaporation line (EL2) with the groundwaters in the PCSX area.

567 Although groundwaters in the SPCSX area are different from those in the NPCSX  
568 area, their isotopic data points still fell onto the EL2 (Fig. 9), which further indicates  
569 that the groundwaters in the SPCSX are a mixture of waters from the Daxing'Anling  
570 Mountain and other sources. Another source for groundwater recharge in the SPCSX  
571 could be represented by remote water such as flash floods coming from the north  
572 Yinshan Mountains, because it can be clearly observed from digital maps that many  
573 transient rivers or streams originated from the Yinshan Mountains flow into the  
574 south and southeastern Otindag (Fig. 1). Supportive evidence for this idea can also  
575 be observed in the summer rainy season. During rainy days or under storm  
576 conditions, fast-flowing floods caused by occasional short, heavy rainstorms can form  
577 in playas, wadi channels and low-lying depressions in the unconfined to  
578 semi-confined areas of the Yinshan Mountains' piedmont. These waters may  
579 temporarily recharge shallow aquifers in the SPCSX area.

#### 581 4. 6. Speciation modeling and hydrogeological conceptual model

582 Speciation modeling. Selected results of speciation modeling are provided in  
583 Table 6. All samples are undersaturated with respect to calcite, aragonite, dolomite,  
584 halite and gypsum. The values of log  $P_{CO_2}$ , ranging between -4.77 and -1.45 in the  
585 samples from the sedimentary sandy aquifer, indicating that groundwater in the  
586 study area is not at equilibrium with atmospheric  $P_{CO_2}$ .

587 Based on the above analyses, a conceptual model of groundwater recharge was  
588 suggested to facilitate understanding of the hydrogeological conditions in the study  
589 area. Local and regional modern precipitation is a negligible source. Quaternary  
590 unconsolidated sediments with large exposed area form the main aquifer in the  
591 study area. Groundwater is recharged by cold water from remote mountain areas,  
592 and it flows from east to west along the Solonker Suture Zone. Evaporation is a minor  
593 process during groundwater hydrogeochemical evolution. Mineral dissolution may  
594 contribute to groundwater salinization, because saturation indices of all minerals are  
595 less than zero, indicating that these minerals still can dissolve into groundwater.  
596 These clues mean that the origin of groundwater in the desert is mainly controlled by  
597 geological structures and processes. The tectonic settings are more important than  
598 climatic and topographical settings to explain the origin of groundwater in the  
599 desert.

600 In a view of orogenic belt of the global middle-latitude regions, various  
601 groundwater and hydrogeological case studies have established a link between  
602 geological perspectives and origin of groundwater flows. Tague and Grant (2004)  
603 identify, for instance, the dominant control of a young volcanic geological unit on the  
604 groundwater regime of the studied region in Oregon, this geological formation  
605 having an exceptionally high permeability. Pfister et al. (2017) show that bedrock  
606 permeability significantly influences the ratio between average summer and winter  
607 run-off of 16 investigated catchments in Luxembourg. For a selection of Swiss  
608 catchments, Naef et al. (2015) associate lower groundwater flow with slowly draining

带格式的：字体：加粗

带格式的：缩进：首行缩进： 0 字符

带格式的：字体：加粗

带格式的：图案：清除

带格式的：下标

带格式的：图案：15%（自动设置前景，白色背景）

带格式的: 图案: 清除

带格式的: 图案: 清除

609 porous bedrock and low streamflow during dry periods for catchments dominated by  
610 Moraine deposits. Kaser and Hunkeler (2016) have shown that alluvial aquifers, even  
611 if they represent only a small portion of the catchment surface, can contribute  
612 significantly to the catchment groundwater outflow especially during low-flow  
613 periods. Alluvial aquifers can thus also be relevant for total catchment groundwater  
614 storage. Chen and Wang (2009) proposed that earthquake is a possible mechanism  
615 for groundwater releasing in the Qilian Mountains and discharging it in the Hexi  
616 Corridor. Carlier et al. (2018) statistically analyzed 22 catchments of the Swiss Plateau  
617 and Prealpes to establish relationships between streamflow indicators and various  
618 geological and hydrogeological properties of the bedrock and Quaternary deposits,  
619 along with meteorological, soil, land use, and topographical characteristics. The study  
620 shows that the geological characteristics dominate catchment response during high  
621 and low groundwater flow conditions.

622 These studies focused the influence of base/surrounding rock, topography,  
623 recharge source and permeability on groundwater flow in orogeny area. According to  
624 the hydrologically active bedrock hypothesis (Uchida et al. 2008) the bedrock is an  
625 active reservoir that significantly contributes to baseflow (Tague and Grant 2004;  
626 Andermann et al. 2012; Welch and Allen 2012; Birkel et al. 2014). The hydraulic  
627 conductivity of the bedrock controls storage processes (Hale et al. 2016; Pfister et al.  
628 2017). Most importantly, the ratio of the hydraulic conductivity to recharge rates has  
629 been shown to be relevant for water table elevation (Gleeson and Manning 2008).  
630 Haitjema and Mitchell-Bruker (2005) propose a criterion based on the  
631 Dupuit-Forchheimer approximation combining this ratio with geometrical aquifer  
632 properties and topographical characteristics to determine whether the water table is  
633 controlled by the topography or the recharge. From the above review it can be seen  
634 that various studies have used spatially distributed, synthetic groundwater models to  
635 identify and explore how topography, recharge and/or bedrock permeability  
636 influence groundwater fluxes and flow patterns (e.g., Gleeson and Manning 2008;  
637 Welch et al. 2012; Welch and Allen 2012; Welch and Allen 2014).

638 These studies highlight the complex interplay of topography and hydrogeology  
639 on groundwater flow. They, however, mainly focus on the geology of the bedrock, no  
640 studies mentioned the important role of tectonic structure on the groundwater flow.  
641 Thus, based on this study in the Otindag Desert, we proposed a simple conceptual  
642 model of multiprocesses that constrain the mechanism of groundwater recharge in  
643 the desert, namely mountain water (M) – tectonic fault hydrology (T) – unconfined  
644 vadose zone with underlying buried fault (V) – groundwater formation and recharge  
645 (G), i.e. the MTVG mechanism. Although the model is still conceptual but not  
646 practical at present, it provides a new perspective into the origin and evolution of  
647 groundwater resources in the middle-latitude deserts of the arid Asia.

## 648 5. Conclusions

650 In the middle-latitude desert zone of northern China, many deserts such as the  
651 Otindag and Badanjilin Deserts, are unexpectedly rich in groundwater resources,  
652 although they have no surface runoff and have been under an arid or hyper-arid  
653 climate for a long period of time. How groundwaters originated and recharged in  
654 these deserts are thus key questions that are still under debate. For some earth  
655 scientists, the direct recharge is thought to be very important for groundwaters in

656 the wide desert lands of northern China, due to the lack of surface runoffs. However,  
657 groundwater availability is very much a function of the local- and regional-scale  
658 geological and climatic settings. To achieve an integrated understanding of the  
659 groundwater recharge and its controlling mechanisms is of great significance. In this  
660 study, groundwater recharge was explored using multiple environmental tracers in  
661 the Otindag Desert of northern China, a region that is under the influence of the East  
662 Asian Summer Monsoon (EASM) climate. Compared to modern summer precipitation,  
663 the groundwaters, river waters and spring waters are depleted in  $\delta D$  and  $\delta^{18}O$ . All  
664 these waters shared a same Craig line, indicating a genetic relationship on their  
665 recharge sources. The stable isotopic signals of the groundwaters is more depleted  
666 than those of the modern summer precipitation and this suggests that the  
667 groundwaters studied could only be sourced from cold water different from the  
668 EASM precipitation. In general, the analyses revealed that the highland remote water  
669 resources from the Daxing'Anling and Yinshan Mountains were isotopically and  
670 geochemically traced to be a major source for the groundwater in the Otindag. It  
671 suggests that the modern indirect recharge mechanism, instead of the direct  
672 recharge and the palaeo-water recharge, is the most significant for groundwater  
673 recharge in the eastern Otindag. This study provides a new perspective into the  
674 origin and evolution of groundwater resources in the middle-latitude desert zone of  
675 northern China.

676

#### 677 **Acknowledgements**

678 This study was financially supported by the National Natural Science Foundation  
679 of China (41771014-~~and 41602196~~), ~~and~~ the National Key Research and Development  
680 Program of China (2016YFA0601900), and the National Natural Science Foundation of  
681 China (41602196). We thank the China Meteorological Data Sharing Service system  
682 for providing the weather data. Sincere thanks are also extended to Profs. Xiaoping  
683 Yang, Xunming Wang, Jule Xiao and other workmates, e.g., Ziting Liu, Hongwei Li, and  
684 DeguoZhangfor their generous help in the research work.

685

#### 686 **References:**

- 687 Andermann, C., Longuevergne, L., Bonnet, S., Crave, A., Davy, P., and Gloaguen, R.:  
688 Impact of transient groundwater storage on the discharge of Himalayan rivers.  
689 Nature Geoscience, 5, 127-132, 2012.
- 690 Bazuhair, A.S., and Wood, W.W.: Chloride mass-balance method for estimating  
691 ground water recharge in arid areas: examples from western Saudi Arabia.  
692 Journal of Hydrology, 186, 153-159, 1996.
- 693 Bense, V.F., Gleeson, T., Loveless, S.E., Bour, O., and Scibek, J.: Fault zone  
694 hydrogeology. Earth-Science Reviews, 127, 171-192, 2013.
- 695 Birkel, C., Soulsby, C., and Tetzlaff, D.: Developing a consistent process-based  
696 conceptualization of catchment functioning using measurements of internal  
697 state variables. Water Resources Research, 50, 3481-3501, 2014.
- 698 Blasch, K.W., and Bryson, J.R.: Distinguishing sources of ground water recharge by  
699 using  $\delta^2H$  and  $\delta^{18}O$ . Ground Water, 45, 294-308, 2007.
- 700 Boronina, A., Renard, P., Balderer, W., and Stichler, W.: Application of tritium in  
701 precipitation and in groundwater of the Kouris catchment (Cyprus) for  
702 description of the regional groundwater flow. Applied Geochemistry, 20,

703 | 1292-1308, 2005.

704 | [Carlier, C., Wirth, S.B., Cochand, F., Hunkeler, D., and Brunner, P.: Geology controls](#)  
705 | [streamflow dynamics. \*Journal of Hydrology\*, 566, 756–769, 2018.](#)

706 |

707 | Chebotarev, I.I.: Metamorphism of natural waters in the crust of weathering.  
708 | *Geochimica et Cosmochimica Acta*, 8, 22-32, 1955.

709 | Chen, F., Chen, J., Holmes, J., Boomer, I., Austin, P., Gates, J.B., Wang, N., Brooks, S.J.,  
710 | and Zhang, J.: Moisture changes over the last millennium in arid central Asia: a  
711 | review, synthesis and comparison with monsoon region. *Quaternary Science*  
712 | *Reviews*, 29, 1055-1068, 2010.

713 | Chen, J., Chen, X., and Wang, T.: Isotopes tracer research of wet sand layer water  
714 | sources in Alxa Desert. *Advances in Water Science*, 25, 196-206 , 2014 (in  
715 | Chinese).

716 | Chen, J., Li, L., Wang, J., Barry, D.A., Sheng, X., Gu, W., Zhao, X., and Chen, L.: Water  
717 | resources: groundwater maintains dune landscape. *Nature*, 432, 459-460, 2004.

718 | Chen, J., Liu, X., Wang, C., Rao, W., Tan, H., Dong, H., Sun, X., Wang, Y., and Su, Z.:  
719 | Isotopic constraints on the origin of groundwater in the Ordos Basin of northern  
720 | China. *Environmental Earth Sciences*, 66, 505-517, 2012a.

721 | Chen, J., Sun, X., Gu, W., Tan, H., Rao, W., Dong, H., Liu, X., and Su, Z.: Isotopic and  
722 | hydrochemical data to restrict the origin of the groundwater in the Badain Jaran  
723 | Desert, Northern China. *Geochemistry International* 50, 455-465, 2012b.

724 | [Chen, J.S., and Wang, C.Y.: Rising springs along the Silk Road. \*Geology\* 37, 243-246,](#)  
725 | [2009.](#)

726 | Chen, J., Yang, Q., and Hao, G.: Using hydrochemical and environmental isotopical  
727 | data to analyse groundwater recharge in the Hunshandake Sandy Land. *Inner*  
728 | *Mongolia Science Technology & Economy*, 17, 9-12, 2008 (in Chinese).

729 | Clark, I.D.: *Groundwater Geochemistry and Isotopes*. CRC Press, Boca Raton, 2015.

730 | Craig, H.: Isotopic Variations in Meteoric Waters. *Science*, 133, 1702-1703, 1961.

731 | Dansgaard, W.: Stable isotopes in precipitation. *Tellus*, 16, 436-468, 1964.

732 | Dogramaci, S., Skrzypek, G., Dodson, W., and Grierson, P.F.: Stable isotope and  
733 | hydrochemical evolution of groundwater in the semi-arid Hamersley Basin of  
734 | subtropical northwest Australia. *Journal of hydrology*, 475, 281-293, 2012.

735 | Doll, P., and Fiedler, K.: Global-scale modeling of groundwater recharge. *Hydrology*  
736 | *and Earth System Sciences*, 12, 863-885, 2008.

737 | Doll, P.: Vulnerability to the impact of climate change on renewable groundwater  
738 | resources: a global-scale assessment. *Environmental Research Letters*, 4, 035006,  
739 | doi:10.1088/1748-9326/4/3/035006, 2009.

740 | Drever, J.I.: Catchment mass balance. In: Saether, O.M., and de Caritat, P. (Eds.),  
741 | *Geochemical Processes, Weathering and Groundwater Recharge in Catchments*.  
742 | A.A, Balkema, Rotterdam, pp. 241-261, 1997.

743 | Edmunds, W.M., Ma, J., Aeschbach-Hertig, W., Kipfer, R., and Darbyshire, D.P.F.:  
744 | Groundwater recharge history and hydrogeochemical evolution in the Minqin  
745 | Basin, North West China. *Applied Geochemistry*, 21, 2148-2170, 2006.

746 | Eizenhöfer, P.R., Zhao, G., Zhang, J., and Sun, M.: Final closure of the Paleo-Asian  
747 | Ocean along the Solonker Suture Zone: Constraints from geochronological and  
748 | geochemical data of Permian volcanic and sedimentary rocks. *Tectonics*, 33,  
749 | 441-463, 2014.

750 Freeze, R.A., and Cherry, J.A.: Groundwater. Prentice-Hall, Inc, New Jersey, 1979.

751 Gat, J.R.: Precipitation, groundwater and surface waters: control of climate  
752 parameters on their isotopic composition and their utilization as  
753 palaeoclimatological tools. In: Palaeoclimates and palaeowaters: a collection of  
754 environmental isotope studies. Proc. Adv. Gp. Meeting, Vienna, 25–28 Nov 1980,  
755 pp 3–12, IAEA, Vienna, 1983.

756 Gat, J.R., and Issar, A.: Desert isotope hydrology: water sources of the Sinai Desert.  
757 Geochimica et & Cosmochimica Acta, 38, 1117-1131, 1974.

758 Gates, J., Edmunds, W.M., Ma, J., and Scanlon, B.: Estimating groundwater recharge  
759 in a cold desert environment in northern China using chloride. Hydrogeology  
760 Journal, 16, 893-910, 2008.

761 Giordano, M.: Global groundwater? Issues and solutions. Annual Review of  
762 Environment and Resources, 34, 153-178, 2009.

763 [Gleeson, T., and Manning, A.H.: Regional groundwater flow in mountainous terrain:  
764 Three-dimensional simulations of topographic and hydrogeologic controls.  
765 Water Resources Research, 44, 1-16, 2008.](#)

766 Guendouz, A., Moulla, A.S., Edmunds, W.M., Zouari, K., Shand, P., and Mamou, A.:  
767 Hydrogeochemical and isotopic evolution of water in the Complexe Terminal  
768 aquifer in the Algerian Sahara. Hydrogeology Journal, 11, 483-495, 2003.

769 [Haitjema, H.M., and Mitchell-Bruker, S.: Are water tables a subdued replica of the  
770 topography? Ground Water, 43, 781-786, 2005.](#)

771 [Hale, V.C., McDonnell, J.J., Stewart, M.K., Solomon, D.K., Doolittle, J., Ice, G.G., and  
772 Pack, R.T.: Effect of bedrock permeability on stream base flow mean transit time  
773 scaling relationships: 2. Process study of storage and release. Water Resources  
774 Research, 52, 1375-1397, 2016.](#)

775 Healy, R.W.: Estimating groundwater recharge. Cambridge University Press, New York,  
776 2010.

777 Herczeg, A.L., and Leaney, F.: Review: environmental tracers in arid-zone hydrology.  
778 Hydrogeology Journal, 19, 17-29, 2011.

779 Jahn, B.M.: The Central Asian Orogenic Belt and growth of the continental crust in  
780 the Phanerozoic. Geological Society London Special Publications, 226, 73-100,  
781 2004.

782 Jian, P., Liu, D., Kroner, A., Windley, B.F., Shi, Y., Zhang, W., Zhang, F., Miao, L., Zhang,  
783 L., and Tomurhuu, D.: Evolution of a Permian intraoceanic arc-trench system in  
784 the Solonker suture zone, Central Asian Orogenic Belt, China and Mongolia.  
785 Lithos, 118, 169-190, 2010.

786 Jin, K., Rao, W., Tan, H., Song, Y., Yong, B., Zheng, Y., Chen, T., and Han, L.: H-O isotopic  
787 and chemical characteristics of a precipitation-lake water-groundwater system  
788 in a desert area. Journal of Hydrology, 559, 848-860, 2018.

789 Jobbágy, E., Noretto, M., Villagra, P., and Jackson, R.: Water subsidies from mountains  
790 to deserts: their role in sustaining groundwater-fed oases in a sandy landscape.  
791 Ecological Applications, 21, 678-694, 2011.

792 [Kaser, D., and Hunkeler, D.: Contribution of alluvial groundwater to the outflow of  
793 mountainous catchments. Water Resources Research, 52, 680-697, 2016.](#)

794 Kazemi, G.A., Lehr, J.H., and Perrochet, P.: Groundwater age. John Wiley & Sons,  
795 Hoboken, 2006.

796 Li, J.: Permian geodynamic settings of Notheast China and adjacent regions: closure

797 of the Paleo-Asian Ocean and subduction of the Paleo-Pacific Plate. *Journal of*  
798 *Asian Earth Sciences*, 26, 207-224.

799 Li, S., Sun, W., Li, X., and Zhang, B.: Sedimentary characteristics and environmental  
800 evolution of Otindag sandy land in Holocene. *Journal of Desert Research*, 15,  
801 323-331, 1995 (in Chinese).

802 Liu, Z., and Yang, X.: Geochemical-geomorphological evidence for the provenance of  
803 aeolian sands and sedimentary environments in the Hunshandake Sandy Land,  
804 eastern Inner Mongolia, China. *Acta Geologica Sinica (English Edition)*, 87,  
805 871-884, 2013.

806 Love, A.J., Herczeg, A.L., Leaney, F.W., Stadter, M.H., Dighton, J.C., and Armstrong, D.:  
807 Groundwater residence time and palaeohydrology in the Otway Basin, South  
808 Australia. *Journal of Hydrology*, 153, 157–187, 1994.

809 Love, A.J., Herczeg, A.L., Sampson, L., Cresswell, R.G., and Fifield, L.K.: Sources of  
810 chloride and implications for <sup>36</sup>Cl dating of old groundwater, south-western  
811 Great Artesian basin, Australia. *Water Resources Research*, 36(6), 1561-1574,  
812 2000.

813 Ma, J., Ding, Z., Gates, J.B., and Su, Y.: Chloride and the environmental isotopes as the  
814 indicators of the groundwater recharge in the Gobi Desert, northwest China.  
815 *Environmental Geology*, 55, 1407-1419, 2008.

816 Ma, J., and Edmunds, W.M.: Groundwater and lake evolution in the BadainJaran  
817 Desert ecosystem, Inner Mongolia. *Hydrogeology Journal*, 14, 1231-1243, 2006.

818 Ma, J., Pan, F., Chen, L., Edmunds, W.M., Ding, Z., He, J., Zhou, K., and Huang, T.:  
819 Isotopic and geochemical evidence of recharge sources and water quality in the  
820 Quaternary aquifer beneath Jinchang city, NW China. *Applied Geochemistry*, 25,  
821 996-1007, 2010.

822 Merlivat, L., and Jouzel, J.: Global climatic interpretation of the deuterium-oxygen 18  
823 relationship for precipitation. *Journal of Geophysical Research*, 84, 5029-5033,  
824 1979.

825 Meybeck, M.: Global occurrence of major elements in rivers. In: Drever, J.I. (Ed.),  
826 *Surface and Ground Water, Weathering, and Soils*. Holland, H.D., and Turekian,  
827 K.K. (Exec.Eds), *Treatise on Geochemistry*, vol. 5. Elsevier-Pergamon, Oxford, pp.  
828 207-223, 2004.

829 [Naef, F., Margreth, M., and Florianic, M.: Festlegung von Restwassermengen: Q347,](#)  
830 [eine entscheidende, aber schwer zu fassende Größe. \*Wasser Energie Luft, Heft\*](#)  
831 [4\(107. Jahrgang\), 277–284, 2015.](#)

832 Petrides, B., Cartwright, I., and Weaver, T.R.: The evolution of groundwater in the  
833 Tyrrell catchment, south-central Murray Basin, Victoria, Australia. *Hydrogeology*  
834 *Journal*, 14, 1522-1543, 2006.

835 [Pfister, L., Martinez-Carreras, N., Hissler, C., Klaus, J., Carrer, G.E., Stewart, M.K., and](#)  
836 [McDonnell, J.J.: Bedrock geology controls on catchment storage, mixing, and](#)  
837 [release: A comparative analysis of 16 nested catchments. \*Hydrological Processes\*,](#)  
838 [31, 1828-1845, 2017.](#)

839 Rizk, Z.S., and El-Etr, H.A.: Hydrogeology and hydrogeochemistry of some springs in  
840 the United Arab Emirates. *Arabian Journal for Science and Engineering*, 22,  
841 95-111, 1997.

842 Scanlon, B.R., Keese, K.E., Flint, A.L., Flint, L.E., Gaye, C.B., Edmunds, W.M., and  
843 Simmers, I.: Global synthesis of groundwater recharge in semiarid and arid

844 regions. *Hydrological Processes*, 20, 3335-3370, 2006.

845 Seiler, K.P., and Gat, J.R.: Groundwater Recharge From Run-Off, Infiltration and  
846 Percolation. Springer, The Netherlands, 2007.

847 Stolp, B.J., Solomon, D.K., Suckow, A., Vitvar, T., Rank, D., Aggarwal, P.K., and Han, L.F.:  
848 Age dating base flow at springs and gaining streams using helium-3 and tritium:  
849 Fischa-Dagnitz system, southern Vienna Basin, Austria. *Water Resources*  
850 *Research*, 46, W07503, doi:10.1029/2009WR008006, 2010.

851 Sultan, M., Sturchio, N., Gheith, H., Hady, Y.A., and Anbeawy, M.: Chemical and  
852 Isotopic Constraints on the Origin of Wadi EliTarfa Ground Water, Eastern Desert,  
853 Egypt. *Ground Water*, 38, 743-751, 2000.

854 Sun, D., Wu, F., Zhang, Y., and Gao, S.: The final closing time of the west Lamulun  
855 River-Changchun-Yanji plate suture zone-Evidence from the Dayushan granitic  
856 pluton, Jilin Province. *Journal of Jilin University (Earth Science Edition)*, 34,  
857 174-181, 2004 (in Chinese).

858 Sun, J., Ye, J., Wu, W., Ni, X., Bi, S., Zhang, Z., Liu, W., and Meng, J.: Late  
859 Oligocene-Miocene mid-latitude aridification and wind patterns in the Asian  
860 interior. *Geology*, 38, 515-518, 2010.

861 [Tague, C., and Grant G.E.: A geological framework for interpreting the low-flow](#)  
862 [regimes of Cascade streams, Willamette River basin, Oregon. \*Water Resources\*](#)  
863 [\*Research\*, 40\(4\), 1-9, 2004.](#)

864 Tian, F., Wang, Y., Liu, J., Tang, W., and Jiang, N.: Late Holocene climate change  
865 inferred from a lacustrine sedimentary sequence in southern Inner Mongolia,  
866 China. *Quaternary International*, 452, 22-32, 2017.

867 [Uchida, T., Miyata, S., and Asano Y.: Effects of the lateral and vertical expansion of the](#)  
868 [water flowpath in bedrock on temporal changes in hillslope discharge.](#)  
869 [\*Geophysical Research Letters\*, 35, 2-6, 2008.](#)

870

871 Wang, P., Yu, J., Zhang, Y., and Liu, C.: Groundwater recharge and hydrogeochemical  
872 evolution in the Ejina Basin, northwest China. *Journal of Hydrology*, 476, 72-86,  
873 2013.

874 Wang, Q., and Liu, X.Y.: Paleoplate tectonics between Cathaysia and Angaraland in  
875 Inner Mongolia of China. *Tectonics*, 5, 1073-1088, 1986.

876 Wang, W., and Feng, Z.D.: Holocene moisture evolution across the Mongolian Plateau  
877 and its surrounding areas: a synthesis of climatic records. *Earth-Science Reviews*,  
878 122, 38-57, 2013.

879 [Welch, L.A., and Allen, D.M.: Consistency of groundwater flow patterns in](#)  
880 [mountainous topography: Implications for valley bottom water replenishment](#)  
881 [and for defining groundwater flow boundaries. \*Water Resources Research\*, 48,](#)  
882 [1-17, 2012.](#)

883 [Welch, L.A.A., Allen, D.M.M., and van Meerveld, H.J.: Topographic controls on deep](#)  
884 [groundwater contributions to mountain headwater streams and sensitivity to](#)  
885 [available recharge. \*Canadian Water Resources Journal\*, 37, 349-371, 2012.](#)

886 [Welch, L.A., and Allen, D.M.: Hydraulic conductivity characteristics in mountains and](#)  
887 [implications for conceptualizing bedrock groundwater flow. \*Hydrogeology\*](#)  
888 [\*Journal\*, 22, 1003-1026, 2014.](#)

889 Wu, J., An, N., Ji, Y., and Wei, X.: Analysis on Characteristics of Precipitation and  
890 Runoff in Silas MuLun River Basin. *Meteorology Journal of Inner Mongolia*,

- 891 23-25, 2014 (in Chinese).
- 892 Xiao, J., Si, B., Zhai, D., Itoh, S., and Lomtadze, Z.: Hydrology of Dali Lake in  
893 central-eastern Inner Mongolia and Holocene East Asian monsoon variability.  
894 *Journal of Paleolimnology*, 40, 519-528, 2008.
- 895 Yang, X., Li, H., and Conacher, A.: Large-scale controls on the development of sand  
896 seas in northern China. *Quaternary International*, 250, 74-83, 2012.
- 897 Yang, X., Ma, N., Dong, J., Zhu, B., Xu, B., Ma, Z., and Liu, J.: Recharge to the  
898 inter-dune lakes and Holocene climatic changes in the BadainJaran Desert,  
899 western China. *Quaternary Research*, 73, 10-19, 2010.
- 900 Yang, X., Scuderi, L.A., Wang, X., Scuderi, L.J., Zhang, D., Li, H., Forman, S., Xu, Q.,  
901 Wang, R., Huang, W., and Yang, S.: Groundwater sapping as the cause of  
902 irreversible desertification of Hunshandake Sandy Lands, Inner Mongolia,  
903 northern China. *PNAS*, 112, 702-706, 2015.
- 904 Yang, X., Wang, X., Liu, Z., Li, H., Ren, X., Zhang, D., Ma, Z., Rioual, P., Jin, X., and  
905 Scuderi, L.: Initiation and variation of the dune fields in semi-arid China – with a  
906 special reference to the Hunshandake Sandy Land, Inner Mongolia. *Quaternary  
907 Science Reviews*, 78, 369-380, 2013.
- 908 Yang, X., and Williams, M.A.J.: The ion chemistry of lakes and late Holocene  
909 desiccation in the BadainJaran Desert, Inner Mongolia, China. *Catena*, 51, 45-60,  
910 2003.
- 911 Yang, X., Zhu, B., Wang, X., Li, C., Zhou, Z., Chen, J., Yin, J., and Lu, Y.: Late Quaternary  
912 environmental changes and organic carbon density in the Hunshandake Sandy  
913 Land, eastern Inner Mongolia, China. *Global and Planetary Change*, 61, 70-78,  
914 2008.
- 915 Yao, S., Zhu, Z., Zhang, S., Zhang, S., and Li, Y.: Using SWAT model to simulate the  
916 discharge of the river Shandianhe in Inner Mongolia. *Journal of Arid Land  
917 Resources and Environment*, 27, 175-180, 2013 (in Chinese).
- 918 Zhang, Z., Li, K., Li, J., Tang, W., Chen, Y., and Luo, Z.: Geochronology and  
919 geochemistry of the Eastern Erenhot ophiolitic complex: implications for the  
920 tectonic evolution of the Inner Mongolia-Daxinganling Orogenic Belt. *Journal of  
921 Asian Earth Sciences*, 97, 279-293, 2015.
- 922 Zhao, J., Ma, Y., Luo, X., Yue, D., Shao, T., and Dong, Z.: The discovery of surface runoff  
923 in the megadunes of BadainJaran Desert, China, and its significance. *Science  
924 China Earth Sciences*, 60, 707-719, 2017.
- 925 Zhao, L., Xiao, H., Dong, Z., Xiao, S., Zhou, M., Cheng, G., Yin, L., and Yin, Z.: Origins of  
926 groundwater inferred from isotopic patterns of the Badain Jaran Desert,  
927 Northwestern China. *Ground Water*, 50, 715-725, 2012.
- 928 Zhen, Z., Li, C., Li, W., Hu, Q., Liu, X., Liu, Z., and Yu, R.: Characteristics of  
929 environmental isotopes of surface water and groundwater and their recharge  
930 relationships in Lake Dali basin. *Journal of Lake Sciences*, 26, 916-922, 2014 (in  
931 Chinese).
- 932 Zhu, B.Q., Yu, J.J., Rioual, P., Gao, Y., Zhang, Y.C., and Xiong, H.G.: Climate effects on  
933 recharge and evolution of natural water resources in middle-latitude  
934 watersheds under arid climate. In: Ramkumar, M. U., Kumaraswamy, K, and  
935 Mohanraj, R. (Eds.), *Environmental Management of River Basin Ecosystems*.  
936 Springer Earth System Sciences, Springer-Verlag, Heidelberg, pp. 91-109, 2015.
- 937 Zhu, B.Q., Wang, X.M., and Rioual, P.: Multivariate indications between environment

938 and ground water recharge in a sedimentary drainage basin in northwestern  
939 China. *Journal of Hydrology*, 2017, 549, 92-113, 2017.

940 Zhu, G.F., Li, Z.Z., Su, Y.H., Ma, J.Z., and Zhang, Y.Y.: Hydrogeochemical and isotope  
941 evidence of groundwater evolution and recharge in Minqin Basin, Northwest  
942 China. *Journal of Hydrology*, 333, 239-251, 2007.

943 Zhu, G.F., Su, Y.H., and Feng, Q.: The hydrochemical characteristics and evolution of  
944 groundwater and surface water in the Heihe River Basin, northwest China.  
945 *Hydrogeology Journal*, 16, 167-182, 2008.

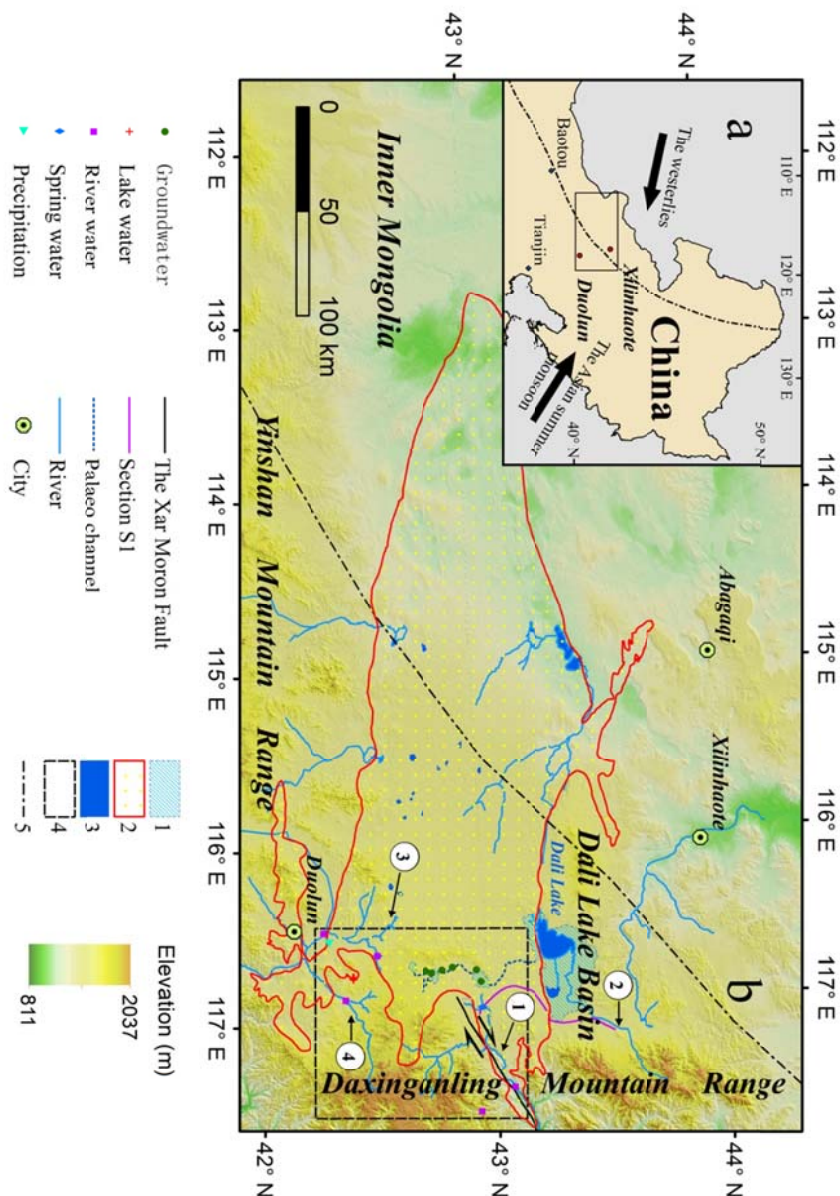
946 Zhu, Z., Wu, Z., Liu, S., and Di, X.: *An Outline of Chinese Deserts*. Science Press,  
947 Beijing, 1980 (in Chinese).

948

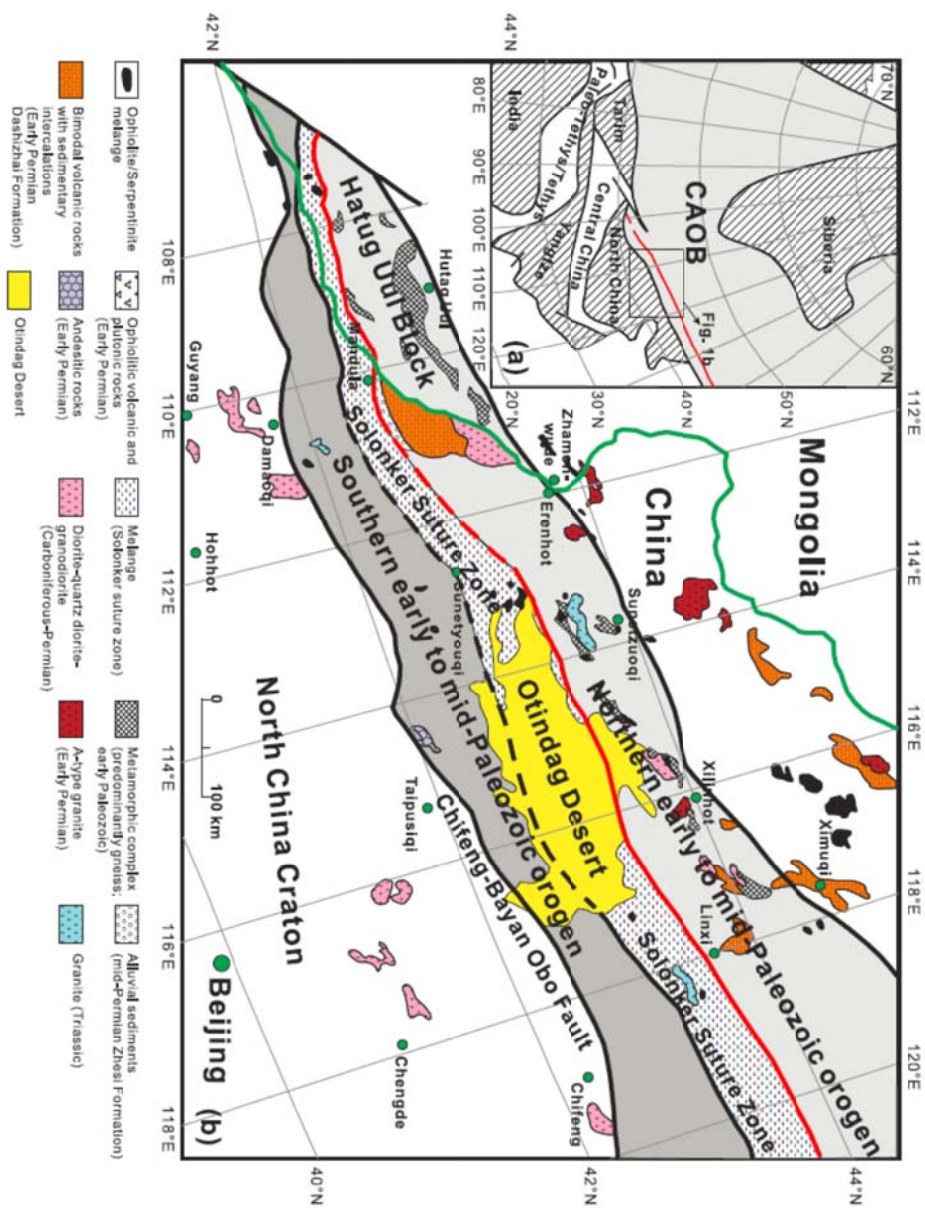
949

950 **Figure Captions:**

951 **Fig. 1.** The Geographical location of the Otindag Desert in northern China. (a) The  
952 study area shown at a large scale, and (b) the study area shown at a smaller scale,  
953 with detailed information about the boundary and tectonic settings of the desert  
954 land. 1, the palaeo lake area of the megalake Dali; 2, the boundary of the Otindag; 3,  
955 the modern lake area; 4, the boundary of Fig. 2; 5, the boundary between the  
956 westerlies and the East Asian Summer Monsoon (EASM) climate systems. ①, the  
957 Xilamulun River. ②, the Gonggeer River. ③, the Shepi River. ④, the Tuligen River.  
958 The boundary between the westerlies and the EASMin (a) and (b) is modified from  
959 Chen et al. (2010). The palaeo lake area of the megalake Dali and the palaeo channel  
960 in (b) is modified from Yang et al. (2015). The location of the Xar Moron Fault is  
961 referenced from Eizenhöfer et al. (2014). Section S1 is an elevation section starting  
962 from the upstream of the Dali Lake and ending with a spring sample (s2) in the  
963 riverhead of Xilamulun River.

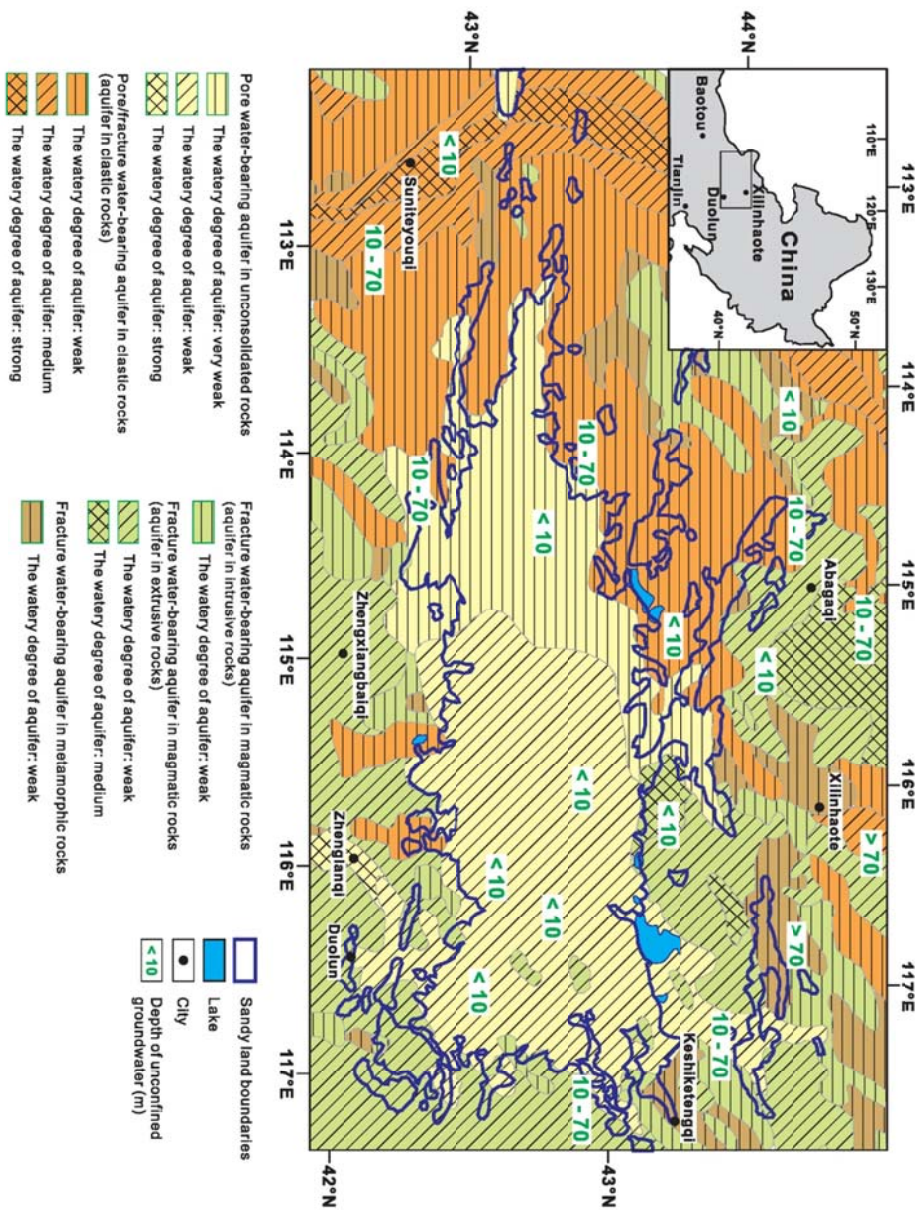


965  
 973 **Fig. 2.** (a) Tectonic framework of the north China-Mongolian segment of the Central  
 974 Asian Orogenic Belt (modified after Jahn, 2004). (b) Geological sketch map of the  
 975 northern China-Mongolia tract (modified after Jian et al., 2010). The Solonker suture  
 976 zone represents the tectonic boundary between the northern (Hutag Uul  
 977 Block-Northern orogen) and the southern (southern orogen-Northern margin of  
 978 North China craton) continental blocks. Note that the red line marks the early  
 979 Permian paleobiogeographical boundary (Wang and Liu, 1986; Li, 2006), which  
 980 coincides with the northern boundary of the suture zone.



974  
 975  
 976  
 977  
 978  
 979  
 980  
 981  
 982

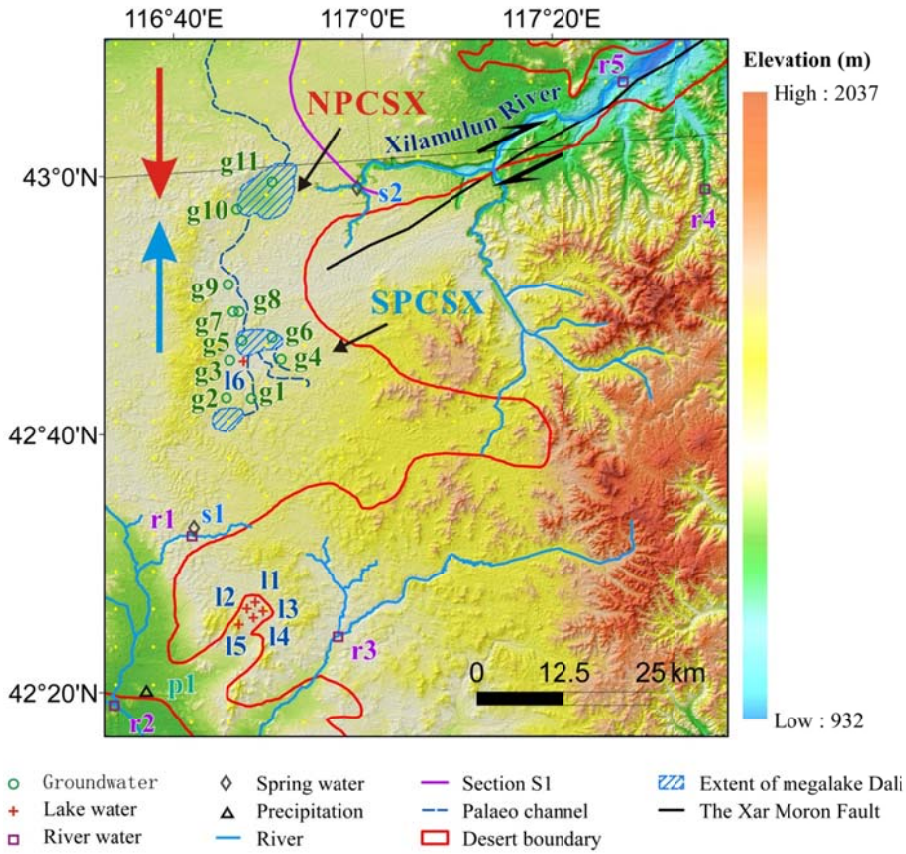
**Fig. 3.** The hydrogeological division map of the Otindag Desert.



983  
984  
985  
986  
987  
988  
989  
990  
991  
992  
993

994  
995  
996

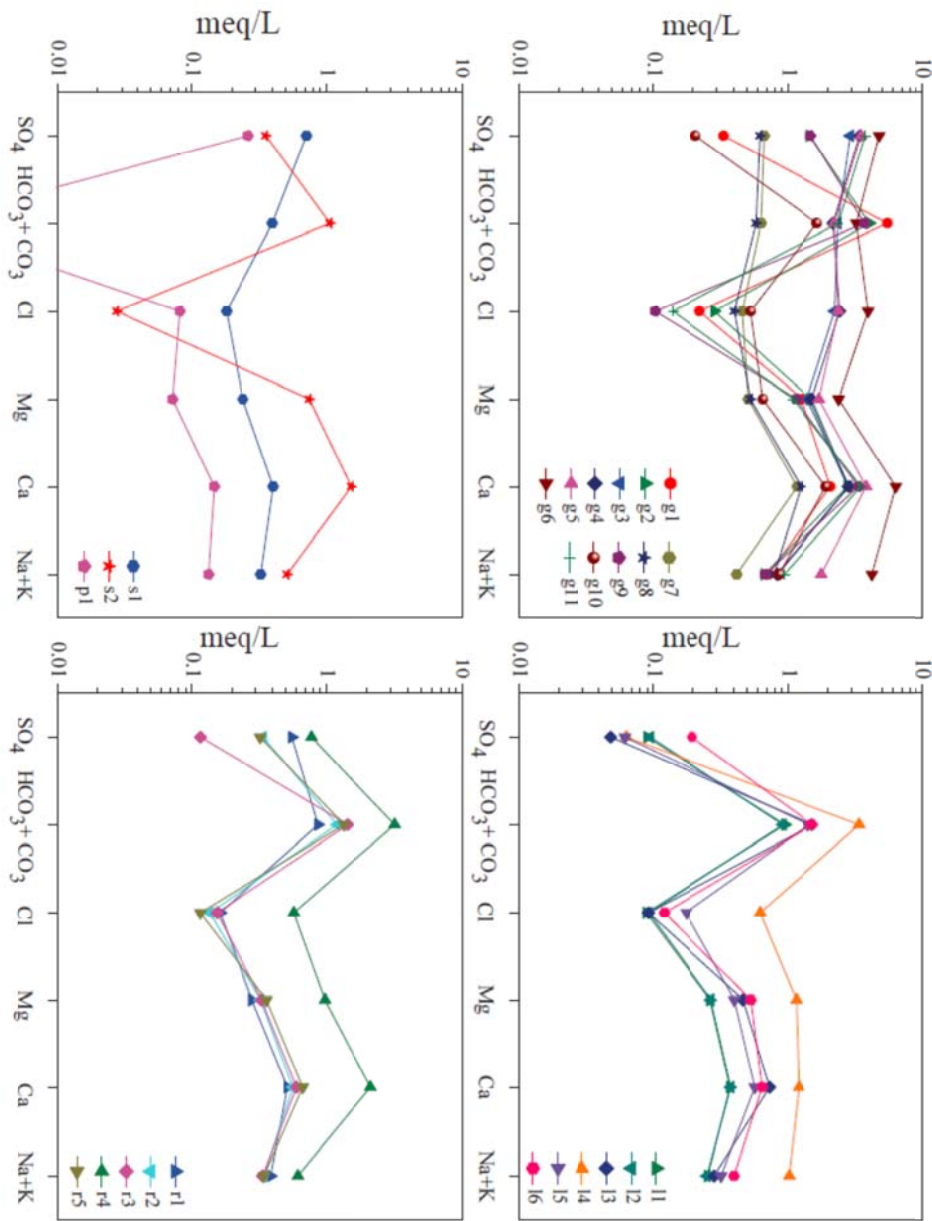
**Fig. 4.** The locations of the water sampling sites in this study.



997  
998  
999  
1000  
1001  
1002  
1003  
1004  
1005  
1006  
1007  
1008  
1009  
1010  
1011  
1012  
1013  
1014  
1015

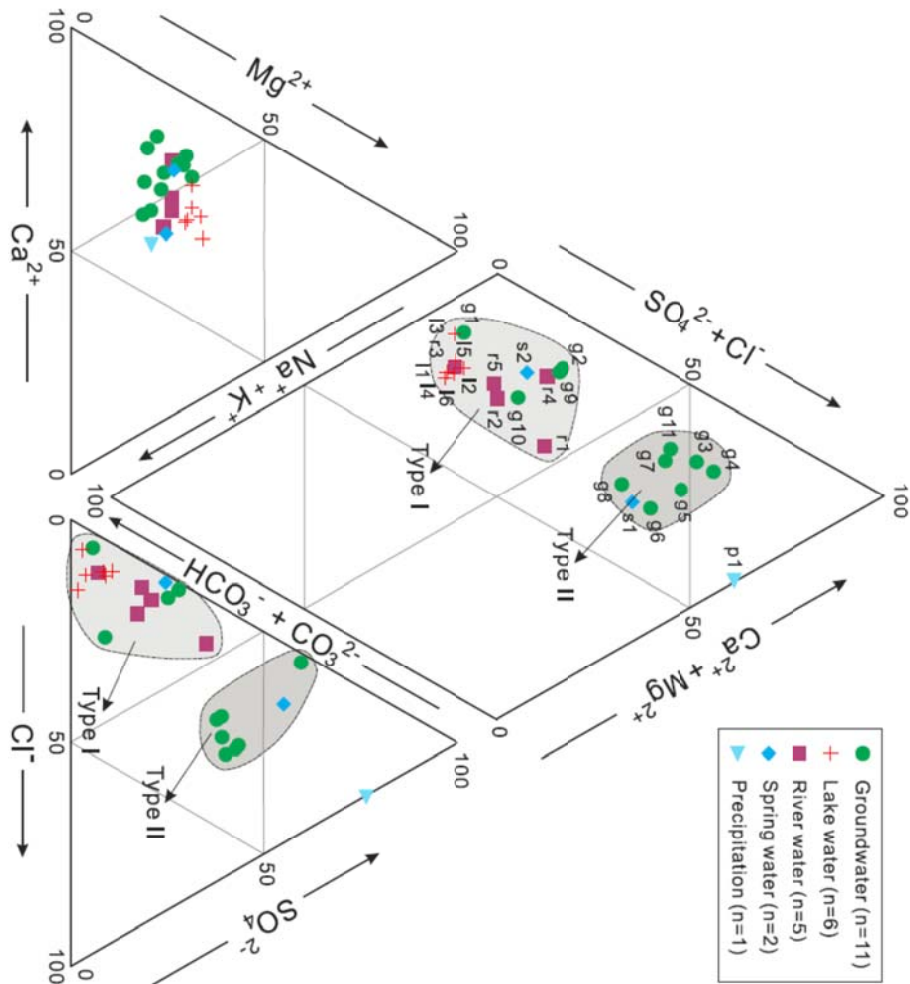
1015  
1016  
1017  
1018  
1019  
1020  
1021  
1022

1023 **Fig. 5.** The fingerprint diagram showing the variations of multiple ions'  
1024 concentrations in the studied water samples in an equivalent unit. The  $\text{HCO}_3+\text{CO}_3$   
1025 concentration in the sample p1 was not shown, due to its value being lower than the  
1026 detection limit.



1028  
 1029  
 1030  
 1031  
 1032  
 1033  
 1034  
 1035  
 1036  
 1037  
 1038

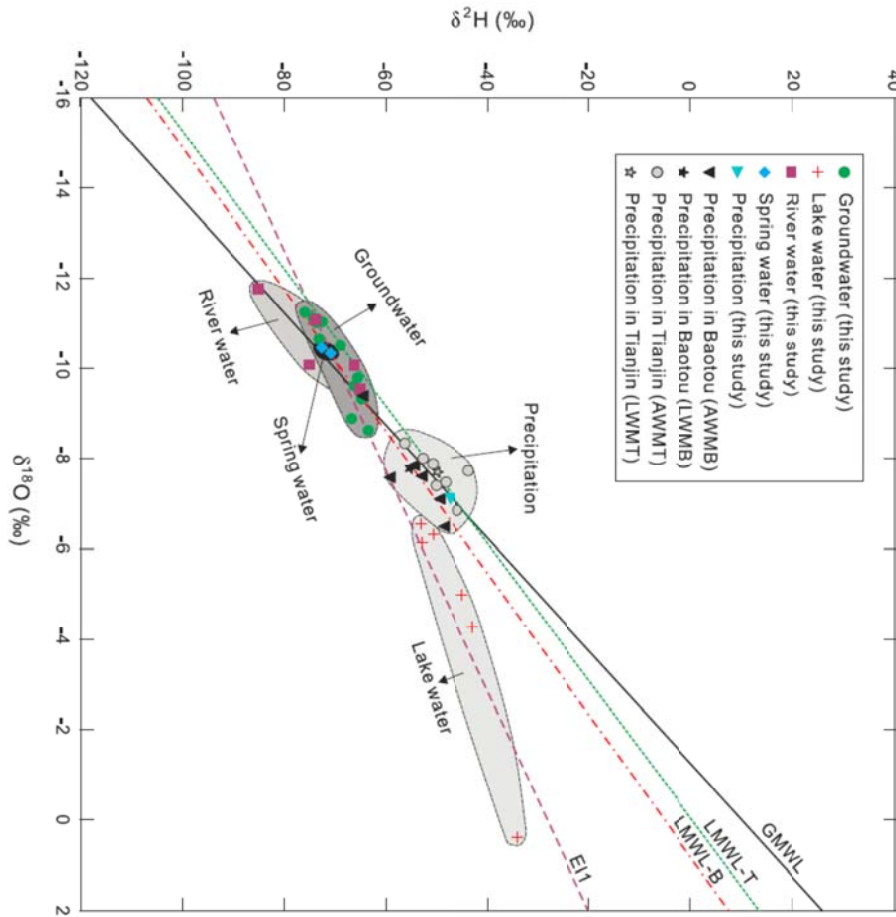
1041 **Fig. 6.** The Piper diagram showing the relative abundances of major cations and  
 1042 anions in the studied water samples. Major water types are also shown in this  
 1043 diagram.



1042  
 1043  
 1044  
 1045  
 1046  
 1047  
 1048  
 1049  
 1050  
 1051  
 1052  
 1053  
 1054  
 1055

1056  
1057  
1058  
1059  
1060  
1061

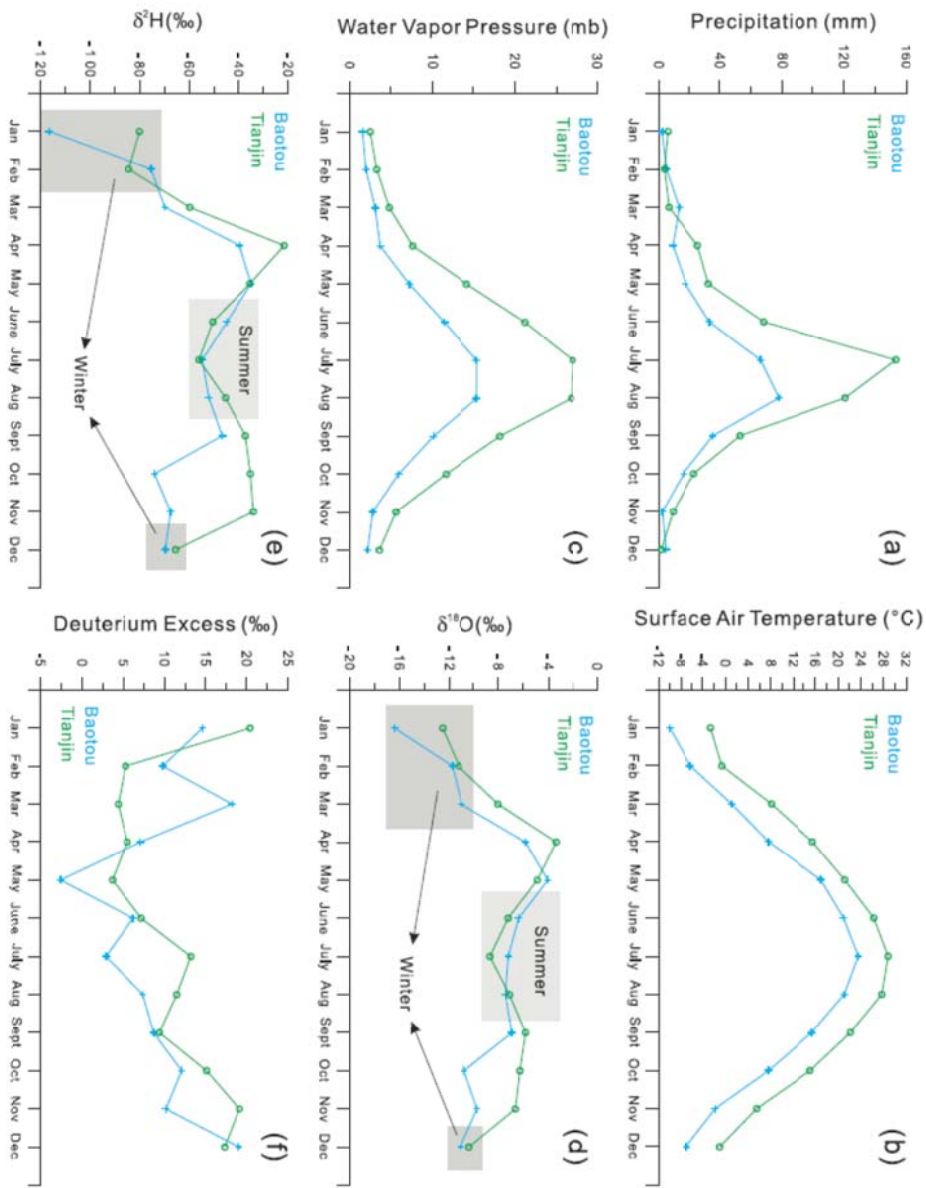
1071 **Fig. 7.** The bivariate diagram of  $\delta D$  and  $\delta^{18}O$ , i.e. the Craig diagram, for the natural  
1072 water samples in this study. Different relationships between the groundwaters, lake  
1073 waters, river waters, spring waters and the precipitation waters are illustrated.  
1074 AWMB, the annual weighted mean value at the Baotou station; AWMT, the annual  
1075 weighted mean value at the Tianjin station; LWMB, the long-term weighted means at  
1076 the Baotou station; LWMT, the long-term weighted means at the Tianjin station;  
1077 GMWL, the Global Meteoric Water Line; LMWL-B, the local meteoric water line  
1078 calculated based on the data from the Baotou station; LWML-T, the local meteoric  
1079 water line calculated based on the data from the Tianjin station; EL1, the evaporation  
1080 line calculated based on the data of water samples collected in this study.



1072  
1073  
1074

1074  
1075  
1076  
1077  
1078  
1079  
1080  
1081  
1082  
1083  
1084  
1085

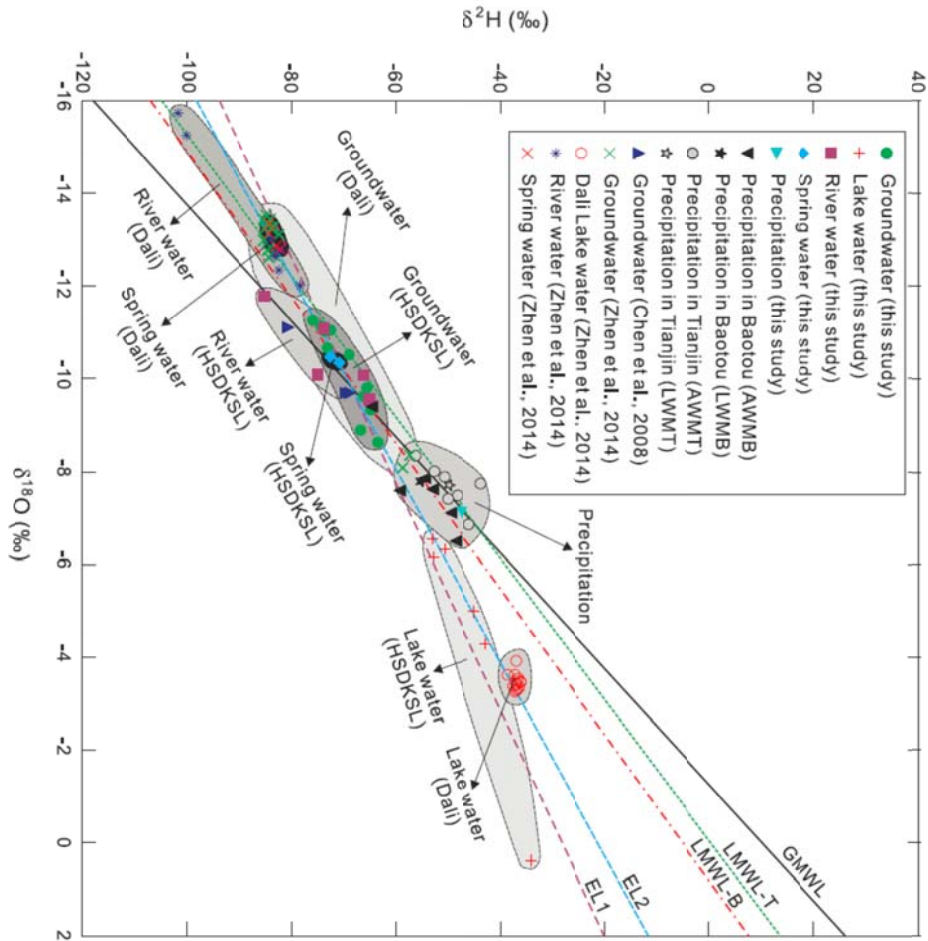
1086 **Fig. 8.** The seasonal mean distributions of (a) precipitation, (b) surface air  
1087 temperature and (c) water vapor pressure from the Baotou and Tianjin weather  
1088 stations (station sites seen in **Fig. 1a**) in the surrounding areas of the Otindag for the  
1089 period 1981-2010. The seasonal mean distributions of (d)  $\delta^{18}\text{O}$  and (e)  $\delta\text{D}$  values in  
1090 precipitation from the Baotou and Tianjin weather stations in the surrounding areas  
1091 of the Otindag for the period 1986-2001.



1093  
 1094  
 1095  
 1096  
 1097  
 1098  
 1099  
 1100  
 1101  
 1102  
 1104  
 1105

**Fig. 9.** The bivariate diagram of  $\delta\text{D}$  and  $\delta^{18}\text{O}$ , i.e. the Craig diagram, for the natural water samples collected in the Otindag (this study) and the Dali Basin. Different

1110 relationships between the groundwaters, lake waters, river waters, spring waters and  
 1111 the precipitation waters are clearly illustrated. AWMB, AWMT, LWMB, LWMT, GMWL,  
 1112 LMWL-B, LWML-T, and EL1 are the same as in Fig. 7. EL2, the evaporation line  
 1113 calculated based on the data from the groundwater, lake water, river water and  
 1114 spring water samples collected from the Otindag and Dali Basin. The data for the Dali  
 1115 were taken from Chen et al. (2008) and Zhen et al. (2014).



1111  
 1112  
 1113  
 1114  
 1115  
 1116  
 1117  
 1118  
 1119  
 1120  
 1121  
 1122  
 1123

1123

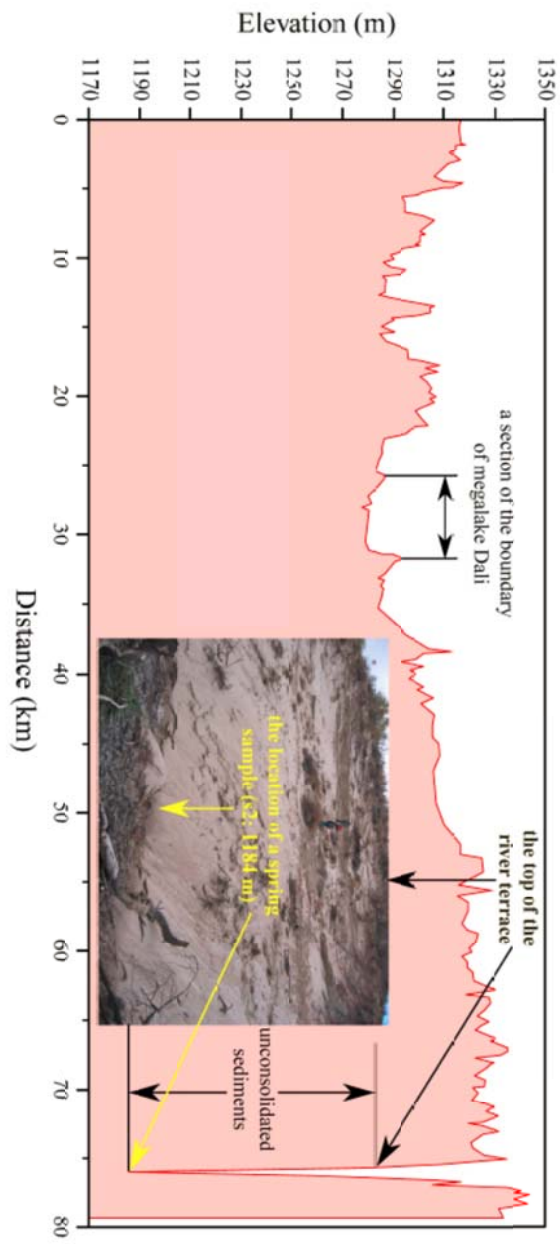
1124

1125

1126

1127 **Fig. 10.** (a) Sketch map showing the relationship between the groundwaters in the  
1128 NPCSX and SPCSX areas, based on variations of (a) the chloride concentrations, (b)  
1129 the TDS concentrations, (c) the  $\delta^{18}\text{O}$  values and (d) the  $\delta\text{D}$  values of these water  
1130 samples versus their distances away from the water sample g1 along the palaeo river  
1131 channel (PCSX) from south to north. The dashed line in (c) and (d) represents the  
1132 corresponding values of the spring water sample s2, and divides samples into the  
1133 NPCSX and SPCSX parts. (e) Variations of tritium contents vs. deuterium excess for  
1134 the groundwater samples in the study area. The sample g6 was omitted due to its  
1135 potential contamination.





1147  
1148

1148

**Table Captions:**

1149

**Table 1.**The physical parameters measured for the natural water samples in the study area.

Sample ID	Water type	Latitude (N, degree)	Longitude (E, degree)	Elevation (m a.s.l)	Depth (m)	Temperature (°C)	pH	Eh (mV)	EC (µS/cm)	TDS (mg/L)	Salinity (%)	Alkalinity (meq/L)	Hardness (°dH)
g1	Groundwater	42.736306	116.747333	1396	12	5.8	6.72	3	769	410	0.6	5.47	9.42
g2	Groundwater	42.736306	116.747333	1396	26	6.0	6.91	-10	736	393	0.5	4.07	12.0
g3	Groundwater	42.760194	116.760139	1355	32	7.7	6.88	-6	725	384	0.5	2.39	11.9
g4	Groundwater	42.759694	116.760417	1360	7	10.0	6.74	1	725	387	0.5	2.20	12.3
g5	Groundwater	42.759556	116.760556	1362	27	7.6	6.46	16	691	368	0.5	2.23	15.6
g6	Groundwater	42.760111	116.760250	1365	7	10.3	6.26	22	1240	660	0.8	3.25	24.5
g7	Groundwater	42.806361	116.747806	1352	20	6.8	6.71	2	297	158	0.2	0.63	4.70
g8	Groundwater	42.806361	116.747806	1352	16	6.5	6.92	-8	276	147	0.2	0.58	5.00
g9	Groundwater	42.850333	116.735722	1347	30	7.2	6.74	-1	487	260	0.4	3.73	12.7
g10	Groundwater	42.949861	116.759194	1321	37	9.9	6.75	-2	337	179	0.2	1.66	7.23
g11	Groundwater	42.967111	116.827528	1317	60	8.6	6.99	-14	571	302	0.4	2.40	12.9
l1	Lake water	42.424611	116.769194	1368	/	16.9	9.44	-151	126	67	0.1	0.95	1.79

l2	Lake water	42.424611	116.769194	1368	/	19.6	9.18	-137	132	70	0.1	0.92	1.82
l3	Lake water	42.424611	116.757806	1365	/	20.2	7.38	-36	196	105	0.1	1.53	3.36
l4	Lake water	42.427083	116.757639	1366	/	20.5	7.87	-64	448	238	0.2	3.42	6.61
l5	Lake water	42.421806	116.756917	1360	/	20.1	8.23	-83	173	92	0.1	1.43	2.73
l6	Lake water	42.736389	116.747222	1374	/	10.7	8.35	-89	194	103	0.1	1.53	3.30
r1	River water	42.530917	116.641250	1355	/	20.6	7.31	-33	180	96	0.1	0.88	2.23
r2	River water	42.310883	116.494817	1231	/	14.9	7.67	-52	178	95	0.1	1.21	2.50
r3	River water	42.385778	116.886194	1362	/	9.5	7.62	-48	177	94	0.1	1.45	2.62
r4	River water	42.931417	117.585306	1217	/	10.5	7.97	-69	474	252	0.3	3.22	8.73
r5	River water	43.079083	117.457389	1006	/	12.9	7.87	-62	191	101	0.1	1.37	2.88
s1	Spring water	42.530917	116.641250	1359	/	20.9	6.63	5	165	88	0.1	0.40	1.81
s2	Spring water	42.965417	116.975361	1184	/	19.0	7.47	-46	371	195	0.2	1.07	6.40
p1	Precipitation	42.330750	116.551694	1260	/	20.2	4.61	109	78	42	0.0	/	0.61

1150

1151 **Table 2.** The concentrations of major cations and anions measured for the water samples in the study area.

Sample	F <sup>-</sup> (mg/L)	Cl <sup>-</sup> (mg/L)	NO <sub>2</sub> <sup>-</sup> (mg/L)	NO <sub>3</sub> <sup>-</sup> (mg/L)	SO <sub>4</sub> <sup>2-</sup> (mg/L)	CO <sub>3</sub> <sup>2-</sup> (mg/L)	HCO <sub>3</sub> <sup>-</sup> (mg/L)	Li <sup>+</sup> (mg/L)	Na <sup>+</sup> (mg/L)	NH <sub>4</sub> <sup>+</sup> (mg/L)	K <sup>+</sup> (mg/L)	Mg <sup>2+</sup> (mg/L)	Ca <sup>2+</sup> (mg/L)
g1	0.13	7.90	2.32	0.48	16.1	0.00	335	0.02	13.8	10.5	4.59	15.5	41.8
g2	0.21	10.2	0.00	6.15	70.6	0.10	248	0.02	13.4	6.56	3.45	17.9	56.0
g3	0.11	79.6	0.00	0.00	141	0.00	145	0.01	17.9	2.28	1.76	17.1	57.3
g4	0.10	86.9	0.00	5.73	165	0.00	134	0.02	18.0	0.00	2.02	18.5	57.3
g5	0.07	84.8	0.00	0.76	169	0.00	136	0.00	39.7	1.02	2.72	20.9	76.9
g6	0.07	141	0.00	111	229	0.00	198	0.00	79.8	0.00	29.47	29.3	126.7
g7	0.37	16.3	0.00	306	32.0	0.00	38.7	0.06	7.83	0.00	3.09	6.21	23.4
g8	0.29	14.3	0.00	35.5	29.9	0.00	35.5	0.02	16.2	0.11	3.38	6.44	25.1
g9	0.10	3.66	0.15	1.19	71.6	0.00	227	0.06	12.9	0.55	4.50	14.1	67.5
g10	0.24	18.8	0.00	49.5	9.97	0.00	101	0.00	18.5	0.00	2.09	7.92	38.7
g11	0.28	4.94	0.00	0.00	182	0.00	146	0.05	20.4	2.59	2.06	13.3	70.6

l1	0.16	3.15	0.00	0.07	4.32	0.00	57.9	0.01	5.42	0.00	0.86	3.24	7.49
l2	0.16	3.30	0.00	1.66	4.57	0.00	55.8	0.00	5.33	0.00	0.84	3.29	7.61
l3	0.11	3.27	0.00	0.61	2.33	0.00	93.3	0.01	5.88	0.00	1.19	5.68	14.7
l4	0.17	22.1	0.00	0.39	3.04	0.10	208	0.00	9.21	0.70	24.2	14.1	24.2
l5	0.09	6.24	0.00	0.65	2.97	0.10	86.8	0.01	6.72	0.00	1.16	4.91	11.4
l6	0.18	4.29	0.00	0.80	9.34	0.10	93.0	0.01	8.41	0.00	1.36	6.47	13.0
r1	0.30	5.76	0.00	2.38	26.7	0.30	52.4	0.01	7.15	0.00	2.99	3.41	10.3
r2	0.19	4.82	0.00	0.65	16.4	0.10	73.1	0.01	6.82	0.00	1.92	3.96	11.4
r3	0.64	5.46	0.00	0.43	5.57	0.00	88.1	0.01	7.11	0.00	1.13	4.04	12.1
r4	1.08	20.4	0.00	19.3	37.3	0.50	195	0.01	13.0	0.00	1.96	11.9	42.8
r5	0.19	4.10	0.00	1.08	15.6	0.00	82.6	0.01	6.71	0.00	2.08	4.38	13.4
s1	0.16	6.44	0.00	1.95	34.3	0.00	24.3	0.02	6.56	0.00	1.62	2.92	8.10
s2	0.05	0.98	0.00	0.45	17.2	0.00	64.9	0.02	9.87	0.00	3.32	9.10	30.8
p1	0.61	2.90	0.00	9.46	12.7	0.00	0.00	0.00	2.09	2.07	1.64	0.88	2.95

1152

1153

1154

1155 **Table 3.** The analytical data of stable and radioactive isotopes measured for the water samples in this study.

Sample ID	$\delta D$ (‰)	$\sigma_{\text{‰}}$	$\delta^{18}O$ (‰)	$\sigma_{\text{‰}}$	deuterium excess (d)	Tritium ( $^3H$ ) (TU)
g1	-66.7	0.199	-8.90	0.026	4.50	/
g2	-64.8	0.291	-9.34	0.039	9.93	/
g3	-63.4	0.269	-8.64	0.008	5.66	/
g4	-66.1	0.149	-9.62	0.062	10.9	7.25
g5	-65.5	0.111	-9.80	0.027	13.0	9.98
g6	-68.9	0.287	-10.5	0.039	15.2	22.9
g7	-73.1	0.298	-10.7	0.041	12.2	/

g8	-73.7	0.220	-11.0	0.037	14.5	19.6
g9	-72.5	0.181	-11.0	0.015	15.8	24.3
g10	-74.4	0.201	-11.1	0.026	14.7	18.7
g11	-75.9	0.340	-11.3	0.015	14.2	1.86
l1	-53.1	0.229	-6.55	0.002	-0.704	/
l2	-50.7	0.304	-6.32	0.026	-0.161	/
l3	-42.9	0.239	-4.29	0.034	-8.55	/
l4	-34.2	0.243	0.381	0.040	-37.2	/
l5	-45.1	0.206	-4.99	0.009	-5.16	/
l6	-52.9	0.187	-6.15	0.049	-3.67	/
r1	-66.2	0.118	-10.1	0.015	14.4	/
r2	-65.0	0.148	-9.55	0.012	11.4	/
r3	-73.8	0.315	-11.1	0.021	14.9	/
r4	-85.2	0.244	-11.8	0.005	9.09	/
r5	-75.0	0.195	-10.1	0.003	5.69	/
s1	-70.8	0.074	-10.3	0.007	11.9	/
s2	-72.6	0.281	-10.5	0.046	11.1	/
p1	-47.4	0.374	-7.14	0.017	9.69	/

1156  
1157  
1158  
1159  
1160

**Table 4.** The statistical frequency of rainfall events being >20 mm per year during the recent 30 years from 1985 to 2014. The data come from the China Meteorological Data Sharing Service System.

Station	One time/year	Two times/year	Three times/year	Four times/year	Five times/year	Six times/year	Seven times/year	Mean times/year
Duolun	2	8	8	4	4	3	1	3.4
Xilinhaote	8	5	2	6	3	2	0	2.5

1161

1162 **Table 5.** The measured contents of tritium in the groundwater samples studied and the calculated ages of these samples.

Sample-ID	Tritium content (T.U.)	Possible ages (years)
g1	not measured	not clear
g2	not measured	not clear
g3	not measured	not clear
g4	7.25	20-40
g5	9.97	13-33
g6	22.9	0-20
g7	not measured	not clear
g8	19.6	0-20
g9	24.3	0-17
g10	18.7	0-22
g11	1.86	40-65

1163

1164 **Table 6.** Mineral saturation Index (MSI) of the water samples studied.

Sample-ID	Mineral (Formula)	Anhydrite (CaSO <sub>4</sub> )	Aragonite (CaCO <sub>3</sub> )	Calcite (CaCO <sub>3</sub> )	Dolomite (CaMg(CO <sub>3</sub> ) <sub>2</sub> )	Fluorite (CaF <sub>2</sub> )	Gypsum (CaSO <sub>4</sub> ·2H <sub>2</sub> O)	Halite (NaCl)	CH <sub>4</sub> (g) (CH <sub>4</sub> )	CO <sub>2</sub> (g) (CO <sub>2</sub> )	H <sub>2</sub> (g) (H <sub>2</sub> )	H <sub>2</sub> O(g) (H <sub>2</sub> O)	NH <sub>3</sub> (g) (NH <sub>3</sub> )	O <sub>2</sub> (g) (O <sub>2</sub> )
g1	SI	-2.76	-1.21	-1.05	-2.5	-2.69	-2.5	-8.48	-58.68	-1.5	-21.44	-2.04	-8.5	-47.28
	Log IAP	-7.1	-9.45	-9.45	-19.11	-13.56	-7.1	-6.95	-61.37	-2.71	-24.5	0	-6.32	-50
	Log KT	-4.34	-8.24	-8.4	-16.61	-10.86	-4.6	1.54	-2.69	-1.2	-3.06	2.04	2.18	-2.72
g2	SI	-2.04	-0.99	-0.83	-2.12	-2.19	-1.79	-8.39	-60.49	-1.76	-21.82	-2.04	-8.51	-46.44
	Log IAP	-6.39	-9.23	-9.23	-18.74	-13.05	-6.39	-6.86	-63.18	-2.97	-24.88	0	-6.33	-49.16
	Log KT	-4.34	-8.24	-8.4	-16.62	-10.86	-4.6	1.54	-2.69	-1.21	-3.06	2.04	2.18	-2.73
g3	SI	-1.77	-1.25	-1.09	-2.62	-2.8	-1.51	-7.38	-60.71	-1.96	-21.76	-1.99	-8.9	-45.9
	Log IAP	-6.11	-9.49	-9.49	-19.29	-13.63	-6.11	-5.84	-63.41	-3.2	-24.83	0	-6.77	-48.65
	Log KT	-4.34	-8.25	-8.4	-16.66	-10.83	-4.6	1.54	-2.71	-1.23	-3.07	1.99	2.14	-2.74

带格式的: 字体: 加粗

g4	SI	-1.72	-1.43	-1.27	-2.92	-2.94	-1.47	-7.35	-59.85	-1.88	-21.48	-1.92	-45.59	
	Log IAP	-6.06	-9.69	-9.69	-19.64	-13.73	-6.06	-5.8	-62.58	-3.15	-24.56	0	-48.35	
	Log KT	-4.34	-8.26	-8.41	-16.72	-10.8	-4.59	1.55	-2.73	-1.27	-3.08	1.92	-2.77	
g5	SI	-1.6	-1.74	-1.59	-3.66	-3.09	-1.35	-7.02	-57.1	-1.73	-20.92	-1.99	-9.68	-47.62
	Log IAP	-5.94	-9.99	-9.99	-20.32	-13.93	-5.94	-5.48	-59.81	-2.96	-23.99	0	-7.54	-50.36
	Log KT	-4.34	-8.25	-8.4	-16.66	-10.83	-4.6	1.54	-2.71	-1.23	-3.07	1.99	2.14	-2.74
g6	SI	-1.39	-1.67	-1.52	-3.54	-3.01	-1.13	-6.53	-55.63	-1.45	-20.52	-1.91	-47.4	
	Log IAP	-5.73	-9.93	-9.93	-20.27	-13.8	-5.73	-4.98	-58.36	-2.73	-23.6	0	-50.16	
	Log KT	-4.34	-8.26	-8.41	-16.73	-10.79	-4.59	1.55	-2.73	-1.27	-3.08	1.91	-2.77	
g7	SI	-2.79	-2.45	-2.29	-5.1	-2.12	-2.54	-8.44	-59.68	-2.43	-21.42	-2.01	-46.93	
	Log IAP	-7.13	-10.69	-10.69	-21.74	-12.97	-7.13	-6.91	-62.38	-3.65	-24.49	0	-49.66	
	Log KT	-4.34	-8.24	-8.4	-16.64	-10.85	-4.6	1.54	-2.7	-1.22	-3.07	2.01	-2.73	
g8	SI	-2.65	-2.11	-1.95	-4.43	-2.19	-2.4	-8.15	-61.48	-2.6	-21.84	-2.02	-10.23	-46.21
	Log IAP	-6.99	-10.35	-10.35	-21.06	-13.04	-6.99	-6.61	-64.18	-3.82	-24.9	0	-8.07	-48.94
	Log KT	-4.34	-8.24	-8.4	-16.63	-10.85	-4.6	1.54	-2.7	-1.22	-3.06	2.02	2.17	-2.73
g9	SI	-1.96	-1.14	-0.98	-2.58	-2.77	-1.7	-8.85	-59.22	-1.67	-21.48	-2	-9.68	-46.66
	Log IAP	-6.3	-9.38	-9.38	-19.23	-13.6	-6.3	-7.31	-61.92	-2.9	-24.55	0	-7.53	-49.39
	Log KT	-4.34	-8.24	-8.4	-16.65	-10.84	-4.6	1.54	-2.7	-1.23	-3.07	2	2.15	-2.74
g10	SI	-2.99	-1.63	-1.47	-3.51	-2.24	-2.73	-7.98	-60.04	-2	-21.5	-1.92	-45.59	
	Log IAP	-7.32	-9.88	-9.88	-20.23	-13.04	-7.32	-6.44	-62.77	-3.27	-24.58	0	-48.35	
	Log KT	-4.34	-8.25	-8.41	-16.72	-10.8	-4.59	1.55	-2.73	-1.27	-3.08	1.92	-2.76	
g11	SI	-1.59	-1.01	-0.86	-2.34	-1.92	-1.33	-8.54	-61.8	-2.04	-21.98	-1.96	-8.69	-45.12
	Log IAP	-5.92	-9.26	-9.26	-19.02	-12.74	-5.92	-6.99	-64.51	-3.29	-25.05	0	-6.57	-47.87
	Log KT	-4.34	-8.25	-8.41	-16.69	-10.82	-4.59	1.54	-2.72	-1.25	-3.07	1.96	2.12	-2.75
l1	SI	-3.95	0.37	0.52	0.92	-5.34	-3.7	-9.28	-85.36	-4.77	-26.88	-1.73	-32.25	
	Log IAP	-8.29	-7.92	-7.92	-15.97	-16.04	-8.29	-7.72	-88.15	-6.14	-29.99	0	-35.08	
	Log KT	-4.34	-8.29	-8.44	-16.9	-10.7	-4.58	1.56	-2.79	-1.37	-3.11	1.73	-2.83	
l2	SI	-3.9	0.18	0.33	0.58	-3.36	-3.66	-9.27	-83.39	-4.49	-26.36	-1.65	-32.33	
	Log IAP	-8.24	-8.12	-8.12	-16.38	-14.02	-8.24	-7.7	-86.2	-5.89	-29.49	0	-35.18	
	Log KT	-4.34	-8.3	-8.45	-16.96	-10.66	-4.58	1.57	-2.81	-1.4	-3.13	1.65	-2.85	
l3	SI	-3.92	-1.1	-0.95	-2.03	-3.4	-3.69	-9.24	-67.05	-2.47	-22.76	-1.64	-39.32	
	Log IAP	-8.27	-9.4	-9.4	-19	-14.06	-8.27	-7.67	-69.87	-3.88	-25.89	0	-42.18	

	<u>Log KT</u>	<u>-4.34</u>	<u>-8.31</u>	<u>-8.45</u>	<u>-16.98</u>	<u>-10.66</u>	<u>-4.58</u>	<u>1.57</u>	<u>-2.82</u>	<u>-1.41</u>	<u>-3.13</u>	<u>1.64</u>		<u>-2.86</u>
<u>l4</u>	<u>SI</u>	<u>-3.7</u>	<u>-0.07</u>	<u>0.07</u>	<u>0.2</u>	<u>-2.9</u>	<u>-3.46</u>	<u>-8.24</u>	<u>-71.14</u>	<u>-2.6</u>	<u>-23.74</u>	<u>-1.63</u>	<u>-7.72</u>	<u>-37.26</u>
	<u>Log IAP</u>	<u>-8.04</u>	<u>-8.38</u>	<u>-8.38</u>	<u>-16.78</u>	<u>-13.55</u>	<u>-8.04</u>	<u>-6.67</u>	<u>-73.96</u>	<u>-4.01</u>	<u>-26.87</u>	<u>0</u>	<u>-5.86</u>	<u>-40.11</u>
	<u>Log KT</u>	<u>-4.35</u>	<u>-8.31</u>	<u>-8.46</u>	<u>-16.98</u>	<u>-10.65</u>	<u>-4.58</u>	<u>1.57</u>	<u>-2.82</u>	<u>-1.41</u>	<u>-3.13</u>	<u>1.63</u>	<u>1.86</u>	<u>-2.86</u>
<u>l5</u>	<u>SI</u>	<u>-3.92</u>	<u>-0.36</u>	<u>-0.21</u>	<u>-0.51</u>	<u>-3.69</u>	<u>-3.68</u>	<u>-8.9</u>	<u>-74.69</u>	<u>-3.32</u>	<u>-24.46</u>	<u>-1.64</u>		<u>-35.96</u>
	<u>Log IAP</u>	<u>-8.26</u>	<u>-8.67</u>	<u>-8.67</u>	<u>-17.48</u>	<u>-14.34</u>	<u>-8.26</u>	<u>-7.33</u>	<u>-77.51</u>	<u>-4.73</u>	<u>-27.59</u>	<u>0</u>		<u>-38.81</u>
	<u>Log KT</u>	<u>-4.34</u>	<u>-8.31</u>	<u>-8.45</u>	<u>-16.97</u>	<u>-10.66</u>	<u>-4.58</u>	<u>1.57</u>	<u>-2.82</u>	<u>-1.41</u>	<u>-3.13</u>	<u>1.64</u>		<u>-2.86</u>
<u>l6</u>	<u>SI</u>	<u>-3.39</u>	<u>-0.32</u>	<u>-0.16</u>	<u>-0.49</u>	<u>-2.91</u>	<u>-3.13</u>	<u>-8.95</u>	<u>-74.42</u>	<u>-3.47</u>	<u>-24.7</u>	<u>-1.9</u>		<u>-38.88</u>
	<u>Log IAP</u>	<u>-7.72</u>	<u>-8.58</u>	<u>-8.58</u>	<u>-17.23</u>	<u>-13.7</u>	<u>-7.72</u>	<u>-7.4</u>	<u>-77.16</u>	<u>-4.74</u>	<u>-27.79</u>	<u>0</u>		<u>-41.66</u>
	<u>Log KT</u>	<u>-4.34</u>	<u>-8.26</u>	<u>-8.41</u>	<u>-16.74</u>	<u>-10.79</u>	<u>-4.59</u>	<u>1.55</u>	<u>-2.74</u>	<u>-1.28</u>	<u>-3.09</u>	<u>1.9</u>		<u>-2.77</u>
<u>r1</u>	<u>SI</u>	<u>-3.01</u>	<u>-1.57</u>	<u>-1.43</u>	<u>-3.05</u>	<u>-2.69</u>	<u>-2.77</u>	<u>-8.91</u>	<u>-66.73</u>	<u>-2.65</u>	<u>-22.62</u>	<u>-1.63</u>		<u>-39.46</u>
	<u>Log IAP</u>	<u>-7.36</u>	<u>-9.88</u>	<u>-9.88</u>	<u>-20.03</u>	<u>-13.35</u>	<u>-7.36</u>	<u>-7.34</u>	<u>-69.55</u>	<u>-4.06</u>	<u>-25.75</u>	<u>0</u>		<u>-42.32</u>
	<u>Log KT</u>	<u>-4.35</u>	<u>-8.31</u>	<u>-8.46</u>	<u>-16.99</u>	<u>-10.65</u>	<u>-4.58</u>	<u>1.57</u>	<u>-2.82</u>	<u>-1.41</u>	<u>-3.13</u>	<u>1.63</u>		<u>-2.86</u>
<u>r2</u>	<u>SI</u>	<u>-3.18</u>	<u>-1.09</u>	<u>-0.94</u>	<u>-2.14</u>	<u>-2.97</u>	<u>-2.94</u>	<u>-9</u>	<u>-69.01</u>	<u>-2.88</u>	<u>-23.34</u>	<u>-1.78</u>		<u>-40.05</u>
	<u>Log IAP</u>	<u>-7.52</u>	<u>-9.37</u>	<u>-9.37</u>	<u>-18.98</u>	<u>-13.7</u>	<u>-7.52</u>	<u>-7.44</u>	<u>-71.79</u>	<u>-4.22</u>	<u>-26.44</u>	<u>0</u>		<u>-42.86</u>
	<u>Log KT</u>	<u>-4.34</u>	<u>-8.28</u>	<u>-8.43</u>	<u>-16.85</u>	<u>-10.73</u>	<u>-4.58</u>	<u>1.56</u>	<u>-2.77</u>	<u>-1.34</u>	<u>-3.1</u>	<u>1.78</u>		<u>-2.81</u>
<u>r3</u>	<u>SI</u>	<u>-3.62</u>	<u>-1.12</u>	<u>-0.97</u>	<u>-2.3</u>	<u>-1.8</u>	<u>-3.36</u>	<u>-8.91</u>	<u>-67.72</u>	<u>-2.78</u>	<u>-23.24</u>	<u>-1.93</u>		<u>-42.26</u>
	<u>Log IAP</u>	<u>-7.95</u>	<u>-9.38</u>	<u>-9.38</u>	<u>-19.01</u>	<u>-12.61</u>	<u>-7.95</u>	<u>-7.36</u>	<u>-70.44</u>	<u>-4.04</u>	<u>-26.32</u>	<u>0</u>		<u>-45.02</u>
	<u>Log KT</u>	<u>-4.34</u>	<u>-8.25</u>	<u>-8.41</u>	<u>-16.71</u>	<u>-10.8</u>	<u>-4.59</u>	<u>1.55</u>	<u>-2.72</u>	<u>-1.26</u>	<u>-3.08</u>	<u>1.93</u>		<u>-2.76</u>
<u>r4</u>	<u>SI</u>	<u>-2.41</u>	<u>0.06</u>	<u>0.21</u>	<u>0</u>	<u>-0.93</u>	<u>-2.15</u>	<u>-8.11</u>	<u>-70.67</u>	<u>-2.78</u>	<u>-23.94</u>	<u>-1.9</u>		<u>-40.48</u>
	<u>Log IAP</u>	<u>-6.74</u>	<u>-8.2</u>	<u>-8.2</u>	<u>-16.73</u>	<u>-11.72</u>	<u>-6.75</u>	<u>-6.56</u>	<u>-73.4</u>	<u>-4.06</u>	<u>-27.02</u>	<u>0</u>		<u>-43.25</u>
	<u>Log KT</u>	<u>-4.34</u>	<u>-8.26</u>	<u>-8.41</u>	<u>-16.74</u>	<u>-10.79</u>	<u>-4.59</u>	<u>1.55</u>	<u>-2.73</u>	<u>-1.28</u>	<u>-3.08</u>	<u>1.9</u>		<u>-2.77</u>
<u>r5</u>	<u>SI</u>	<u>-3.15</u>	<u>-0.8</u>	<u>-0.65</u>	<u>-1.61</u>	<u>-2.88</u>	<u>-2.89</u>	<u>-9.07</u>	<u>-70.47</u>	<u>-3.03</u>	<u>-23.74</u>	<u>-1.84</u>		<u>-39.99</u>
	<u>Log IAP</u>	<u>-7.48</u>	<u>-9.07</u>	<u>-9.07</u>	<u>-18.4</u>	<u>-13.63</u>	<u>-7.48</u>	<u>-7.52</u>	<u>-73.23</u>	<u>-4.34</u>	<u>-26.84</u>	<u>0</u>		<u>-42.78</u>
	<u>Log KT</u>	<u>-4.33</u>	<u>-8.27</u>	<u>-8.42</u>	<u>-16.8</u>	<u>-10.75</u>	<u>-4.59</u>	<u>1.55</u>	<u>-2.76</u>	<u>-1.31</u>	<u>-3.1</u>	<u>1.84</u>		<u>-2.79</u>
<u>s1</u>	<u>SI</u>	<u>-2.99</u>	<u>-2.83</u>	<u>-2.68</u>	<u>-5.51</u>	<u>-3.34</u>	<u>-2.76</u>	<u>-8.9</u>	<u>-61.12</u>	<u>-2.44</u>	<u>-21.26</u>	<u>-1.62</u>		<u>-42.08</u>
	<u>Log IAP</u>	<u>-7.34</u>	<u>-11.14</u>	<u>-11.14</u>	<u>-22.5</u>	<u>-13.99</u>	<u>-7.34</u>	<u>-7.33</u>	<u>-63.95</u>	<u>-3.86</u>	<u>-24.39</u>	<u>0</u>		<u>-44.94</u>
	<u>Log KT</u>	<u>-4.35</u>	<u>-8.31</u>	<u>-8.46</u>	<u>-16.99</u>	<u>-10.65</u>	<u>-4.58</u>	<u>1.57</u>	<u>-2.83</u>	<u>-1.42</u>	<u>-3.13</u>	<u>1.62</u>		<u>-2.86</u>
<u>s2</u>	<u>SI</u>	<u>-2.8</u>	<u>-0.89</u>	<u>-0.74</u>	<u>-1.73</u>	<u>-3.79</u>	<u>-2.56</u>	<u>-9.55</u>	<u>-67.85</u>	<u>-2.72</u>	<u>-22.94</u>	<u>-1.67</u>		<u>-39.38</u>
	<u>Log IAP</u>	<u>-7.14</u>	<u>-9.19</u>	<u>-9.19</u>	<u>-18.68</u>	<u>-14.46</u>	<u>-7.14</u>	<u>-7.98</u>	<u>-70.66</u>	<u>-4.12</u>	<u>-26.06</u>	<u>0</u>		<u>-42.23</u>
	<u>Log KT</u>	<u>-4.34</u>	<u>-8.3</u>	<u>-8.45</u>	<u>-16.95</u>	<u>-10.67</u>	<u>-4.58</u>	<u>1.57</u>	<u>-2.81</u>	<u>-1.39</u>	<u>-3.12</u>	<u>1.67</u>		<u>-2.85</u>

1165  
1166

	<u>SI</u>	<u>-3.81</u>		<u>-2.59</u>	<u>-3.57</u>	<u>-9.73</u>		<u>-17.22</u>	<u>-1.64</u>	<u>-10.5</u>	<u>-50.4</u>
<u>p1</u>	<u>Log IAP</u>	<u>-8.15</u>		<u>-13.25</u>	<u>-8.15</u>	<u>-8.16</u>		<u>-20.35</u>	<u>0</u>	<u>-8.63</u>	<u>-53.26</u>
	<u>Log KT</u>	<u>-4.34</u>		<u>-10.66</u>	<u>-4.58</u>	<u>1.57</u>		<u>-3.13</u>	<u>1.64</u>	<u>1.87</u>	<u>-2.86</u>

1 **Potential source of groundwater recharge in the middle-latitude desert of Otindag,**  
2 **China?**

3 Bing-Qi Zhu<sup>1\*</sup>, Xiao-Zong Ren<sup>2</sup>, Patrick Rioual<sup>3</sup>

4 <sup>1</sup>KLWCRESPP, IGSNRR, CAS, Beijing, China

5 <sup>2</sup>SGS, TYNU, Jinzhong, China

6 <sup>3</sup>KLCGE, IGGCAS, Beijing, China

7 *Correspondence to:* Bing-Qi Zhu ([zhubingqi@sina.com](mailto:zhubingqi@sina.com))

8 **Abstract.** The Otindag Desert in the middle-latitude desert zone of northern  
9 Hemisphere (NH) is essential to livestock-economy and environment of northern  
10 China. Many areas in this zone are unexpectedly rich with groundwater resources  
11 although they have been under arid or hyper-arid climate. Widespread fresh  
12 groundwater deep to 60 m was found at the eastern part of the Otindag Desert. The  
13 occurrence of this massive fresh groundwater raises doubts on the long-lasting  
14 hypothesis in academic circles that regional atmospheric precipitation or  
15 palaeowater is the source of water in the middle-latitude desert aquifers of northern  
16 China. Understanding of the recharge sources of this fresh groundwater is important  
17 in evaluating the feasibility of groundwater exploitation and utilization. In this study  
18 we conducted hydrogeochemical and isotopical analyses to assess possible origin and  
19 recharge of these groundwaters. The analytical results indicate that the fresh  
20 groundwater is neither originated from regional atmospheric precipitation derived  
21 from the Asian Summer Monsoon system, nor from palaeowater that formed during  
22 the last glacial period. These findings suggest that the groundwater in this desert is  
23 possible to originate from remote mountain areas via the faults of the Solonker  
24 Suture zone. In addition, it is concluded that the hydrogeological linkage between  
25 desert aquifers and mountain systems through the suture zone is crucial to the  
26 hydrological functioning of the Otindag aquifer. This suggests that the modern  
27 indirect recharge mechanism, instead of the direct recharge and the palaeo-water  
28 recharge, is the most significant for groundwater recharge in the Otindag Desert. This  
29 study provides a new perspective into the origin and evolution of groundwater  
30 resources in the middle-latitude desert zone of HA.

31

32 **Keywords:** fresh groundwater recharge; atmospheric precipitation; direct recharge;  
33 indirect recharge; palaeowater recharge; fault hydrology; middle-latitude desert;  
34 Otindag Desert.

35

36 **1. Introduction**

37 The deficit of rainfall occurs globally in semi-arid to arid regions. It is usually  
38 made up by extracting groundwater to supply the needs of a growing population and  
39 a higher standard of living. Many areas in the middle-latitude desert zone of  
40 northern China such as the Badanjilin Desert, the Mu US sandy Land and the Hobq  
41 Desert (Chen et al., 2012a; Chen et al., 2012b), are unexpectedly rich with large  
42 groundwater resources although they have been under arid or hyper-arid climate for  
43 a long time (Sun et al., 2010). How these groundwaters originated and how they are  
44 recharged in these deserts are thus fundamental scientific questions. Until now,

45 however, no consensus has been achieved in academic circles.

46 The Otindag Desert is one of the largest sandy lands located at the monsoon  
47 margin of northern China and is the geographical centre of the northeastern Asian  
48 Continent (Fig. 1), which can be regarded as a significant repository of information  
49 relating to the groundwater recharge in the arid Inner Asia. At present, the eastern  
50 Otindag is also a typical case for its unexpected groundwater resources, because  
51 there is abundant groundwater in this desert land and even rivers originate there due  
52 to the spillover of spring water, such as the tributaries of Xilamulun River in its north  
53 and the Shandian River in its south (Fig. 1). Climatically, the monsoon margin of  
54 northern China refers to a strip along the present East Asian Summer Monsoon  
55 (EASM) limits and is considered to be sensitive to climate change (Wang and Feng,  
56 2013). Geologically, the Otindag Desert lies in a tectonic depression of the central  
57 Solonker suture zone with a few faults stretching east and west (Fig. 2), with its  
58 northern margin along a fault marked by a series of lake basins. Thus, the large-scale  
59 hydrogeological conditions of the Otindag Desert belong to a fault zone under the  
60 influence of the EASM climate.

61 Until now, however, whether the climate or other factors affected the  
62 groundwater recharge in the Otindag is still not known. Little data about the  
63 groundwater and its origin is available in the literature, and knowledge and reliable  
64 data on various hydrogeological characteristics of the desert such as the catchment  
65 extent, input/output, the hysteretic hydraulic functions, the transient hydraulic  
66 conditions, in-homogeneities, and on transfer functions to overcome scale problems  
67 are also missing. Under such conditions, conventional methods such as water  
68 balance and hydraulic methods sometimes fail in determining groundwater recharge,  
69 particularly in extreme environments (arid, semi-arid, or cold) (Drever, 1997).  
70 Because pristine aquatic conditions may significantly differ from managed conditions  
71 in arid environment, and thus groundwater recharge is not a fixed number, but may  
72 vary with the boundary conditions of the recharge system (Seiler and Gat, 2007).

73 Groundwater recharge can be broadly classified into two categories: the direct  
74 recharge by native water resources and the indirect recharge by external water  
75 resources (Herczeg and Leaney, 2011). Water infiltration of atmospheric precipitation  
76 through the unsaturated zone to the groundwater is hydrologically defined as the  
77 direct recharge, and the indirect recharge is defined as recharge from mappable  
78 features such as rivers, canals, lakes and originates from remote areas (Scanlon et al.,  
79 2006; Healy, 2010). It is well known that groundwater recharge can be influenced by  
80 environmental factors, including climate change, underlying soil and geology, land  
81 cover and the growth in human population that affects withdrawal and economic  
82 development (Zhu et al., 2015, 2017). Among these environmental factors, climate  
83 and land cover largely determine precipitation and evapotranspiration, whereas the  
84 underlying soil and geology dictate whether a water surplus (precipitation minus  
85 evapotranspiration) can be transmitted and stored in the subsurface (Doll, 2008,  
86 2009; Giordano, 2009).

87 For some earth scientists, the direct recharge is thought to be very important  
88 for groundwaters in the wide desert lands of north China due to the lack of surface  
89 runoffs (Yang et al., 2010; Yang and Williams, 2003; Zhao et al., 2017). They argued  
90 that although the amount of atmospheric precipitation is small, the vast catchment  
91 area in the desert region could concentrate the rainfall into large inland basins,

92 creating an aquifer with large storage capacity and great thickness. However, some  
93 hydrologists estimated by the chloride mass balance method that the direct recharge  
94 was 1.4 mm/year, which represents approximately only 1.7% of the mean annual  
95 precipitation in a cold large desert (Badanjilin) in northern China (Gates et al., 2008).  
96 A similar estimation of 1 mm/year was given for Gobi deserts from the Hexi Corridor  
97 to the Inner Mongolia Plateau in northwestern China (Ma et al., 2008). Consequently,  
98 they thought that heavy potential evaporation and little precipitation make it difficult  
99 for direct recharge to meet the supply of groundwater in these desert areas. Thus,  
100 the indirect recharge is considered to be an important mechanism for groundwater  
101 recharge in these desert areas. For example, Zhao et al. (2012) suggested that little  
102 precipitation had recharged into groundwaters in the Badain Jaran Desert. Chen et al.  
103 (2004) argued that the groundwaters in the Badanjilin Desert were recharged by  
104 palaeo-glacial melt water through faults and deep carbonate layers far away from the  
105 local desert. Many studies also suggested that palaeowaters stored in an aquifer  
106 during wetter climate periods could recharge to groundwater under certain  
107 conditions in arid lands (Edmunds et al., 2006; Ma and Edmunds, 2006). Other kinds  
108 of indirect recharge, such as mountain front recharge from adjacent mountain blocks,  
109 are also proposed to offer an important inflow to aquifers within arid to semiarid  
110 catchments (Blasch and Bryson, 2007).

111 In this paper, we focus to answer the question that whether groundwater  
112 recharge in Otindag is mainly direct or indirect, using hydrochemical and isotopic  
113 indicators as tracers to offer a valuable support for identifying the contributions of  
114 precipitation recharge on groundwater, since these indicators reflect the  
115 composition of water molecules and are sensitive to physical processes such as  
116 mixing and evaporation (Sultan et al., 2000; Guendouz et al., 2003; Petrides et al.,  
117 2006; Scanlon et al., 2006; Zhu et al., 2007, 2008; Jobbágy et al., 2011). The detailed  
118 objectives are: (1) to recognize the major sources of groundwater in the area, and (2)  
119 to identify the key mechanism of groundwater recharge in the desert.

120

## 121 **2. Regional settings**

122 Geographical location. The Otindag Desert lies between latitudes 42° and 44°N  
123 and longitudes 112° and 118° E (Fig. 1). It is an east part of the great middle-latitude  
124 desert zone between northwestern and northeastern China which extends from the  
125 Taklamakan Desert in northwestern China to the Kelqin Desert in northeastern China,  
126 near the west coast of the Pacific Ocean. The desert has an area of approximately  
127 21,400 square kilometers located in the eastern Inner Mongolia and at the monsoon  
128 margin of northern China (Fig. 1). It is the fourth largest sandy lands in China (Yang et  
129 al., 2012) and is bordered by a flat steppe terrain of Dali Basin to the north, the  
130 Yinshan Mountains and mountainous loess landscape to the south, and the the  
131 Greater Khingan (Daxing'Anling) Mountains to the east (Fig. 1). The Otindag Desert is  
132 essential to livestock-economy and environment of northern China. Settlements  
133 in this desert are constrained to oases to frequent springs, groundwater with high  
134 level and areas where cultivation and irrigation are feasible. Some herdsmen live a  
135 precarious life by grazing livestock in the desert.

136 Topography and geomorphology. The relief in the Otindag Desert is varied with  
137 a combination of extensive dune fields and rugged piedmonts and mountains along  
138 the eastern and southern rims. In the east, the Daxing'Anling Mountains has an

139 average elevation ranging from 1,100 to 1,400 m and extend from the Heilong River  
140 Valley into the upper reach valleys of the Xilumulun River from northeast to  
141 southwest, with a gradual increase in height northwards from about 180 m near  
142 Huma to Huanggangliang, where the highest mountaintop reach 2,029 m. In the  
143 south and southeast, the Yinshan Mountains decline gradually near Duolun and  
144 Zhenglanqi, and in some areas leave wide alluvial plains. The terrain of the Otindag  
145 Desert is less rough and elevations decrease from ca. 1300 m in the southeast to ca.  
146 1000 m in the northwest. Over the greater part of this desert the ground cover  
147 consists of fixed and semi-fixed sandy dunes, with a few mobile dunes in area of little  
148 vegetation. The dominated dune types are represented from parabolic to barchans,  
149 linear and grid-formed types, ranging from a few meters to over 40 m in height (Zhu  
150 et al., 1980; Yang et al., 2008).

151 Climate, vegetation and soil. The climate of the Otindag Desert was not uniform  
152 in geological period, with much sand movement, occasional rainy years, and several  
153 wetter intervals during the Holocene (Yang et al., 2015; Tian et al., 2017). At present  
154 the whole desert belongs to the arid and semi-arid temperate zone, with a mean  
155 annual temperature of 2 °C in the north and 4°C in the south (Liu and Yang, 2013). At  
156 the regional scale, the climate of the desert is typically controlled by the East Asian  
157 Monsoon system, characterized by a warm summer, with precipitation transported  
158 by the EASM, and by a cold and dry winter under the influence of the East Asian  
159 Winter Monsoon (EAWM). The rainfall in the desert exhibits a wide variation in space  
160 and time. Influence of the EASM changes from southeast to northwest in the desert,  
161 varying with the distance increase from the Pacific Ocean and leading to the mean  
162 annual rainfall decreasing from ~450 mm in the southeast to ~150 mm in the  
163 northwest (Yang et al., 2013). The spatial inequality of rainfall makes a great impact  
164 on the availability of near-surface moisture, consequently on the distribution of  
165 vegetation, soil and the animal husbandry potential of local communities. The major  
166 soil type is the grey desert soil in the west and changes to the sierozems and  
167 chernozem or chestnut soil in the east. Through the desert, vegetation is sparse in  
168 the west and relatively abundant in the east. The native vegetation is scrub  
169 woodland in the east and is steppe in the west, showing a natural characteristic of  
170 the temperate desert or semi-desert. It is greatly affected by temperature, rainfall  
171 and elevation in the growing season due to the scarcity of surface runoff.

172 Geology. The Otindag Desert is located in a tectonic depression of the Solonker  
173 Suture Zone (Jian et al., 2010) bounded by the Northern Early to Mid-Paleozoic  
174 Orogen Zone and the Hatug Uul Block to the north, the Southern Early to  
175 Mid-Paleozoic Orogen Zone and the North China Craton system to the south (Fig. 2).  
176 A few faults such as the Xar Moron Fault and Chifeng-Bayan Obo Fault stretch east  
177 and west, with its northern margin along the Solonker Suture Zone marked by a  
178 series of lake basins (Figs. 1 and 2). The tectonostratigraphic units and overall  
179 structural trends are mainly oriented NE–SW (Fig. 2), which may be interpreted as  
180 resulting from overall compressive stresses oriented principally in the NW–SE  
181 quadrants during orogenesis (Jian et al., 2010; Zhang et al., 2015). Diverse rock types  
182 from unlithified and lithified clastic sediments through to carbonate, crystalline, and  
183 volcanic rocks are distributed in and around the Otindag Desert (Zhang et al., 2015)  
184 (Figs. 2 and 3). Tertiary and Quaternary sandstones and mudstones are the common  
185 basement rocks under the dunes of the Otindag, and extensive volcanic basalts

186 forming flat terrains are to the north (Zhu et al., 1980; Li et al., 1995).

187 Hydrology and hydrogeology. The Otindag Desert originated during the Late  
188 Quaternary (Yang et al., 2015) and various alluvial fans formed at the margins of this  
189 desert during the early to middle Holocene. These are composed of conglomerate  
190 and sand deposits, where major periodic streams or wadis debouched into the  
191 Otindag. At present two rivers run through the eastern margin of the Otindag Desert,  
192 i.e. the Xilamulun River in the north and the Shandian River and its two tributaries,  
193 the Shepi River and Tuligen River in the south. Both stem from the eastern and  
194 southeastern parts of the Otindag (Fig. 1). The Xilamulun River, 380 km in length and  
195  $32.54 \times 10^3 \text{ km}^2$  in area, is a neighboring river both to the northeastern Otindag and  
196 the southeastern Dali Basin, the northern catchment of the Otindag Desert. The  
197 Xilamulun River flows to the east and finally goes into the Xiliao River, with an annual  
198 mean runoff of  $6.58 \times 10^8 \text{ m}^3$  (Wu et al., 2014). The Shandian River is the upper  
199 reach of the Luan River, with a length of 254 km and a catchment area of  $4.11 \times 10^3$   
200  $\text{km}^2$  (Yao et al., 2013). Spotted salt crusts can extensively develop on land surface  
201 due to the high rate of evaporation. Sabkhas and salt pans often form in areas  
202 surrounding the flat shorelines of some lakes in the Otindag. During rainy season,  
203 some rain and floodwaters (generally coming from the Yinshan piedmonts) are  
204 retained in low-lying areas, which may temporarily recharge shallow aquifers. Under  
205 storm conditions, fast-flowing floods often form in some wadi channels with rich soil  
206 due to the occasional short, heavy rainstorms.

207 Groundwater resources in the Otindag Desert and its surrounding areas depend  
208 on several kinds of aquifers with different water-bearing formations and units (Fig. 3).  
209 Coarse- to fine-grained sedimentary rocks, magmatic rocks and metamorphic rocks of  
210 the Inner Mongolia-Daxing'Anling Orogenic Belt (Zhang et al., 2015) form the major  
211 regional aquifer unit (Fig. 3). They are composed mainly of alluvial sediments  
212 (mid-Permian Zhesi Formation), melange (Solonker suture zone), A-type granite  
213 (early Permian), bimodal volcanic rocks with sedimentary intercalations (early  
214 Permian Dashizhai Formation), diorite-quartz diorite-granodiorite rocks  
215 (Carboniferous-Permian) and metamorphic complex (predominantly gneiss, early  
216 Paleozoic) (Fig. 2). The aquifer is generally unconfined in dune fields of the Otindag  
217 Desert, unconfined to semi-confined in the Yinshan Mountains' piedmont, and  
218 semi-confined to confined in the Daxing'Anling uplands (Fig. 3). Water-level  
219 measurement in June 2010 indicated that the general depth of unconfined  
220 groundwater level ranges between 10 to 70 m in the Otindag Desert (Fig. 3). Local  
221 granular aquifers in the central desert are composed of coarse fluvial, lacustrine and  
222 aeolian sediments, but their extent and thickness vary throughout the watershed  
223 (Zhu et al., 1980; Li et al., 1995). The generally coarse-grained texture of the  
224 unconsolidated rock formations provides primary porosity in terms of groundwater  
225 flow in the desert.

226

### 227 **3. Methods**

228 The isotopes and ion chemistries of different water samples in the Otindag  
229 Desert, including natural samples collected from local and regional precipitation,  
230 depression springs, shallow and deep aquifers, perpetual lakes and outflowing rivers,  
231 are analyzed here and discussed. Relationships between the study area and the  
232 regional prevailing EASM climate, the dominant topographical, geological (tectonic)

233 and hydrogeological conditions, are also explored and interpreted, using multiple  
234 graphs and diagrams. Fieldworks took place during the summer season of 2011 and  
235 the spring season of 2012. Water samples were mainly retrieved from shallow and  
236 deep wells located over a wide area in dune fields of the study regions. The detailed  
237 locations of the sampling sites are shown in Fig. 4.

238 In this study, we designed two groups of parameters to characterize the  
239 physiochemistry of each water sample. One is the field-measured parameters and  
240 another is the lab-measured parameters. The former includes those parameters that  
241 will change in a shorter period of time when they are not directly measured in the  
242 field, such as the total dissolved solid (TDS, mg/L), electrical conductivity (EC in  
243 micro-Siemens per centimeter or  $\mu\text{S}/\text{cm}$ ), hydrogen-ion concentration (pH) and  
244 temperature ( $^{\circ}\text{C}$ ). The analysis for major cations ( $\text{F}^-$ ,  $\text{Cl}^-$ ,  $\text{NO}_2^-$ ,  $\text{NO}_3^-$ ,  $\text{SO}_4^{2-}$ ,  $\text{HCO}_3^-$ ,  
245  $\text{CO}_3^{2-}$  and  $\text{H}_2\text{PO}_4^-$ ) and anions ( $\text{Li}^+$ ,  $\text{Na}^+$ ,  $\text{NH}_4^+$ ,  $\text{K}^+$ ,  $\text{Mg}^{2+}$  and  $\text{Ca}^{2+}$ ) are determined for all  
246 of the water samples collected. Contents of stable ( $^2\text{H}$  and  $^{18}\text{O}$ ) and radioactive  
247 isotopes ( $^3\text{H}$ ) in the rain and groundwater samples are precisely measured. The  
248 analytical data of the physiochemical parameters and the stable and radioactive  
249 isotopes of the water samples collected in this study are listed in Tables 1, 2 and 3,  
250 respectively.

251

## 252 4. Results and Discussions

253

### 254 4. 1. Hydrochemical characteristics of natural waters

255 The natural water samples collected in this study are generally neutral to slightly  
256 alkaline, with the pH values varying between 6.26 and 9.44 (except the precipitation  
257 sample p1, 4.61) (Table 1) and a median value of 7.27. The TDS values range between  
258 67 and 660 mg/L (average 211 mg/L) (Table 1), all belonging to fresh water (TDS <  
259 1000 mg/L) in the salination classification of natural water (Meybeck, 2004). The  
260 variations in ion concentrations of the major cations and anions in the studied water  
261 samples were displayed in a fingerprint diagram with a semi-logarithm y-axis (Fig. 5).  
262 The rain water sample is the most depleted in ions among these samples. The  
263 groundwater samples have the highest concentrations of cations and anions and the  
264 lake, river and spring waters had intermediate values. The calcium concentration is  
265 the highest among cations in almost all of the water samples, and the  $\text{HCO}_3^- + \text{CO}_3^{2-}$   
266 concentration (bicarbonate + carbonate, alkalinity) is the highest among anions in  
267 most of the water samples. For several groundwater samples (g3, g4, g5, g6 and g11),  
268 spring sample (s1) and precipitation sample (p1), they have higher  $\text{SO}_4^{2-}$   
269 concentrations than alkalinity (Fig. 5).

270 Two chemically distinct water types are recognized for the studied waters via a  
271 Piper diagram (Fig. 6), calcium bicarbonate and calcium sulphate. No Chloride-type  
272 and sodium-type waters occur in the study area (Fig. 6). It has been reported that the  
273 global groundwater tends to evolve chemically towards the composition of seawater  
274 (Chebotarev, 1955), and this evolution is associated with regional changes in  
275 dominant anions but not cations. This general evolution of groundwater can be  
276 illustrated as a anion evolution line (Freeze and Cherry, 1979):  $\text{HCO}_3^- \rightarrow \text{HCO}_3^- + \text{SO}_4^{2-}$   
277  $\rightarrow \text{SO}_4^{2-} + \text{HCO}_3^- \rightarrow \text{SO}_4^{2-} + \text{Cl}^- \rightarrow \text{Cl}^- + \text{SO}_4^{2-} \rightarrow \text{Cl}^-$ , which travels along the flow paths  
278 and increasing ages. It can be deduced from this line that bicarbonate water is the  
279 early product of groundwater evolution with low salinity, renewable water resources

280 or low residence time, while sulfate waters is the intermediate or advanced product  
281 of groundwater evolution with higher salinity passing through gypsum and anhydrite  
282 aquifers (Clark, 2015). The distribution pattern of water chemical types occurred in  
283 the study area indicates a primary stage of groundwater evolution in the Otindag  
284 Desert.

285 The  $\delta D$  values of the groundwater samples collected in this study varied from  
286  $-63.42\text{‰}$  to  $-75.92\text{‰}$  (Table 3), with an average  $-69.53\text{‰}$ . The  $\delta^{18}O$  values ranged  
287 between  $-8.64\text{‰}$  and  $-11.26\text{‰}$  (Table 3), with an average  $-10.17\text{‰}$ . The spring water  
288 samples were relatively concentrated in  $\delta D$  and  $\delta^{18}O$  and were greatly similar to  
289 those of the groundwater samples (Fig. 7). The  $\delta D$  and  $\delta^{18}O$  values in the river water  
290 samples were slightly more variable and were also similar to those of the  
291 groundwater (Fig. 7). The lake water samples were enriched in  $\delta D$  and  $\delta^{18}O$  by  
292 comparison to the groundwater samples (Fig. 6). The precipitation sample p1 was  
293 also enriched in  $\delta D$  and  $\delta^{18}O$  by comparison to the groundwater samples (Fig. 7). The  
294 content of radioactive isotope of tritium ( $^3H$ ) measured in seven well groundwater  
295 samples with 6-60 m depth ranged from 1.86 to 24.35 TU (Table 3), with an average  
296 14.95 TU, higher than the mean tritium concentration (9.8 TU) of groundwater in the  
297 Vienna Basin, Austria (Stolp et al., 2010), the seat of the International Atomic Energy  
298 Agency (IAEA).

299 If we plot the relationships between oxygen and hydrogen isotopes of  
300 groundwater, spring, river and lake water samples, we observed that most of the  
301 data points fell on a straight line that can be expressed by a regression equation:  $\delta D$   
302  $= 4.09\delta^{18}O - 28.31$  ( $R^2=0.93$ ,  $n=24$ ) (EL1 in Fig. 7). This local groundwater line (LGWL)  
303 is different from the Global Meteoric Water Line (GMWL,  $\delta D = 8\delta^{18}O + 10$ ) and the  
304 Mediterranean Meteoric Water Line (MMWL,  $\delta D = 8\delta^{18}O + 20$ ) estimated by Craig  
305 (1961), but it is similar to the local groundwater lines established for other deserts in  
306 northern China and central Asia with a same slope but different Y-intercepts, such as  
307  $\delta D = 4.17\delta^{18}O - 31.3$  for the Badanjilin Desert (Jin et al., 2018),  $\delta D = 4.8\delta^{18}O - 15.2$   
308 for the Ejina Desert in China (Wang et al., 2013), and  $\delta D = 4.26\delta^{18}O + 9.23$  for the  
309 Rub Al Khal Desert in the United Arab Emirates (Rizk and El-Etr, 1997). The data  
310 points are scattered for the lake water samples (Fig. 7) in the Otindag, suggesting  
311 that the lake waters are affected by evaporation, but the other waters in the desert  
312 are not so.

313

#### 314 **4. 2. Summer precipitation recharge on groundwater in the Otindag**

315 In order to compare the isotopic signals between groundwater and precipitation  
316 at a regional scale, the isotopic analysis of precipitation from similar areas surrounding  
317 the study area, such as Baotou, were incorporated with local data of summer  
318 precipitation (p1) in this study (Fig. 7). The Baotou station is the nearest long-term  
319 station to the Otindag Desert and was monitored for the isotopic composition of  
320 rainfall for the period 1986-2001 within the International Atomic Energy Agency  
321 Global Network of Isotopes in Precipitation (IAEA-GNIP) database. The stable isotope  
322 data from Baotou was used to represent the regional background of stable isotopic  
323 compositions of the present-day summer meteoric water, especially in the westward  
324 inland areas of the Otindag Desert (Fig. 1). In addition, stable isotope data of the  
325 Tianjin station was also used to represent the regional background of summer  
326 precipitation in the eastern coastal areas of the Otindag Desert (Fig. 1).

327 Based on the isotopic data from the Baotou station, the local meteoric water  
328 lines can be statistically expressed as the isotopic regression equation of  $\delta D =$   
329  $6.36\delta^{18}O - 5.21$  (LMWL-B). It can also be expressed as  $\delta D = 6.57\delta^{18}O + 0.31$  (LWML-T),  
330 based on the data from the Tianjin station (Fig. 7). The precipitation sample p1  
331 collected in this study fell onto the GMWL (Fig. 7). It also showed similar  $\delta D$  and  $\delta^{18}O$   
332 values to those of the precipitation collected in the GNIP stations of Baotou and  
333 Tianjin (Fig. 7).

334 Compared to the summer precipitation data from the GNIP stations and from  
335 the local summer precipitation (p1), the groundwater, spring, and river water  
336 samples were evidently depleted in heavy stable isotopes in the Otindag (Fig. 7).  
337 Except for the lake water samples, most of the groundwater, river water and spring  
338 water samples in the Otindag fall on or lay between the LMWL-B and the LMWL-T  
339 lines, and are located at the lower left area of the precipitation points (Fig. 7).

340 Because the isotopic evolution of  $\delta D$  and  $\delta^{18}O$  in water illustrated in the Craig  
341 line represents a one-way and irreversible process, the water bodies distributed at  
342 the upper right area of the Craig line can not be recharge sources for the water  
343 bodies distributed at the lower left area of the line. Such results indicate that the  
344 groundwater, river water and spring water in the Otindag are not recharged by the  
345 regional precipitation, namely no significant modern direct recharge has taken place  
346 for groundwater in the Otindag.

347 Dogramaci et al. (2012) documented that only intense and remarkable rainfall  
348 events  $>20$  mm could recharge groundwater in the semi-arid Hamersley Basin of  
349 northwest Australia, while the rainfall events  $<20$  mm had limited influences on  
350 groundwater recharge. Chen et al. (2014) described that rainfall events  $\leq 5$  mm in the  
351 summer arid and semi-arid region of northern China would be evaporated into the  
352 atmosphere rapidly before it is infiltrated into the groundwater system. Based on the  
353 analysis on the data records from two meteorological stations around the Otindag,  
354 i.e. the Duolun and Xilinhaote stations (see Fig. 1a), we observed that summer rainfall  
355 events  $>20$  mm on average only occur 2.5-3.4 times per year (Table 4). In some years  
356 (e.g. from 2005 to 2007 at the Xilinhaote Station), no summer rainfall events  $>20$  mm  
357 even occurred. It further indicated the limited contribution of regional summer  
358 precipitation on groundwater recharge in the Otindag.

359 In addition to groundwater, the river and spring water samples from the Otindag  
360 also deviated from the local precipitation in the Craig diagram (Fig. 7). These water  
361 samples came from the Xilamulun, Shepi and Tuligen rivers. They shared the same  
362 evaporation line (EL1) with the groundwater and lake water samples (Fig. 7).  
363 Generally speaking, natural waters that have a same recharge source are distributed  
364 on a same line of evaporation in the  $\delta^2$  and  $\delta^{18}O$  diagram (Chen et al., 2012b). This  
365 indicates that the recharge sources of groundwater, river water, spring water and lake  
366 water in the Otindag are genetically associated each other and differ from the local  
367 precipitation.

#### 369 **4. 3. Winter precipitation and palaeowater recharge on groundwater in the Otindag**

370 Since the groundwater samples in the Otindag are depleted in their  $\delta D$  and  $\delta^{18}O$   
371 values even more than those of the local rainfall (Fig. 7), they must be sourced from  
372 other waters characterized by similar or more depleted signals in their stable  
373 isotopes compositions. Due to the temperature effect (such as evaporation) on

374 isotopic fractionation, only the waters issued from colder environments can be more  
375 depleted in their  $\delta D$  and  $\delta^{18}O$  values even more than those of the local rainfall.

376 Because the Otindag Desert is under the control of the EASM climate (Fig. 1),  
377 the local rainfall in the desert is mainly sourced from summer precipitation. This can  
378 also be illustrated by the seasonal distributions in annual mean precipitation (Fig.8a),  
379 in annual mean air temperature (Fig. 8b) and in annual mean water vapor pressure  
380 (Fig. 8c) over the last forty years at the two surrounding GNIP weather stations in  
381 Baotou and Tianjin. The seasonal distributions of stable isotopes in the two stations  
382 (Fig. 8d-e) show that the summer rainfall is evidently positive in its signals of  $\delta D$  and  
383  $\delta^{18}O$  by comparison with those of the winter rainfall, further suggesting that the  
384 waters issued from cold environments can be more depleted in their  $\delta D$  and  $\delta^{18}O$   
385 values than those of the summer rainfall. Thus we speculate that groundwater in the  
386 Otindag can be potentially derived from (1) modern precipitation in winter, (2)  
387 palaeowater formed in the past glacial period, or (3) remote/mountain waters that  
388 emanate in colder and wetter conditions.

389 The annual mean values of  $\delta D$  and  $\delta^{18}O$  over the last forty years are more  
390 depleted in winter precipitation than in summer precipitation at the Baotou and  
391 Tianjin stations (Fig. 8d-e). This isotopic signal qualifies the regional winter  
392 precipitation to be a potential source of groundwaters in the Otindag. However, the  
393 precipitation amounts and the water vapor pressures (effective moisture) in winter  
394 months are much lower than those in the summer months at both the Baotou and  
395 Tianjin stations (Fig. 8a and 8c). It indicates that the winter seasons in these regions  
396 are relatively colder and drier but not colder and wetter. A colder-wetter winter  
397 season is a necessary condition for winter precipitation to be a water source for the  
398 formation of groundwater under a summer monsoon climate. This is because the  
399 bigger amounts of summer precipitation will easily remove or weaken the depleted  
400 isotopic signals of winter precipitation in groundwater. In this regard, modern winter  
401 precipitation is unlikely to be an important source of groundwater in the Otindag.

402 As to the palaeowaters formed in colder and wetter periods such as the last  
403 glacial, it has been proposed to be a potential water source for groundwaters in the  
404 wide arid lands of the world. The depleted signals of stable isotopes ( $\delta D$  and  $\delta^{18}O$ ) in  
405 groundwater have been recognized in global arid and semi-arid regions, such as the  
406 Sinai Desert in Egypt (Gat and Issar, 1974), Israel (Gat, 1983), South Australia (Love et  
407 al., 1994, 2000), northern China (Ma et al., 2010), Saudi Arabia (Bazuhaire and Wood,  
408 1996) and North Africa (Guendouz et al., 2003). These signals are very often  
409 explained as palaeo-groundwater that recharged by precipitation during past wetter  
410 and colder periods (Love et al., 1994, 2000; Herczeg and Leaney, 2011).

411 Here we use the tritium data as an environmental tracer to estimate the  
412 groundwater age in the Otindag. The tritium data at the GNIP stations of the Baotou  
413 and Tianjin are also referenced as the background values in precipitation of recent  
414 years. The residence time of groundwater in aquifer and the residual tritium of a  
415 water body can be calculated by  $N = N_0 e^{-\lambda t}$  (Yang and Williams, 2003). Where  $N$  =  
416 content of residual tritium in water sample,  $\lambda = 0.0565$ , the radioactive decay  
417 constant,  $N_0$  = content of tritium at the time of rainfall and  $t$  = years after  
418 precipitation. Based on this equation, the residual tritium was theoretically  
419 calculated and the standard for tritium dating was established for seven groundwater  
420 samples in the Otindag Desert (Table 3). As a result, ages of 0-60 years were obtained

421 for these groundwater samples (Table 5). This indicates that recent recharge took  
422 place several decades after the peak in global nuclear tests. We thus conclude that  
423 groundwater is generally not older than 70 years in the study area. It means that  
424 groundwater in the Otindag are not palaeowater recharged.

425 Both the modern summer and winter precipitation recharge and the  
426 palaeowater recharge can be refuted, indicating that direct recharge is not a major  
427 mechanism controlling the groundwater recharge in the Otindag.

428

#### 429 **4. 4. External water recharge on groundwater in the Otindag: Dali Basin**

430 The third hypothesis that “remote/mountain waters emanate under colder and  
431 wetter conditions” is further considered here. In essence, it is an indirect recharge  
432 mechanism as water originates from remote areas (Healy, 2010; Herczeg and  
433 Leaney, 2011).

434 It is worth noting that the values of deuterium and oxygen-18 for groundwater  
435 in the north part of the study area are more depleted in  $\delta D$  and  $\delta^{18}O$  than those in  
436 the south part (Table 3). It suggests that the Otindag groundwater might be  
437 potentially recharged by water resources coming from the northern neighboring  
438 catchment, such as the Dali Basin.

439 Recently published data of  $\delta D$  and  $\delta^{18}O$  in groundwater, lake water, river water  
440 and spring water sampled from the Dali Basin (e.g., Chen et al., 2008; Zhen et al.,  
441 2014) were compiled in this study and were co-analyzed with the data from the  
442 Otindag. About 70 natural water samples from the Dali and Otindag with  $\delta D$  and  
443  $\delta^{18}O$  values are shown in a Craig diagram (Fig. 9). All of these samples fell on or lied  
444 near the evaporation line EL2 in the Craig diagram (Fig. 9), with a regression  
445 equation of  $\delta D = 4.81\delta^{18}O - 21.55$  and a high correlation coefficient ( $R^2=0.98$ ,  $n=70$ ).  
446 Compared to the groundwater samples in the Otindag, water samples from the  
447 groundwaters, rivers and springs from the Dali Basin are more depleted in  $\delta^{18}O$  and  
448  $\delta D$  (Fig. 9). Such results further indicate that, in terms of its isotopic signature, the  
449 groundwater in the Otindag has a close relationship with the natural waters in the  
450 Dali Basin.

451 The similar signals of  $\delta D$  and  $\delta^{18}O$  between the groundwater in the Otindag and  
452 the river water in the Dali (Fig. 9) point towards the idea that the groundwater in the  
453 Otindag might be sourced from the river water in the Dali Basin, since the Dali has  
454 more depleted isotopic signals in water than the Otindag (Fig. 9). Considering the  
455 topographical gradient of elevations between the two regions, however, river water  
456 in the Dali Basin cannot flow into the eastern Otindag, because the terrain elevation  
457 of the Dali Basin is lower than that of the Otindag (Fig. 1). This is also the reason why  
458 the huge Dali Lake that lies in the Dali Basin has no equivalent in the Otindag (Fig. 1).  
459 If there is a hydraulic linkage between the two regions, water should flow from the  
460 Otindag into the the Dali, but not conversely.

461 In view of the hydraulic gradient, river water in the Dali Basin could not be a  
462 recharge source for groundwater in the Otindag. However, in view of the isotopic  
463 gradients, groundwater in the Otindag could not conversely be the source of river  
464 water in the Dali (Fig. 9). Thus, the similar isotopic signals between the river water in  
465 Dali and the groundwater in Otindag indicate that these waters might be recharged  
466 from a common source.

467 Similar isotopic signals also occurred in the groundwaters between the Otindag

468 and the Dali Basin (Fig. 9). In order to understand the linkage of groundwaters  
469 between the two regions, the potential movement of groundwater in the transition  
470 zone of the two regions need to be known. In this study, a groundwater-sampling  
471 project was designed in the field along a N-S section of a palaeo-channel located at  
472 the transition zone between the Dali and Otindag (Figs. 1, 2). The channel was  
473 named "PCSX" in this study, with its north part named "NPCSX" and the south part  
474 named "SPCSX".

475 The GPS elevation of the northernmost sampling site in the NPCSX (g11, about  
476 1317 m a.s.l.) was much lower than that of the southernmost site in the SPCSX (g1,  
477 1396 m a.s.l.) (Fig. 2 and Table 1). Regarding to the topographical gradient in the  
478 channel, there is a drop of about 80 m between the NPCSX and the SPCSX. Under  
479 such slope, the underground hydraulic gradient for groundwater flow can be roughly  
480 parallel with that of the surface water flow, namely that the groundwaterflow should  
481 move downwards from the SPCSX area into the NPCSX area. Thus we can speculate  
482 that groundwater in the NPCSX would have higher salinity than those in the SPCSX  
483 under such flowing direction. In order to verify this speculation, actual variations of  
484 water salinity (chloride and TDS) were detected along the PCSX section. The sampling  
485 site g1 was defined as the initial point and the distances between g1 and other  
486 sampling sites along the PCSX section were calculated, based on their GPS  
487 geographical coordinates measured in the field. The results are shown in Fig. 10a-b.  
488 It is clear that the variations of chloride and TDS concentrations in groundwater do  
489 not increase along the palaeo-channel from south to north (Fig. 10a-b). On the  
490 contrary, both the values of chloride and TDS are lower in the NPCSX area than those  
491 in the SPCSX area. Such kind of spatial variations in the chloride and TDS values  
492 contradict the speculated patterns abovementioned, suggesting that the hydraulic  
493 gradient of groundwater flowing path in this region is not controlled by the  
494 topographical gradient between the NPCSX and SPCSX areas.

495 Compared between the NPCSX and SPCSX regions, the stable isotopic values  
496 ( $\delta^{18}\text{O}$  and  $\delta\text{D}$ ) of groundwaters in the SPCSX region vary greatly with a large  
497 amplitude, while those in the NPCSX are relatively constant (Fig. 10c-d). The constant  
498 variations indicate that the recharge source of groundwater in the NPCSX is relatively  
499 unitary. The isotopic values in the SPCSX are much lighter than those in the NPCSX  
500 along the distance section from south to north (Fig. 10c-d). The heaviest values  
501 occurred in the sample g11 collected from the NPCSX (Fig. 10c-d), indicating a water  
502 being earlier recharged. The spring water sample s2, a representation of discharge  
503 water, is characterized by medium values of  $\delta\text{D}$  and  $\delta^{18}\text{O}$ . These results indicate that  
504 the groundwaters in the SPCSX area, with relatively enriched isotopic signals in  $\delta\text{D}$   
505 and  $\delta^{18}\text{O}$  by comparison with those in the NPCSX area, are composed of a mixture of  
506 the groundwaters in the NPCSX with other waters.

507 The tritium contents were broadly and positively related to the values of  
508 deuterium excess in the groundwater samples in the PCSX (Fig. 10e). For water that  
509 experiences an evaporation process, the d-excess value will increase in the  
510 evaporated water vapor, but will decrease in the residual water body (Dansgaard,  
511 1964; Merlivat and Jouzel, 1979). In this study, except for sample g11 (a sample very  
512 close to the riverhead area), the positive relationship between the tritium and the  
513 deuterium excess generally shows that the d-excess values are higher in the  
514 groundwaters collected from the NPCSX, but are lower in those from the SPCSX (Fig.

515 10e). This distribution pattern indicates that the groundwaters in the NPCSX are  
516 relatively younger and experienced a lower degree of evaporation than those in the  
517 SPCSX. The d-excess gradient, increasing from south to north in the PCSX, further  
518 suggests that groundwater does not flow from the SPCSX area to the NPCSX area,  
519 namely out of the topographical control.

520 Many studies (e.g., Boronina et al., 2005; Kazemi et al., 2006) have  
521 demonstrated that groundwater flows in the direction in which it gets older. In view  
522 of this point, groundwaters in the PCSX region should flow from the NPCSX area to  
523 the SPCSX area, in opposition to the S-N topographical gradient between the Otindag  
524 and Dali regions. Thus groundwater in the Dali are not the source of groundwater in  
525 the Otindag. The similar isotopic signals between groundwaters in the two regions  
526 indicate that these waters might be recharged from a common source in other place.

527

#### 528 **4. 5. Water sources from remote areas for groundwater in the Otindag: mountain** 529 **waters**

530 The discussions above revealed that both the groundwaters in the Otindag and  
531 DaliBasin might be recharged from a common source derived from another place.  
532 Considering the third hypothesis abovementioned that “remote/mountain waters  
533 emanate under colder and wetter conditions”, we propose that this “common source”  
534 of the two regions are from mountain areas surrounding the Otindag and Dali Basin.

535 There are two large permanent rivers and lots of small intermittent streams  
536 entering the Dali Basin (Xiao et al., 2008), including the Xilamulun River to the south  
537 and the Gongger River to the north, both of which are stemming from the Greater  
538 Khingan Mountains (Daxing’Anling Mountains in Chinese pinyin, 1,100-1,400 m above  
539 seal level) (Fig. 1). The Xilamulun River carries a large amount of water (about  
540  $6.58 \times 10^8 \text{ m}^3/\text{y}$ ) from the Daxing’Anling Mountains flowing through the east margins  
541 of the Dali and Otindag (Wu et al., 2014). This is an important clue linking natural  
542 waters between the Otindag and Dali Basin.

543 Variation in the elevation from the Dali Lake to the riverhead of the Xilamulun  
544 River can be clearly found along a land surface topographical section (Fig. 11). The  
545 channel of the Xilamulun River is located in the Xar Moron Fault (Fig. 1), which is a  
546 part of the Solonker Suture Zone (Eizenhöfer et al., 2014) or the  
547 Xilamulun-Changchun-Yanji plate suture zone (Sun et al., 2004) in the regional  
548 tectonical settings (Fig. 2). Outcrop observations indicate that fault zones commonly  
549 have a permeability structure suggesting they should act as complex conduit–barrier  
550 systems in which along-fault flow is encouraged and across-fault flow is impeded  
551 (Bense et al., 2013). Thus the hydraulic gradient of groundwater flow in the Eastern  
552 margins of the Otindag and Dali Basin must be controlled by the fault zone  
553 hydrogeology. This may be the reason why the hydraulic gradient of groundwater  
554 represented by the isotopic and hydrogeochemical gradients of groundwater samples  
555 in this study is not consistent with the local topographical gradient in the Otindag  
556 Desert. On the other hand, the regional aquifer is generally unconfined in dune fields  
557 of the Otindag Desert but semi-confined to confined in the Daxing’Anling uplands (Fig.  
558 3), thus the thick unconsolidated aquifers in the study area (Figs. 3 and 11) will be  
559 favourable conditions for groundwater storage and transportation along the Solonker  
560 Suture Zone. When rivers stem from the Daxing’Anling Mountains and flow  
561 downward to the marginal areas of the Dali and Otindag, leakage water from these

562 rivers can recharge the desert land through thick unconsolidated aquifers. A strong  
563 isotopic evidence is that the lake and river waters in the Dali Basin share the same  
564 evaporation line (EL2) with the groundwaters in the PCSX area.

565 Although groundwaters in the SPCSX area are different from those in the NPCSX  
566 area, their isotopic data points still fell onto the EL2 (Fig. 9), which further indicates  
567 that the groundwaters in the SPCSX are a mixture of waters from the Daxing'Anling  
568 Mountain and other sources. Another source for groundwater recharge in the SPCSX  
569 could be represented by remote water such as flash floods coming from the north  
570 Yinshan Mountains, because it can be clearly observed from digital maps that many  
571 transient rivers or streams originated from the Yinshan Mountains flow into the  
572 south and southeastern Otindag (Fig. 1). Supportive evidence for this idea can also  
573 be observed in the summer rainy season. During rainy days or under storm  
574 conditions, fast-flowing floods caused by occasional short, heavy rainstorms can form  
575 in playas, wadi channels and low-lying depressions in the unconfined to  
576 semi-confined areas of the Yinshan Mountains' piedmont. These waters may  
577 temporarily recharge shallow aquifers in the SPCSX area.

578

#### 579 **4. 6. Speciation modeling and hydrogeological conceptual model**

580 Speciation modeling. Selected results of speciation modeling are provided in  
581 Table 6. All samples are undersaturated with respect to calcite, aragonite, dolomite,  
582 halite and gypsum. The values of  $\log P_{CO_2}$ , ranging between -4.77 and -1.45 in the  
583 samples from the sedimentary sandy aquifer, indicating that groundwater in the  
584 study area is not at equilibrium with atmospheric  $P_{CO_2}$ .

585 Based on the above analyses, a conceptual model of groundwater recharge was  
586 suggested to facilitate understanding of the hydrogeological conditions in the study  
587 area. Local and regional modern precipitation is a negligible source. Quaternary  
588 unconsolidated sediments with large exposed area form the main aquifer in the  
589 study area. Groundwater is recharged by cold water from remote mountain areas,  
590 and it flows from east to west along the Solonker Suture Zone. Evaporation is a minor  
591 process during groundwater hydrogeochemical evolution. Mineral dissolution may  
592 contribute to groundwater salinization, because saturation indices of all minerals are  
593 less than zero, indicating that these minerals still can dissolve into groundwater.  
594 These clues mean that the origin of groundwater in the desert is mainly controlled by  
595 geological structures and processes. The tectonic settings are more important than  
596 climatic and topographical settings to explain the origin of groundwater in the  
597 desert.

598 In a view of orogenic belt of the global middle-latitude regions, various  
599 groundwater and hydrogeological case studies have established a link between  
600 geological perspectives and origin of groundwater flows. Tague and Grant (2004)  
601 identify, for instance, the dominant control of a young volcanic geological unit on the  
602 groundwater regime of the studied region in Oregon, this geological formation  
603 having an exceptionally high permeability. Pfister et al. (2017) show that bedrock  
604 permeability significantly influences the ratio between average summer and winter  
605 run-off of 16 investigated catchments in Luxembourg. For a selection of Swiss  
606 catchments, Naef et al. (2015) associate lower groundwater flow with slowly draining  
607 porous bedrock and low streamflow during dry periods for catchments dominated by  
608 Moraine deposits. Kaser and Hunkeler (2016) have shown that alluvial aquifers, even

609 if they represent only a small portion of the catchment surface, can contribute  
610 significantly to the catchment groundwater outflow especially during low-flow  
611 periods. Alluvial aquifers can thus also be relevant for total catchment groundwater  
612 storage. Chen and Wang (2009) proposed that earthquake is a possible mechanism  
613 for groundwater releasing in the Qilian Mountains and discharging it in the Hexi  
614 Corridor. Carlier et al. (2018) statistically analyzed 22 catchments of the Swiss Plateau  
615 and Prealpes to establish relationships between streamflow indicators and various  
616 geological and hydrogeological properties of the bedrock and Quaternary deposits,  
617 along with meteorological, soil, land use, and topographical characteristics. The study  
618 shows that the geological characteristics dominate catchment response during high  
619 and low groundwater flow conditions.

620 These studies focused the influence of base/surrounding rock, topography,  
621 recharge source and permeability on groundwater flow in orogeny area. According to  
622 the hydrologically active bedrock hypothesis (Uchida et al. 2008) the bedrock is an  
623 active reservoir that significantly contributes to baseflow (Tague and Grant 2004;  
624 Andermann et al. 2012; Welch and Allen 2012; Birkel et al. 2014). The hydraulic  
625 conductivity of the bedrock controls storage processes (Hale et al. 2016; Pfister et al.  
626 2017). Most importantly, the ratio of the hydraulic conductivity to recharge rates has  
627 been shown to be relevant for water table elevation (Gleeson and Manning 2008).  
628 Haitjema and Mitchell-Bruker (2005) propose a criterion based on the  
629 Dupuit-Forchheimer approximation combining this ratio with geometrical aquifer  
630 properties and topographical characteristics to determine whether the water table is  
631 controlled by the topography or the recharge. From the above review it can be seen  
632 that various studies have used spatially distributed, synthetic groundwater models to  
633 identify and explore how topography, recharge and/or bedrock permeability  
634 influence groundwater fluxes and flow patterns (e.g., Gleeson and Manning 2008;  
635 Welch et al. 2012; Welch and Allen 2012; Welch and Allen 2014).

636 These studies highlight the complex interplay of topography and hydrogeology  
637 on groundwater flow. They, however, mainly focus on the geology of the bedrock, no  
638 studies mentioned the important role of tectonic structure on the groundwater flow.  
639 Thus, based on this study in the Otindag Desert, we proposed a simple conceptual  
640 model of multiprocesses that constrain the mechanism of groundwater recharge in  
641 the desert, namely mountain water (M) – tectonic fault hydrology (T) – unconfined  
642 vadose zone with underlying buried fault (V) – groundwater formation and recharge  
643 (G), i.e. the MTVG mechanism. Although the model is still conceptual but not  
644 practical at present, it provides a new perspective into the origin and evolution of  
645 groundwater resources in the middle-latitude deserts of the arid Asia.

646

## 647 **5. Conclusions**

648 In the middle-latitude desert zone of northern China, many deserts such as the  
649 Otindag and Badanjilin Deserts, are unexpectedly rich in groundwater resources,  
650 although they have no surface runoff and have been under an arid or hyper-arid  
651 climate for a long period of time. How groundwaters originated and recharged in  
652 these deserts are thus key questions that are still under debate. For some earth  
653 scientists, the direct recharge is thought to be very important for groundwaters in  
654 the wide desert lands of northern China, due to the lack of surface runoffs. However,  
655 groundwater availability is very much a function of the local- and regional-scale

656 geological and climatic settings. To achieve an integrated understanding of the  
657 groundwater recharge and its controlling mechanisms is of great significance. In this  
658 study, groundwater recharge was explored using multiple environmental tracers in  
659 the Otindag Desert of northern China, a region that is under the influence of the East  
660 Asian Summer Monsoon (EASM) climate. Compared to modern summer precipitation,  
661 the groundwaters, river waters and spring waters are depleted in  $\delta D$  and  $\delta^{18}O$ . All  
662 these waters shared a same Craig line, indicating a genetic relationship on their  
663 recharge sources. The stable isotopic signals of the groundwaters is more depleted  
664 than those of the modern summer precipitation and this suggests that the  
665 groundwaters studied could only be sourced from cold water different from the  
666 EASM precipitation. In general, the analyses revealed that the highland remote water  
667 resources from the Daxing'Anling and Yinshan Mountains were isotopically and  
668 geochemically traced to be a major source for the groundwater in the Otindag. It  
669 suggests that the modern indirect recharge mechanism, instead of the direct  
670 recharge and the palaeo-water recharge, is the most significant for groundwater  
671 recharge in the eastern Otindag. This study provides a new perspective into the  
672 origin and evolution of groundwater resources in the middle-latitude desert zone of  
673 northern China.

674

#### 675 **Acknowledgements**

676 This study was financially supported by the National Natural Science Foundation  
677 of China (41771014), the National Key Research and Development Program of China  
678 (2016YFA0601900), and the National Natural Science Foundation of China  
679 (41602196). We thank the China Meteorological Data Sharing Service system for  
680 providing the weather data. Sincere thanks are also extended to Profs. Xiaoping Yang,  
681 Xunming Wang, Jule Xiao and other workmates, e.g., Ziting Liu, Hongwei Li, and  
682 DeguoZhang for their generous help in the research work.

683

#### 684 **References:**

- 685 Andermann, C., Longuevergne, L., Bonnet, S., Crave, A., Davy, P., and Gloaguen, R.:  
686 Impact of transient groundwater storage on the discharge of Himalayan rivers.  
687 Nature Geoscience, 5, 127-132, 2012.
- 688 Bazuhair, A.S., and Wood, W.W.: Chloride mass-balance method for estimating  
689 ground water recharge in arid areas: examples from western Saudi Arabia.  
690 Journal of Hydrology, 186, 153-159, 1996.
- 691 Bense, V.F., Gleeson, T., Loveless, S.E., Bour, O., and Scibek, J.: Fault zone  
692 hydrogeology. Earth-Science Reviews, 127, 171-192, 2013.
- 693 Birkel, C., Soulsby, C., and Tetzlaff, D.: Developing a consistent process-based  
694 conceptualization of catchment functioning using measurements of internal  
695 state variables. Water Resources Research, 50, 3481-3501, 2014.
- 696 Blasch, K.W., and Bryson, J.R.: Distinguishing sources of ground water recharge by  
697 using  $\delta^2H$  and  $\delta^{18}O$ . Ground Water, 45, 294-308, 2007.
- 698 Boronina, A., Renard, P., Balderer, W., and Stichler, W.: Application of tritium in  
699 precipitation and in groundwater of the Kouris catchment (Cyprus) for  
700 description of the regional groundwater flow. Applied Geochemistry, 20,  
701 1292-1308, 2005.
- 702 Carlier, C., Wirth, S.B., Cochand, F., Hunkeler, D., and Brunner, P.: Geology controls

703 streamflow dynamics. *Journal of Hydrology*, 566, 756–769, 2018.

704 Chebotarev, I.I.: Metamorphism of natural waters in the crust of weathering.  
705 *Geochimica et Cosmochimica Acta*, 8, 22-32, 1955.

706 Chen, F., Chen, J., Holmes, J., Boomer, I., Austin, P., Gates, J.B., Wang, N., Brooks, S.J.,  
707 and Zhang, J.: Moisture changes over the last millennium in arid central Asia: a  
708 review, synthesis and comparison with monsoon region. *Quaternary Science*  
709 *Reviews*, 29, 1055-1068, 2010.

710 Chen, J., Chen, X., and Wang, T.: Isotopes tracer research of wet sand layer water  
711 sources in Alxa Desert. *Advances in Water Science*, 25, 196-206 , 2014 (in  
712 Chinese).

713 Chen, J., Li, L., Wang, J., Barry, D.A., Sheng, X., Gu, W., Zhao, X., and Chen, L.: Water  
714 resources: groundwater maintains dune landscape. *Nature*, 432, 459-460, 2004.

715 Chen, J., Liu, X., Wang, C., Rao, W., Tan, H., Dong, H., Sun, X., Wang, Y., and Su, Z.:  
716 Isotopic constraints on the origin of groundwater in the Ordos Basin of northern  
717 China. *Environmental Earth Sciences*, 66, 505-517, 2012a.

718 Chen, J., Sun, X., Gu, W., Tan, H., Rao, W., Dong, H., Liu, X., and Su, Z.: Isotopic and  
719 hydrochemical data to restrict the origin of the groundwater in the Badain Jaran  
720 Desert, Northern China. *Geochemistry International* 50, 455-465, 2012b.

721 Chen, J.S., and Wang, C.Y.: Rising springs along the Silk Road. *Geology* 37, 243-246,  
722 2009.

723 Chen, J., Yang, Q., and Hao, G.: Using hydrochemical and environmental isotopical  
724 data to analyse groundwater recharge in the Hunshandake Sandy Land. *Inner*  
725 *Mongolia Science Technology & Economy*, 17, 9-12, 2008 (in Chinese).

726 Clark, I.D.: *Groundwater Geochemistry and Isotopes*. CRC Press, Boca Raton, 2015.

727 Craig, H.: Isotopic Variations in Meteoric Waters. *Science*, 133, 1702-1703, 1961.

728 Dansgaard, W.: Stable isotopes in precipitation. *Tellus*, 16, 436-468, 1964.

729 Dogramaci, S., Skrzypek, G., Dodson, W., and Grierson, P.F.: Stable isotope and  
730 hydrochemical evolution of groundwater in the semi-arid Hamersley Basin of  
731 subtropical northwest Australia. *Journal of hydrology*, 475, 281-293, 2012.

732 Doll, P., and Fiedler, K.: Global-scale modeling of groundwater recharge. *Hydrology*  
733 *and Earth System Sciences*, 12, 863-885, 2008.

734 Doll, P.: Vulnerability to the impact of climate change on renewable groundwater  
735 resources: a global-scale assessment. *Environmental Research Letters*, 4, 035006,  
736 doi:10.1088/1748-9326/4/3/035006, 2009.

737 Drever, J.I.: Catchment mass balance. In: Saether, O.M., and de Caritat, P. (Eds.),  
738 *Geochemical Processes, Weathering and Groundwater Recharge in Catchments*.  
739 A.A, Balkema, Rotterdam, pp. 241-261, 1997.

740 Edmunds, W.M., Ma, J., Aeschbach-Hertig, W., Kipfer, R., and Darbyshire, D.P.F.:  
741 Groundwater recharge history and hydrogeochemical evolution in the Minqin  
742 Basin, North West China. *Applied Geochemistry*, 21, 2148-2170, 2006.

743 Eizenhöfer, P.R., Zhao, G., Zhang, J., and Sun, M.: Final closure of the Paleo-Asian  
744 Ocean along the Solonker Suture Zone: Constraints from geochronological and  
745 geochemical data of Permian volcanic and sedimentary rocks. *Tectonics*, 33,  
746 441-463, 2014.

747 Freeze, R.A., and Cherry, J.A.: *Groundwater*. Prentice-Hall, Inc, New Jersey, 1979.

748 Gat, J.R.: Precipitation, groundwater and surface waters: control of climate  
749 parameters on their isotopic composition and their utilization as

750 palaeoclimatological tools. In: Palaeoclimates and palaeowaters: a collection of  
751 environmental isotope studies. Proc. Adv. Gp. Meeting, Vienna, 25–28 Nov 1980,  
752 pp 3–12, IAEA, Vienna, 1983.

753 Gat, J.R., and Issar, A.: Desert isotope hydrology: water sources of the Sinai Desert.  
754 *Geochimica et Cosmochimica Acta*, 38, 1117-1131, 1974.

755 Gates, J., Edmunds, W.M., Ma, J., and Scanlon, B.: Estimating groundwater recharge  
756 in a cold desert environment in northern China using chloride. *Hydrogeology*  
757 *Journal*, 16, 893-910, 2008.

758 Giordano, M.: Global groundwater? Issues and solutions. *Annual Review of*  
759 *Environment and Resources*, 34, 153-178, 2009.

760 Gleeson, T., and Manning, A.H.: Regional groundwater flow in mountainous terrain:  
761 Three-dimensional simulations of topographic and hydrogeologic controls.  
762 *Water Resources Research*, 44, 1-16, 2008.

763 Guendouz, A., Moulla, A.S., Edmunds, W.M., Zouari, K., Shand, P., and Mamou, A.:  
764 Hydrogeochemical and isotopic evolution of water in the Complexe Terminal  
765 aquifer in the Algerian Sahara. *Hydrogeology Journal*, 11, 483-495, 2003.

766 Haitjema, H.M., and Mitchell-Bruker, S.: Are water tables a subdued replica of the  
767 topography? *Ground Water*, 43, 781-786, 2005.

768 Hale, V.C., McDonnell, J.J., Stewart, M.K., Solomon, D.K., Doolittle, J., Ice, G.G., and  
769 Pack, R.T.: Effect of bedrock permeability on stream base flow mean transit time  
770 scaling relationships: 2. Process study of storage and release. *Water Resources*  
771 *Research*, 52, 1375-1397, 2016.

772 Healy, R.W.: Estimating groundwater recharge. Cambridge University Press, New York,  
773 2010.

774 Herczeg, A.L., and Leaney, F.: Review: environmental tracers in arid-zone hydrology.  
775 *Hydrogeology Journal*, 19, 17-29, 2011.

776 Jahn, B.M.: The Central Asian Orogenic Belt and growth of the continental crust in  
777 the Phanerozoic. *Geological Society London Special Publications*, 226, 73-100,  
778 2004.

779 Jian, P., Liu, D., Kroner, A., Windley, B.F., Shi, Y., Zhang, W., Zhang, F., Miao, L., Zhang,  
780 L., and Tomurhuu, D.: Evolution of a Permian intraoceanic arc-trench system in  
781 the Solonker suture zone, Central Asian Orogenic Belt, China and Mongolia.  
782 *Lithos*, 118, 169-190, 2010.

783 Jin, K., Rao, W., Tan, H., Song, Y., Yong, B., Zheng, Y., Chen, T., and Han, L.: H-O isotopic  
784 and chemical characteristics of a precipitation-lake water-groundwater system  
785 in a desert area. *Journal of Hydrology*, 559, 848-860, 2018.

786 Jobbágy, E., Noretto, M., Villagra, P., and Jackson, R.: Water subsidies from mountains  
787 to deserts: their role in sustaining groundwater-fed oases in a sandy landscape.  
788 *Ecological Applications*, 21, 678-694, 2011.

789 Kaser, D., and Hunkeler, D.: Contribution of alluvial groundwater to the outflow of  
790 mountainous catchments. *Water Resources Research*, 52, 680-697, 2016.

791 Kazemi, G.A., Lehr, J.H., and Perrochet, P.: Groundwater age. John Wiley & Sons,  
792 Hoboken, 2006.

793 Li, J.: Permian geodynamic settings of Northeast China and adjacent regions: closure  
794 of the Paleo-Asian Ocean and subduction of the Paleo-Pacific Plate. *Journal of*  
795 *Asian Earth Sciences*, 26, 207-224.

796 Li, S., Sun, W., Li, X., and Zhang, B.: Sedimentary characteristics and environmental

797 evolution of Otindag sandy land in Holocene. *Journal of Desert Research*, 15,  
798 323-331, 1995 (in Chinese).

799 Liu, Z., and Yang, X.: Geochemical-geomorphological evidence for the provenance of  
800 aeolian sands and sedimentary environments in the Hunshandake Sandy Land,  
801 eastern Inner Mongolia, China. *Acta Geologica Sinica (English Edition)*, 87,  
802 871-884, 2013.

803 Love, A.J., Herczeg, A.L., Leaney, F.W., Stadter, M.H., Dighton, J.C., and Armstrong, D.:  
804 Groundwater residence time and palaeohydrology in the Otway Basin, South  
805 Australia. *Journal of Hydrology*, 153, 157–187, 1994.

806 Love, A.J., Herczeg, A.L., Sampson, L., Cresswell, R.G., and Fifield, L.K.: Sources of  
807 chloride and implications for <sup>36</sup>Cl dating of old groundwater, south-western  
808 Great Artesian basin, Australia. *Water Resources Research*, 36(6), 1561-1574,  
809 2000.

810 Ma, J., Ding, Z., Gates, J.B., and Su, Y.: Chloride and the environmental isotopes as the  
811 indicators of the groundwater recharge in the Gobi Desert, northwest China.  
812 *Environmental Geology*, 55, 1407-1419, 2008.

813 Ma, J., and Edmunds, W.M.: Groundwater and lake evolution in the BadainJaran  
814 Desert ecosystem, Inner Mongolia. *Hydrogeology Journal*, 14, 1231-1243, 2006.

815 Ma, J., Pan, F., Chen, L., Edmunds, W.M., Ding, Z., He, J., Zhou, K., and Huang, T.:  
816 Isotopic and geochemical evidence of recharge sources and water quality in the  
817 Quaternary aquifer beneath Jinchang city, NW China. *Applied Geochemistry*, 25,  
818 996-1007, 2010.

819 Merlivat, L., and Jouzel, J.: Global climatic interpretation of the deuterium-oxygen 18  
820 relationship for precipitation. *Journal of Geophysical Research*, 84, 5029-5033,  
821 1979.

822 Meybeck, M.: Global occurrence of major elements in rivers. In: Drever, J.I. (Ed.),  
823 *Surface and Ground Water, Weathering, and Soils*. Holland, H.D., and Turekian,  
824 K.K. (Exec.Eds), *Treatise on Geochemistry*, vol. 5. Elsevier-Pergamon, Oxford, pp.  
825 207-223, 2004.

826 Naef, F., Margreth, M., and Floriancic, M.: Festlegung von Restwassermengen: Q347,  
827 eine entscheidende, aber schwer zu fassende Größe. *Wasser Energie Luft*, Heft  
828 4(107. Jahrgang), 277–284, 2015.

829 Petrides, B., Cartwright, I., and Weaver, T.R.: The evolution of groundwater in the  
830 Tyrrell catchment, south-central Murray Basin, Victoria, Australia. *Hydrogeology*  
831 *Journal*, 14, 1522-1543, 2006.

832 Pfister, L., Martinez-Carreras, N., Hissler, C., Klaus, J., Carrer, G.E., Stewart, M.K., and  
833 McDonnell, J.J.: Bedrock geology controls on catchment storage, mixing, and  
834 release: A comparative analysis of 16 nested catchments. *Hydrological Processes*,  
835 31, 1828-1845, 2017.

836 Rizk, Z.S., and El-Etr, H.A.: Hydrogeology and hydrogeochemistry of some springs in  
837 the United Arab Emirates. *Arabian Journal for Science and Engineering*, 22,  
838 95-111, 1997.

839 Scanlon, B.R., Keese, K.E., Flint, A.L., Flint, L.E., Gaye, C.B., Edmunds, W.M., and  
840 Simmers, I.: Global synthesis of groundwater recharge in semiarid and arid  
841 regions. *Hydrological Processes*, 20, 3335-3370, 2006.

842 Seiler, K.P., and Gat, J.R.: *Groundwater Recharge From Run-Off, Infiltration and*  
843 *Percolation*. Springer, The Netherlands, 2007.

844 Stolp, B.J., Solomon, D.K., Suckow, A., Vitvar, T., Rank, D., Aggarwal, P.K., and Han, L.F.:  
845 Age dating base flow at springs and gaining streams using helium-3 and tritium:  
846 Fische-Dagnitz system, southern Vienna Basin, Austria. *Water Resources*  
847 *Research*, 46, W07503, doi:10.1029/2009WR008006, 2010.

848 Sultan, M., Sturchio, N., Gheith, H., Hady, Y.A., and Anbeawy, M.: Chemical and  
849 Isotopic Constraints on the Origin of Wadi Elitarfa Ground Water, Eastern Desert,  
850 Egypt. *Ground Water*, 38, 743-751, 2000.

851 Sun, D., Wu, F., Zhang, Y., and Gao, S.: The final closing time of the west Lamulun  
852 River-Changchun-Yanji plate suture zone-Evidence from the Dayushan granitic  
853 pluton, Jilin Province. *Journal of Jilin University (Earth Science Edition)*, 34,  
854 174-181, 2004 (in Chinese).

855 Sun, J., Ye, J., Wu, W., Ni, X., Bi, S., Zhang, Z., Liu, W., and Meng, J.: Late  
856 Oligocene-Miocene mid-latitude aridification and wind patterns in the Asian  
857 interior. *Geology*, 38, 515–518, 2010.

858 Tague, C., and Grant G.E.: A geological framework for interpreting the low-flow  
859 regimes of Cascade streams, Willamette River basin, Oregon. *Water Resources*  
860 *Research*, 40(4), 1-9, 2004.

861 Tian, F., Wang, Y., Liu, J., Tang, W., and Jiang, N.: Late Holocene climate change  
862 inferred from a lacustrine sedimentary sequence in southern Inner Mongolia,  
863 China. *Quaternary International*, 452, 22-32, 2017.

864 Uchida, T., Miyata, S., and Asano Y.: Effects of the lateral and vertical expansion of the  
865 water flowpath in bedrock on temporal changes in hillslope discharge.  
866 *Geophysical Research Letters*, 35, 2-6, 2008.

867 Wang, P., Yu, J., Zhang, Y., and Liu, C.: Groundwater recharge and hydrogeochemical  
868 evolution in the Ejina Basin, northwest China. *Journal of Hydrology*, 476, 72-86,  
869 2013.

870 Wang, Q., and Liu, X.Y.: Paleoplate tectonics between Cathaysia and Angaraland in  
871 Inner Mongolia of China. *Tectonics*, 5, 1073-1088, 1986.

872 Wang, W., and Feng, Z.D.: Holocene moisture evolution across the Mongolian Plateau  
873 and its surrounding areas: a synthesis of climatic records. *Earth-Science Reviews*,  
874 122, 38-57, 2013.

875 Welch, L.A., and Allen, D.M.: Consistency of groundwater flow patterns in  
876 mountainous topography: Implications for valley bottom water replenishment  
877 and for defining groundwater flow boundaries. *Water Resources Research*, 48,  
878 1-17, 2012.

879 Welch, L.A.A., Allen, D.M.M., and van Meerveld, H.J.: Topographic controls on deep  
880 groundwater contributions to mountain headwater streams and sensitivity to  
881 available recharge. *Canadian Water Resources Journal*, 37, 349-371, 2012.

882 Welch, L.A., and Allen, D.M.: Hydraulic conductivity characteristics in mountains and  
883 implications for conceptualizing bedrock groundwater flow. *Hydrogeology*  
884 *Journal*, 22, 1003-1026, 2014.

885 Wu, J., An, N., Ji, Y., and Wei, X.: Analysis on Characteristics of Precipitation and  
886 Runoff in Silas MuLun River Basin. *Meteorology Journal of Inner Mongolia*,  
887 23-25, 2014 (in Chinese).

888 Xiao, J., Si, B., Zhai, D., Itoh, S., and Lomtadze, Z.: Hydrology of Dali Lake in  
889 central-eastern Inner Mongolia and Holocene East Asian monsoon variability.  
890 *Journal of Paleolimnology*, 40, 519-528, 2008.

891 Yang, X., Li, H., and Conacher, A.: Large-scale controls on the development of sand  
892 seas in northern China. *Quaternary International*, 250, 74-83, 2012.

893 Yang, X., Ma, N., Dong, J., Zhu, B., Xu, B., Ma, Z., and Liu, J.: Recharge to the  
894 inter-dune lakes and Holocene climatic changes in the BadainJaran Desert,  
895 western China. *Quaternary Research*, 73, 10-19, 2010.

896 Yang, X., Scuderi, L.A., Wang, X., Scuderi, L.J., Zhang, D., Li, H., Forman, S., Xu, Q.,  
897 Wang, R., Huang, W., and Yang, S.: Groundwater sapping as the cause of  
898 irreversible desertification of Hunshandake Sandy Lands, Inner Mongolia,  
899 northern China. *PNAS*, 112, 702-706, 2015.

900 Yang, X., Wang, X., Liu, Z., Li, H., Ren, X., Zhang, D., Ma, Z., Rioual, P., Jin, X., and  
901 Scuderi, L.: Initiation and variation of the dune fields in semi-arid China – with a  
902 special reference to the Hunshandake Sandy Land, Inner Mongolia. *Quaternary  
903 Science Reviews*, 78, 369-380, 2013.

904 Yang, X., and Williams, M.A.J.: The ion chemistry of lakes and late Holocene  
905 desiccation in the BadainJaran Desert, Inner Mongolia, China. *Catena*, 51, 45-60,  
906 2003.

907 Yang, X., Zhu, B., Wang, X., Li, C., Zhou, Z., Chen, J., Yin, J., and Lu, Y.: Late Quaternary  
908 environmental changes and organic carbon density in the Hunshandake Sandy  
909 Land, eastern Inner Mongolia, China. *Global and Planetary Change*, 61, 70-78,  
910 2008.

911 Yao, S., Zhu, Z., Zhang, S., Zhang, S., and Li, Y.: Using SWAT model to simulate the  
912 discharge of the river Shandianhe in Inner Mongolia. *Journal of Arid Land  
913 Resources and Environment*, 27, 175-180, 2013 (in Chinese).

914 Zhang, Z., Li, K., Li, J., Tang, W., Chen, Y., and Luo, Z.: Geochronology and  
915 geochemistry of the Eastern Erenhot ophiolitic complex: implications for the  
916 tectonic evolution of the Inner Mongolia-Daxinganling Orogenic Belt. *Journal of  
917 Asian Earth Sciences*, 97, 279-293, 2015.

918 Zhao, J., Ma, Y., Luo, X., Yue, D., Shao, T., and Dong, Z.: The discovery of surface runoff  
919 in the megadunes of BadainJaran Desert, China, and its significance. *Science  
920 China Earth Sciences*, 60, 707-719, 2017.

921 Zhao, L., Xiao, H., Dong, Z., Xiao, S., Zhou, M., Cheng, G., Yin, L., and Yin, Z.: Origins of  
922 groundwater inferred from isotopic patterns of the Badain Jaran Desert,  
923 Northwestern China. *Ground Water*, 50, 715-725, 2012.

924 Zhen, Z., Li, C., Li, W., Hu, Q., Liu, X., Liu, Z., and Yu, R.: Characteristics of  
925 environmental isotopes of surface water and groundwater and their recharge  
926 relationships in Lake Dali basin. *Journal of Lake Sciences*, 26, 916-922, 2014 (in  
927 Chinese).

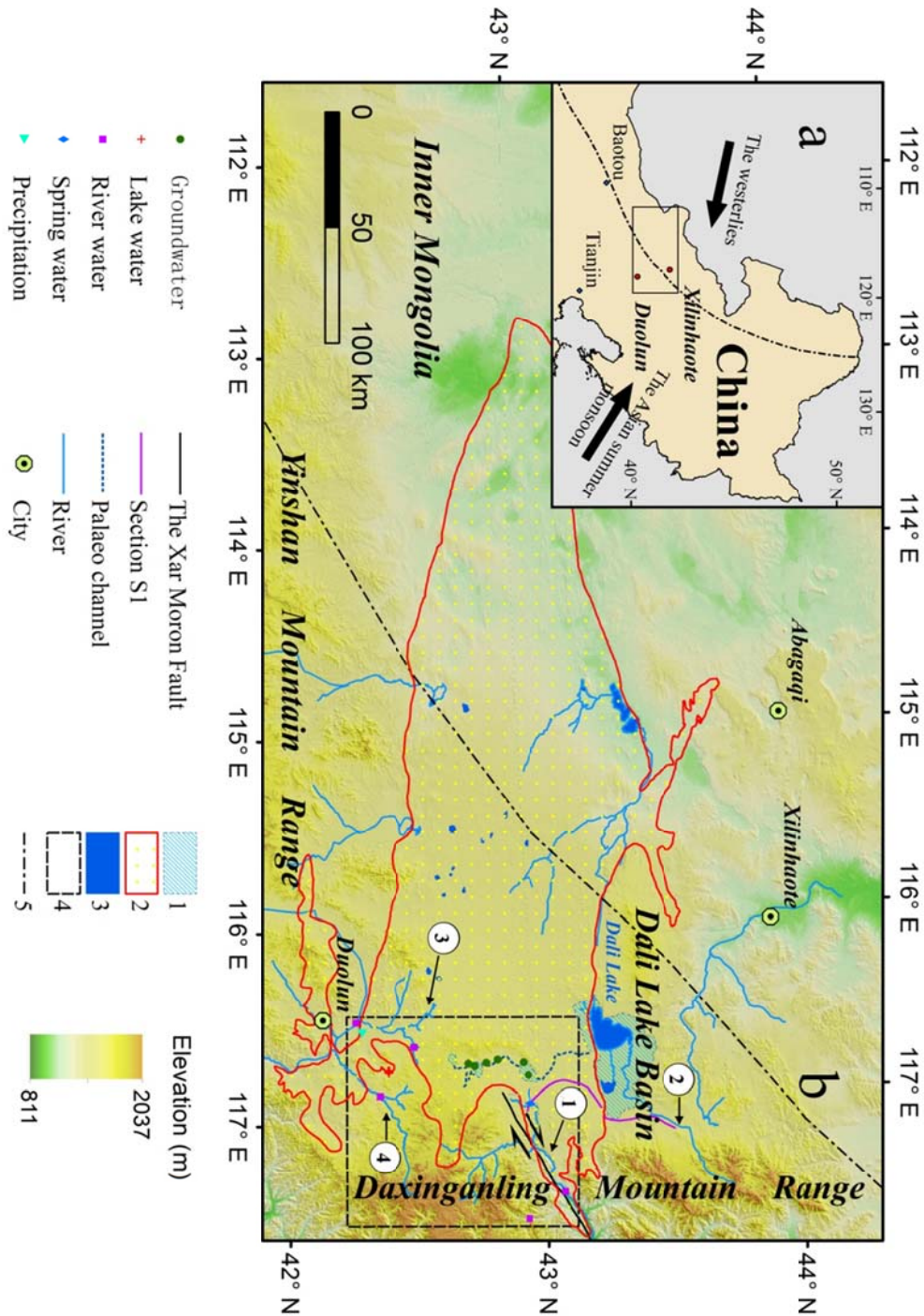
928 Zhu, B.Q., Yu, J.J., Rioual, P., Gao, Y., Zhang, Y.C., and Xiong, H.G.: Climate effects on  
929 recharge and evolution of natural water resources in middle-latitude  
930 watersheds under arid climate. In: Ramkumar, M. U., Kumaraswamy, K, and  
931 Mohanraj, R. (Eds.), *Environmental Management of River Basin Ecosystems*.  
932 Springer Earth System Sciences, Springer-Verlag, Heidelberg, pp. 91-109, 2015.

933 Zhu, B.Q., Wang, X.M., and Rioual, P.: Multivariate indications between environment  
934 and ground water recharge in a sedimentary drainage basin in northwestern  
935 China. *Journal of Hydrology*, 2017, 549, 92-113, 2017.

936 Zhu, G.F., Li, Z.Z., Su, Y.H., Ma, J.Z., and Zhang, Y.Y.: Hydrogeochemical and isotope  
937 evidence of groundwater evolution and recharge in Minqin Basin, Northwest

938 China. Journal of Hydrology, 333, 239-251, 2007.  
939 Zhu, G.F., Su, Y.H., and Feng, Q.: The hydrochemical characteristics and evolution of  
940 groundwater and surface water in the Heihe River Basin, northwest China.  
941 Hydrogeology Journal, 16, 167-182, 2008.  
942 Zhu, Z., Wu, Z., Liu, S., and Di, X.: An Outline of Chinese Deserts. Science Press,  
943 Beijing, 1980 (in Chinese).  
944  
945

946 **Figure Captions:**  
947 **Fig. 1.** The Geographical location of the Otindag Desert in northern China. (a) The  
948 study area shown at a large scale, and (b) the study area shown at a smaller scale,  
949 with detailed information about the boundary and tectonic settings of the desert  
950 land. 1, the palaeo lake area of the megalake Dali; 2, the boundary of the Otindag; 3,  
951 the modern lake area; 4, the boundary of Fig. 2; 5, the boundary between the  
952 westerlies and the East Asian Summer Monsoon (EASM) climate systems. ①, the  
953 Xilamulun River. ②, the Gonggeer River. ③, the Shepi River. ④, the Tuligen River.  
954 The boundary between the westerlies and the EASMin (a) and (b) is modified from  
955 Chen et al. (2010). The palaeo lake area of the megalake Dali and the palaeo channel  
956 in (b) is modified from Yang et al. (2015). The location of the Xar Moron Fault is  
957 referenced from Eizenhöfer et al. (2014). Section S1 is an elevation section starting  
958 from the upstream of the Dali Lake and ending with a spring sample (s2) in the  
959 riverhead of Xilamulun River.



961  
 969 **Fig. 2.** (a) Tectonic framework of the north China-Mongolian segment of the Central  
 970 Asian Orogenic Belt (modified after Jahn, 2004). (b) Geological sketch map of the  
 971 northern China-Mongolia tract (modified after Jian et al., 2010). The Solonker suture  
 972 zone represents the tectonic boundary between the northern (Hutag Uul  
 973 Block-Northern orogen) and the southern (southern orogen-Northern margin of  
 974 North China craton) continental blocks. Note that the red line marks the early  
 975 Permian paleobiogeographical boundary (Wang and Liu, 1986; Li, 2006), which  
 976 coincides with the northern boundary of the suture zone.

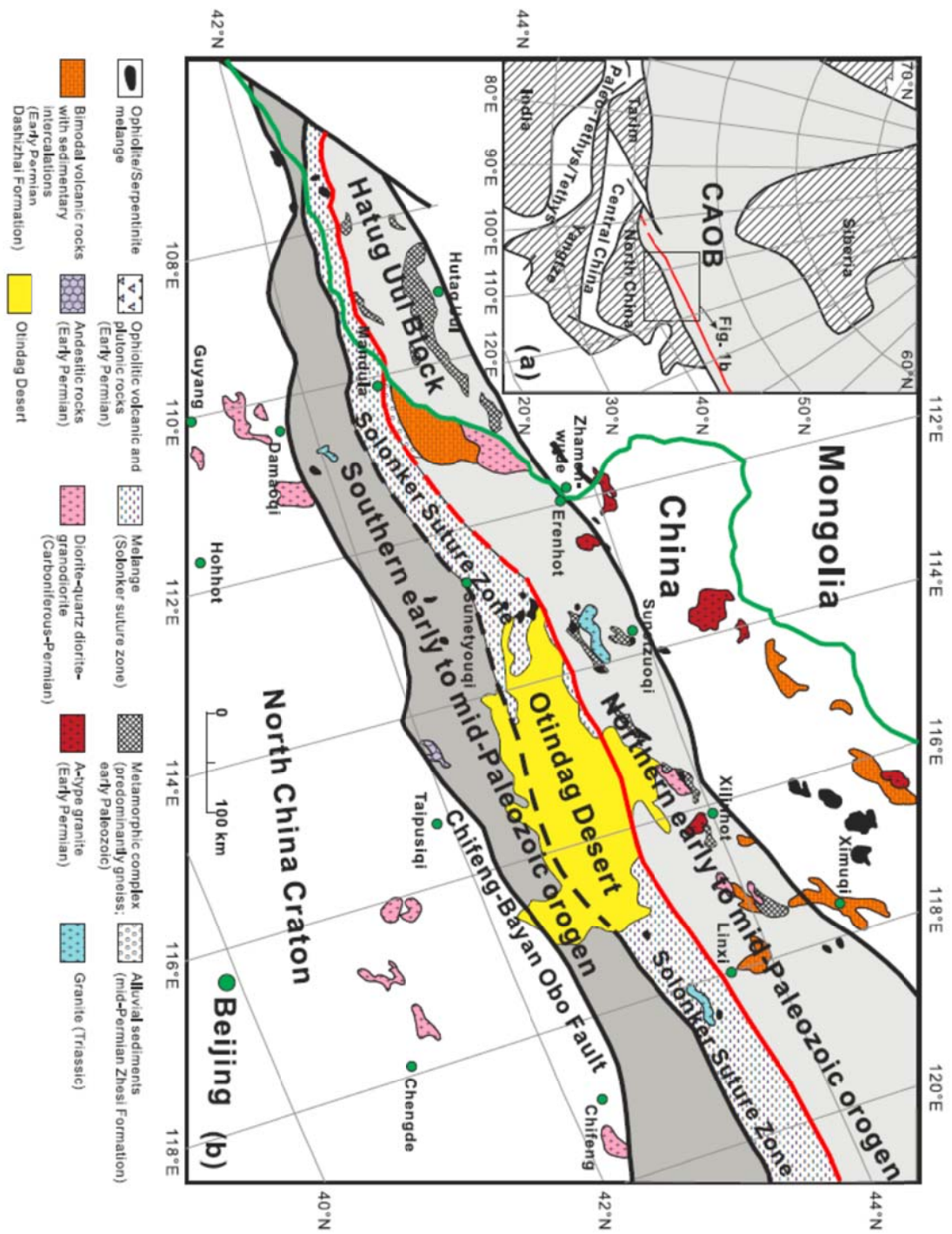
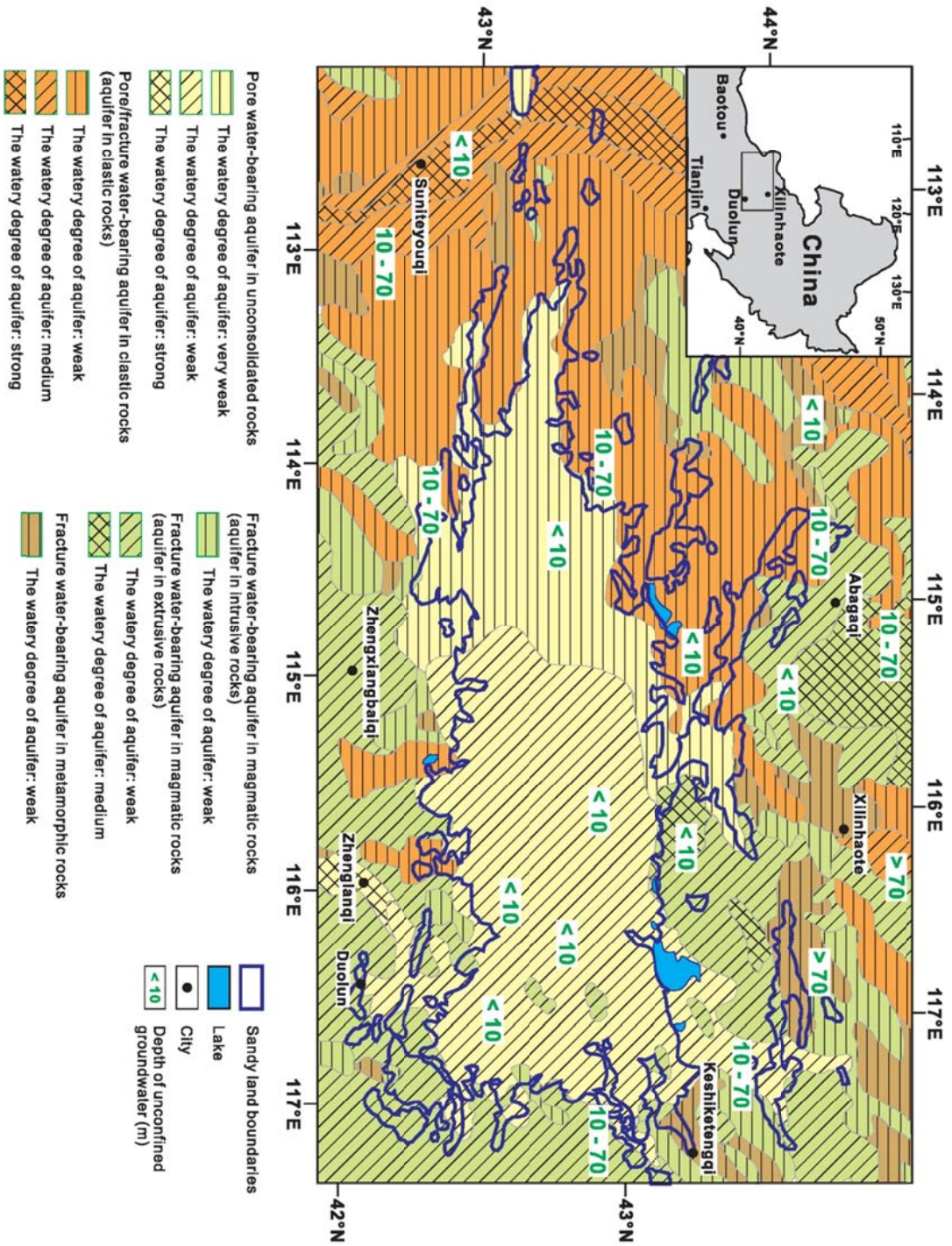


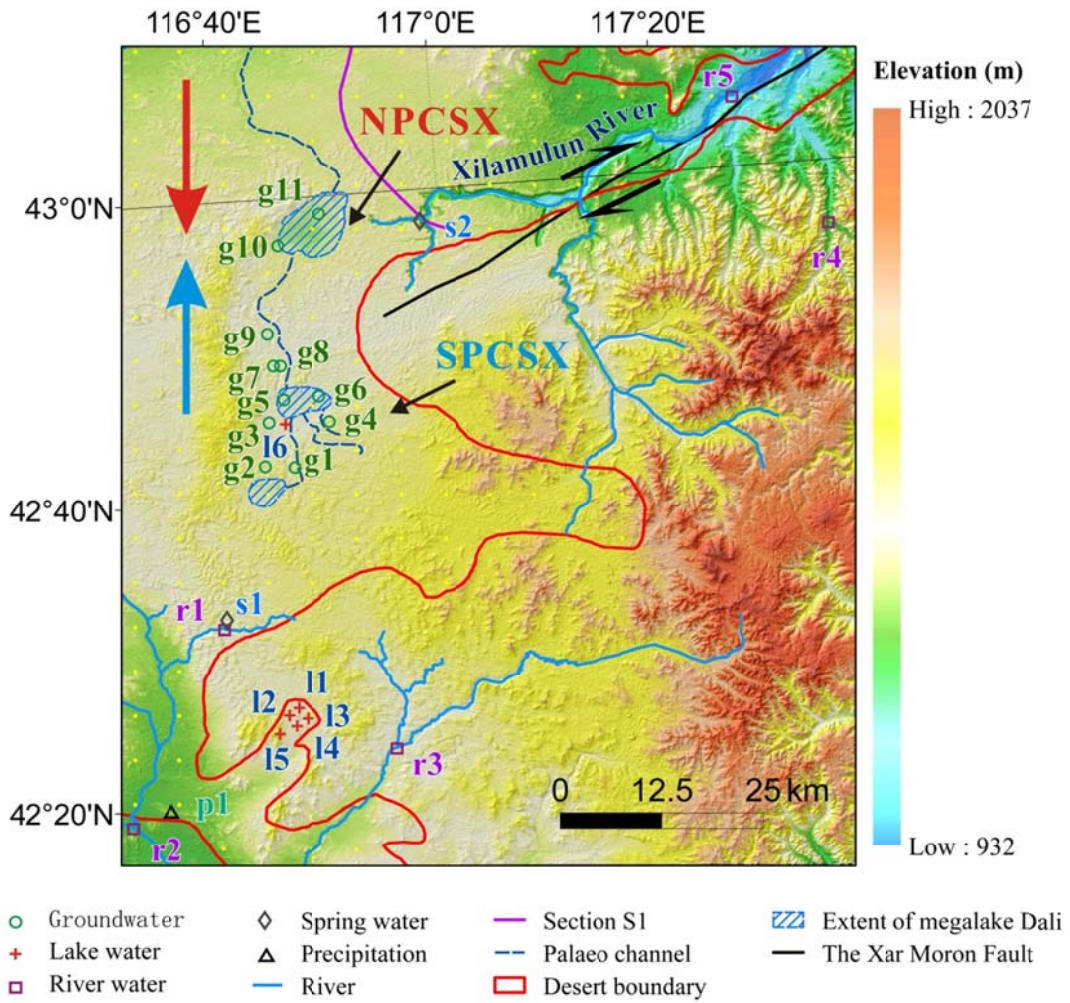
Fig. 3. The hydrogeological division map of the Otindag Desert.



979  
980  
981  
982  
983  
984  
985  
986  
987  
988  
989

990  
 991  
 992

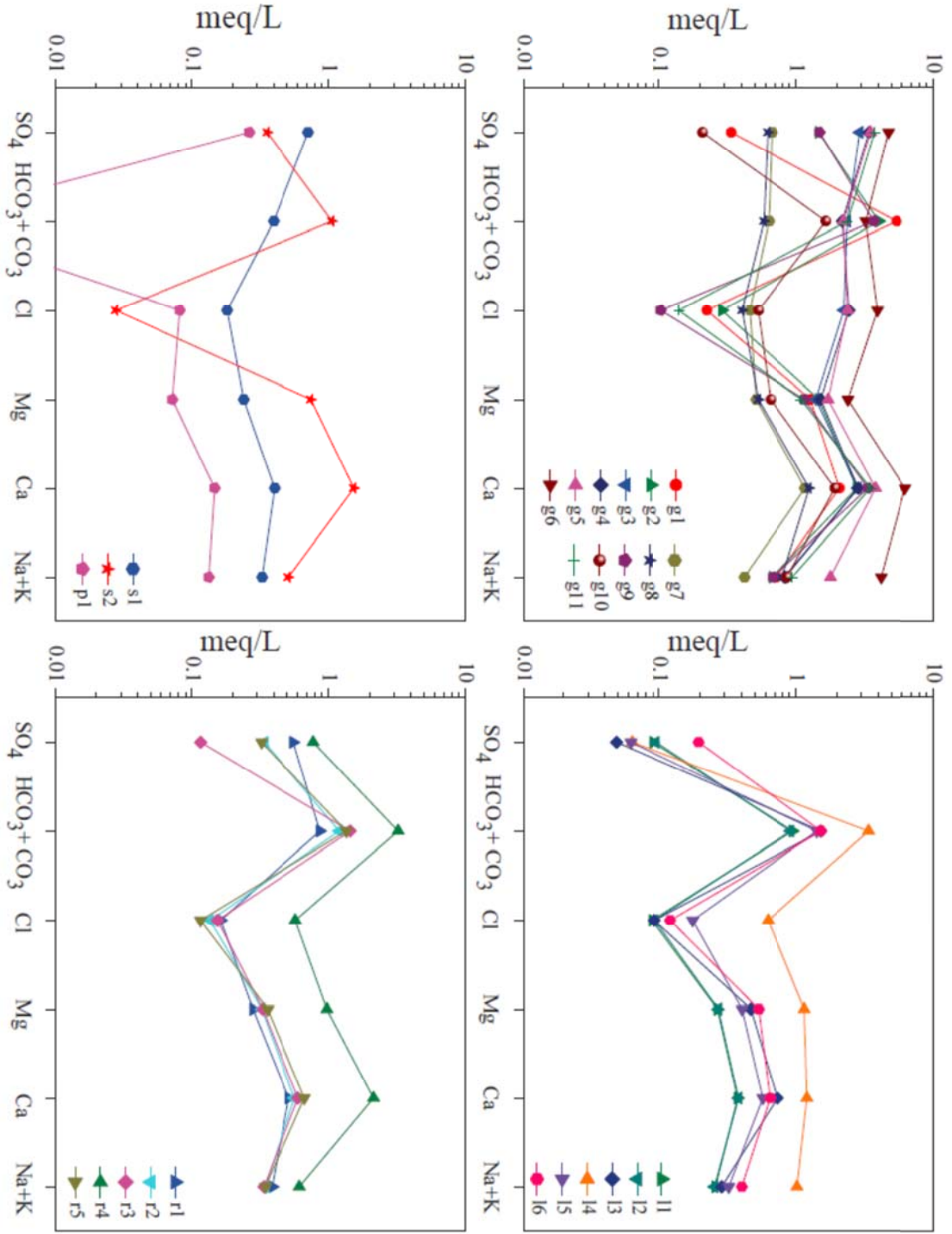
**Fig. 4.** The locations of the water sampling sites in this study.



993  
 994  
 995  
 996  
 997  
 998  
 999  
 1000  
 1001  
 1002  
 1003  
 1004  
 1005  
 1006  
 1007  
 1008  
 1009  
 1010  
 1011

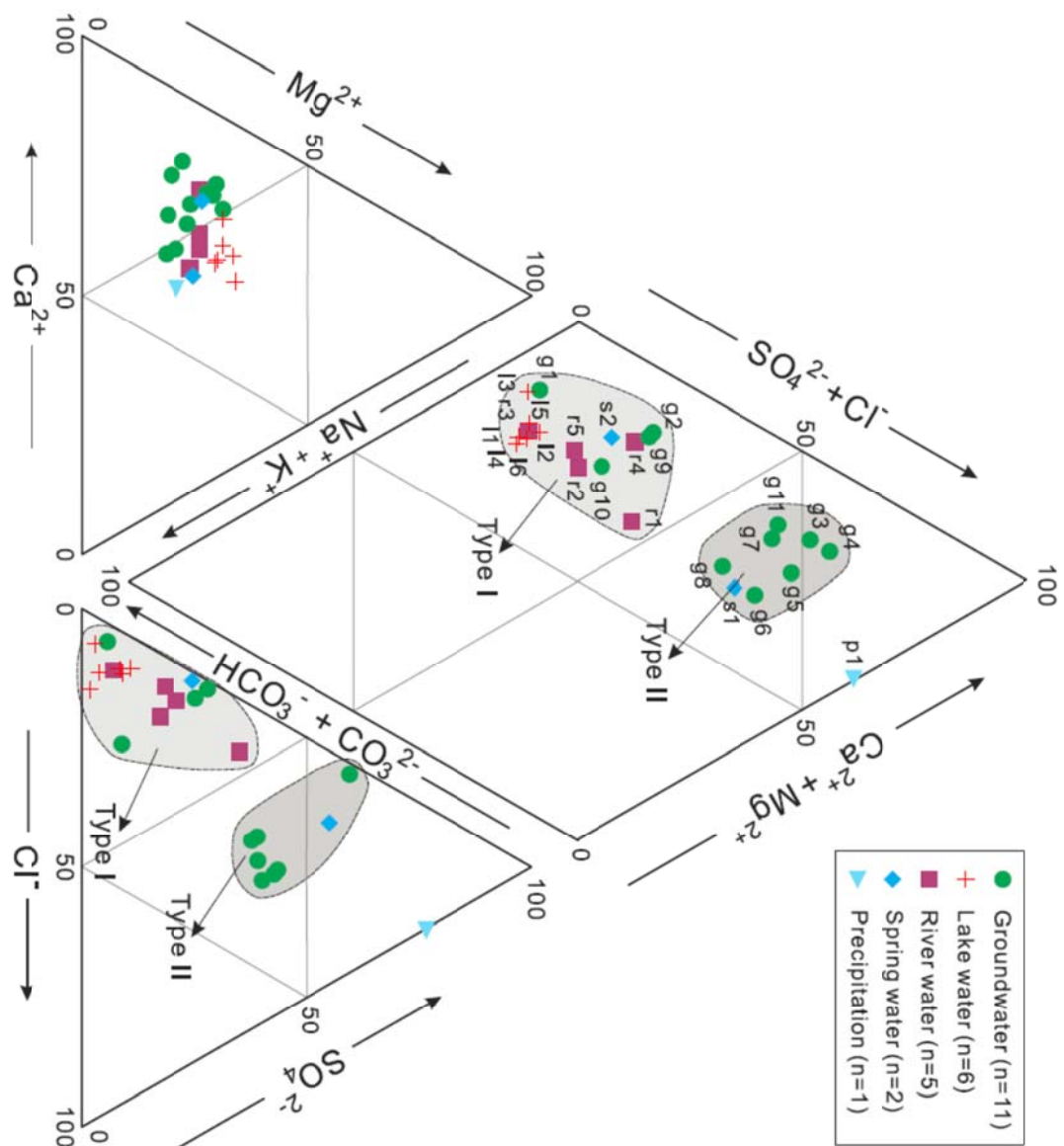
1011  
1012  
1013  
1014  
1015  
1016  
1017  
1018

1019 **Fig. 5.** The fingerprint diagram showing the variations of multiple ions'  
1020 concentrations in the studied water samples in an equivalent unit. The  $\text{HCO}_3+\text{CO}_3$   
1021 concentration in the sample p1 was not shown, due to its value being lower than the  
1022 detection limit.



1024  
 1025  
 1026  
 1027  
 1028  
 1029  
 1030  
 1031  
 1032  
 1033  
 1034

1037 **Fig. 6.** The Piper diagram showing the relative abundances of major cations and  
 1038 anions in the studied water samples. Major water types are also shown in this  
 1039 diagram.



1038  
 1039  
 1040  
 1041  
 1042  
 1043  
 1044  
 1045  
 1046  
 1047  
 1048  
 1049  
 1050  
 1051

1052

1053

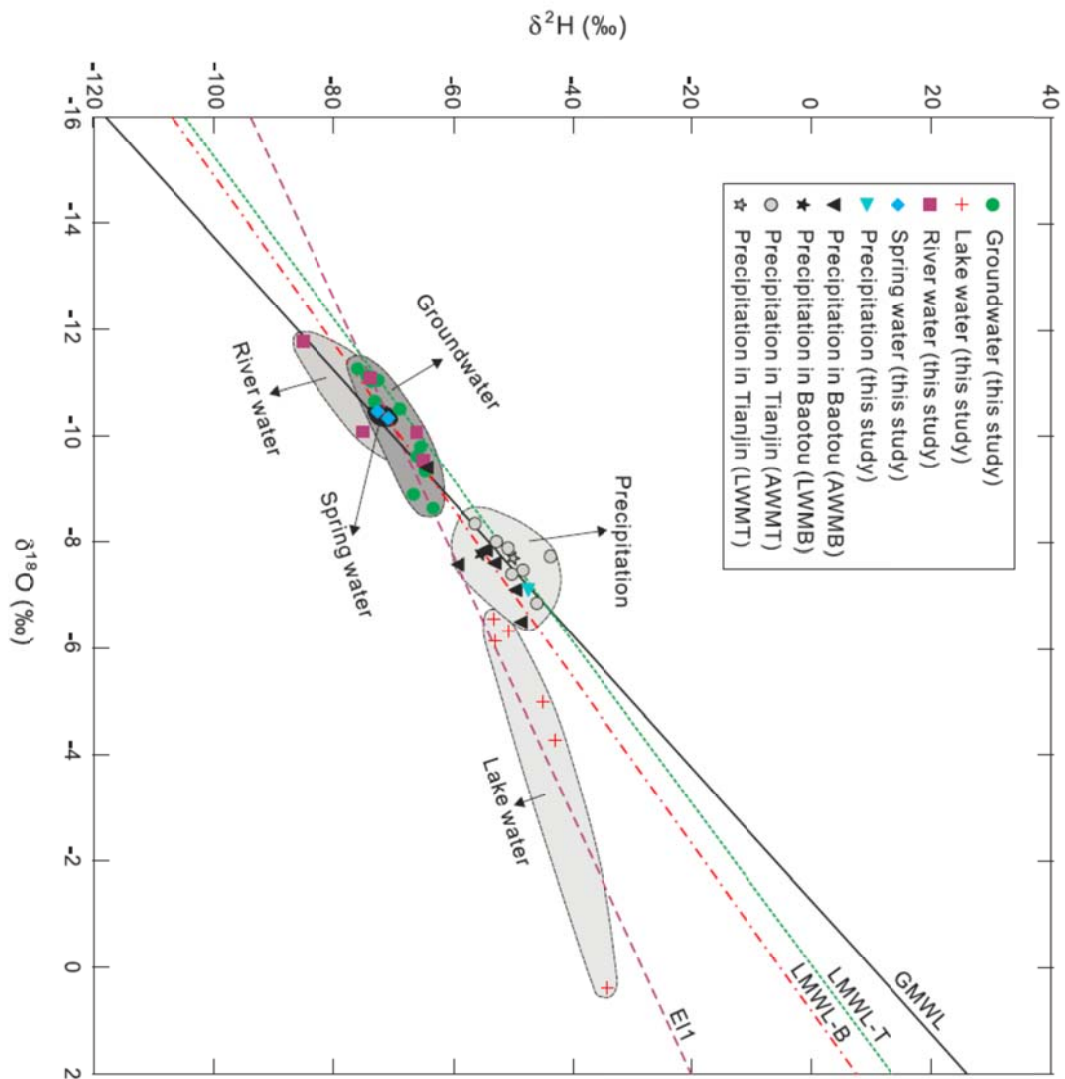
1054

1055

1056

1057

1067 **Fig. 7.** The bivariate diagram of  $\delta D$  and  $\delta^{18}O$ , i.e. the Craig diagram, for the natural  
1068 water samples in this study. Different relationships between the groundwaters, lake  
1069 waters, river waters, spring waters and the precipitation waters are illustrated.  
1070 AWMB, the annual weighted mean value at the Baotou station; AWMT, the annual  
1071 weighted mean value at the Tianjin station; LWMB, the long-term weighted means at  
1072 the Baotou station; LWMT, the long-term weighted means at the Tianjin station;  
1073 GMWL, the Global Meteoric Water Line; LMWL-B, the local meteoric water line  
1074 calculated based on the data from the Baotou station; LWML-T, the local meteoric  
1075 water line calculated based on the data from the Tianjin station; EL1, the evaporation  
1076 line calculated based on the data of water samples collected in this study.



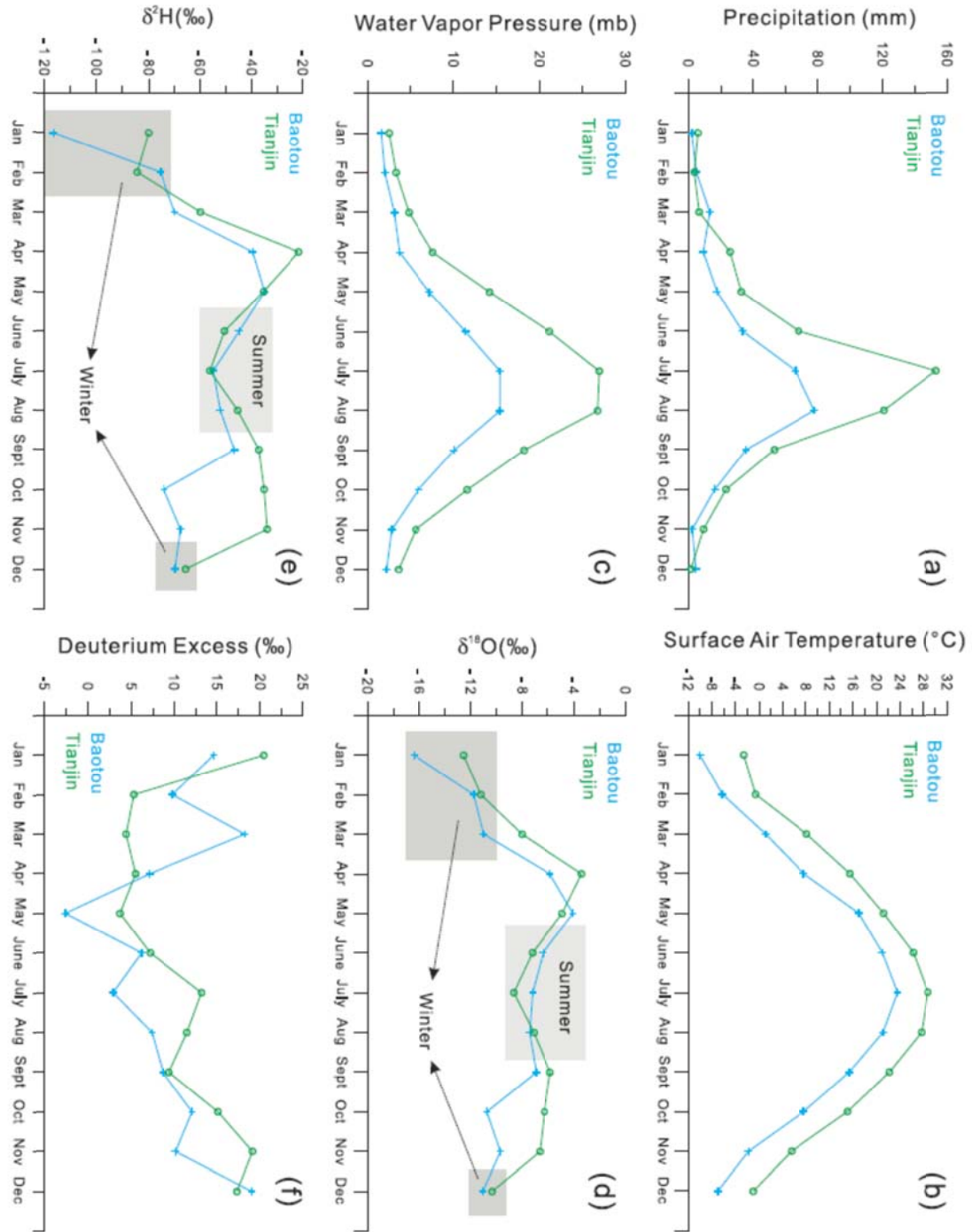
1068

1069

1070

1070  
1071  
1072  
1073  
1074  
1075  
1076  
1077  
1078  
1079  
1080  
1081

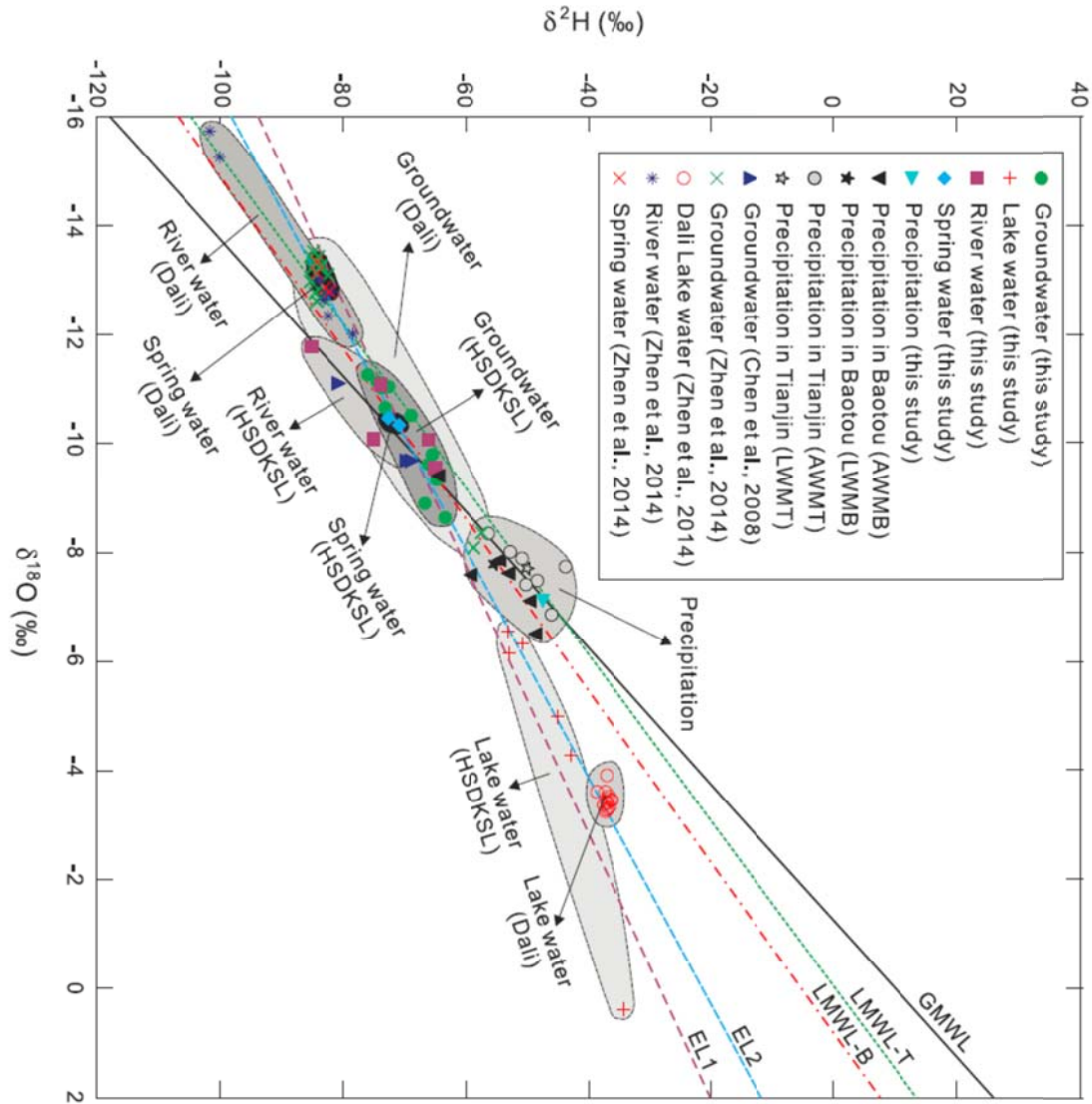
1082 **Fig. 8.** The seasonal mean distributions of (a) precipitation, (b) surface air  
1083 temperature and (c) water vapor pressure from the Baotou and Tianjin weather  
1084 stations (station sites seen in **Fig. 1a**) in the surrounding areas of the Otindag for the  
1085 period 1981-2010. The seasonal mean distributions of (d)  $\delta^{18}\text{O}$  and (e)  $\delta\text{D}$  values in  
1086 precipitation from the Baotou and Tianjin weather stations in the surrounding areas  
1087 of the Otindag for the period 1986-2001.



1089  
 1090  
 1091  
 1092  
 1093  
 1094  
 1095  
 1096  
 1097  
 1098  
 1100  
 1101

**Fig. 9.** The bivariate diagram of  $\delta\text{D}$  and  $\delta^{18}\text{O}$ , i.e. the Craig diagram, for the natural water samples collected in the Otindag (this study) and the Dali Basin. Different

1106 relationships between the groundwaters, lake waters, river waters, spring waters and  
 1107 the precipitation waters are clearly illustrated. AWMB, AWMT, LWMB, LWMT, GMWL,  
 1108 LMWL-B, LWML-T, and EL1 are the same as in Fig. 7. EL2, the evaporation line  
 1109 calculated based on the data from the groundwater, lake water, river water and  
 1110 spring water samples collected from the Otindag and Dali Basin. The data for the Dali  
 1111 were taken from Chen et al. (2008) and Zhen et al. (2014).



1107  
 1108  
 1109  
 1110  
 1111  
 1112  
 1113  
 1114  
 1115  
 1116  
 1117  
 1118  
 1119

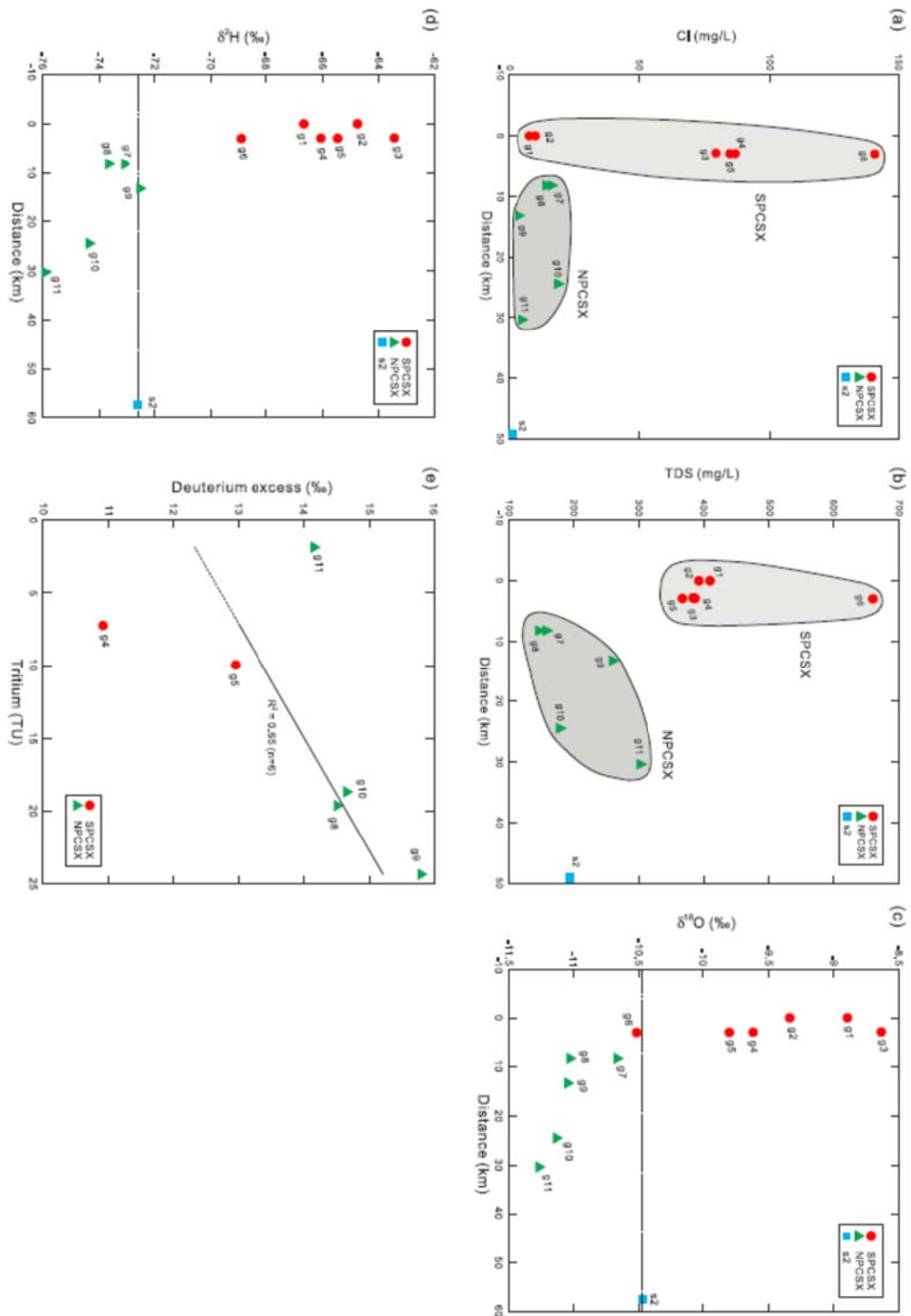
1119

1120

1121

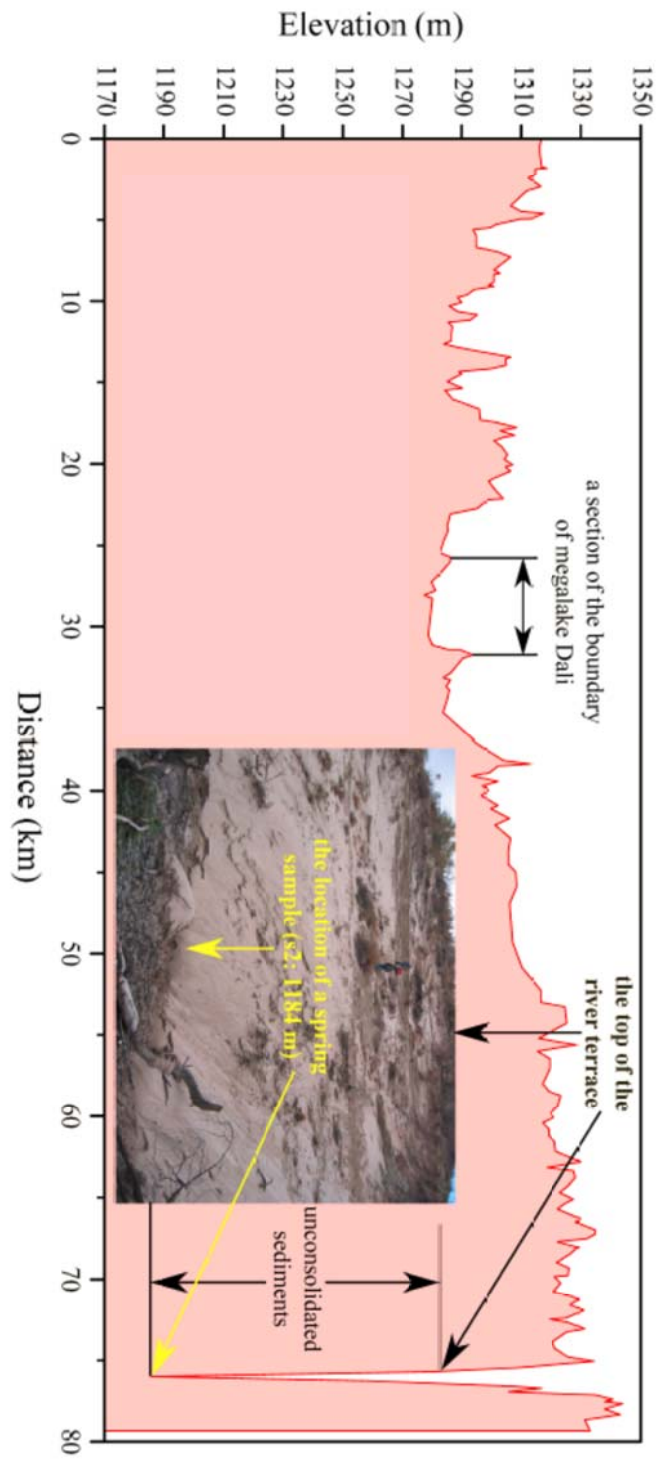
1122

1123 **Fig. 10.** (a) Sketch map showing the relationship between the groundwaters in the  
1124 NPCSX and SPCSX areas, based on variations of (a) the chloride concentrations, (b)  
1125 the TDS concentrations, (c) the  $\delta^{18}\text{O}$  values and (d) the  $\delta\text{D}$  values of these water  
1126 samples versus their distances away from the water sample g1 along the palaeo river  
1127 channel (PCSX) from south to north. The dashed line in (c) and (d) represents the  
1128 corresponding values of the spring water sample s2, and divides samples into the  
1129 NPCSX and SPCSX parts. (e) Variations of tritium contents vs. deuterium excess for  
1130 the groundwater samples in the study area. The sample g6 was omitted due to its  
1131 potential contamination.



1133  
 1134  
 1135  
 1136  
 1137  
 1138  
 1142  
 1143  
 1144  
 1145

**Fig. 11.** Variation of the topographical elevation along the section S1 (see Fig. 1b) from the upstream of the Dali Lake to the location site of the spring water sample (s2) in the riverhead of the Xilamulun River. Note that no river water samples are shown in this figure.



1143  
1144

1144

**Table Captions:**

1145

**Table 1.** The physical parameters measured for the natural water samples in the study area.

Sample ID	Water type	Latitude (N, degree)	Longitude (E, degree)	Elevation (m a.s.l)	Depth (m)	Temperature (°C)	pH	Eh (mV)	EC (µS/cm)	TDS (mg/L)	Salinity (%)	Alkalinity (meq/L)	Hardness (°dH)
g1	Groundwater	42.736306	116.747333	1396	12	5.8	6.72	3	769	410	0.6	5.47	9.42
g2	Groundwater	42.736306	116.747333	1396	26	6.0	6.91	-10	736	393	0.5	4.07	12.0
g3	Groundwater	42.760194	116.760139	1355	32	7.7	6.88	-6	725	384	0.5	2.39	11.9
g4	Groundwater	42.759694	116.760417	1360	7	10.0	6.74	1	725	387	0.5	2.20	12.3
g5	Groundwater	42.759556	116.760556	1362	27	7.6	6.46	16	691	368	0.5	2.23	15.6
g6	Groundwater	42.760111	116.760250	1365	7	10.3	6.26	22	1240	660	0.8	3.25	24.5
g7	Groundwater	42.806361	116.747806	1352	20	6.8	6.71	2	297	158	0.2	0.63	4.70
g8	Groundwater	42.806361	116.747806	1352	16	6.5	6.92	-8	276	147	0.2	0.58	5.00
g9	Groundwater	42.850333	116.735722	1347	30	7.2	6.74	-1	487	260	0.4	3.73	12.7
g10	Groundwater	42.949861	116.759194	1321	37	9.9	6.75	-2	337	179	0.2	1.66	7.23
g11	Groundwater	42.967111	116.827528	1317	60	8.6	6.99	-14	571	302	0.4	2.40	12.9
l1	Lake water	42.424611	116.769194	1368	/	16.9	9.44	-151	126	67	0.1	0.95	1.79
l2	Lake water	42.424611	116.769194	1368	/	19.6	9.18	-137	132	70	0.1	0.92	1.82
l3	Lake water	42.424611	116.757806	1365	/	20.2	7.38	-36	196	105	0.1	1.53	3.36
l4	Lake water	42.427083	116.757639	1366	/	20.5	7.87	-64	448	238	0.2	3.42	6.61
l5	Lake water	42.421806	116.756917	1360	/	20.1	8.23	-83	173	92	0.1	1.43	2.73
l6	Lake water	42.736389	116.747222	1374	/	10.7	8.35	-89	194	103	0.1	1.53	3.30
r1	River water	42.530917	116.641250	1355	/	20.6	7.31	-33	180	96	0.1	0.88	2.23
r2	River water	42.310883	116.494817	1231	/	14.9	7.67	-52	178	95	0.1	1.21	2.50
r3	River water	42.385778	116.886194	1362	/	9.5	7.62	-48	177	94	0.1	1.45	2.62
r4	River water	42.931417	117.585306	1217	/	10.5	7.97	-69	474	252	0.3	3.22	8.73
r5	River water	43.079083	117.457389	1006	/	12.9	7.87	-62	191	101	0.1	1.37	2.88
s1	Spring water	42.530917	116.641250	1359	/	20.9	6.63	5	165	88	0.1	0.40	1.81
s2	Spring water	42.965417	116.975361	1184	/	19.0	7.47	-46	371	195	0.2	1.07	6.40
p1	Precipitation	42.330750	116.551694	1260	/	20.2	4.61	109	78	42	0.0	/	0.61

1146

1147

**Table 2.** The concentrations of major cations and anions measured for the water samples in the study area.

Sample	F <sup>-</sup> (mg/L)	Cl <sup>-</sup> (mg/L)	NO <sub>2</sub> <sup>-</sup> (mg/L)	NO <sub>3</sub> <sup>-</sup> (mg/L)	SO <sub>4</sub> <sup>2-</sup> (mg/L)	CO <sub>3</sub> <sup>2-</sup> (mg/L)	HCO <sub>3</sub> <sup>-</sup> (mg/L)	Li <sup>+</sup> (mg/L)	Na <sup>+</sup> (mg/L)	NH <sub>4</sub> <sup>+</sup> (mg/L)	K <sup>+</sup> (mg/L)	Mg <sup>2+</sup> (mg/L)	Ca <sup>2+</sup> (mg/L)
g1	0.13	7.90	2.32	0.48	16.1	0.00	335	0.02	13.8	10.5	4.59	15.5	41.8
g2	0.21	10.2	0.00	6.15	70.6	0.10	248	0.02	13.4	6.56	3.45	17.9	56.0
g3	0.11	79.6	0.00	0.00	141	0.00	145	0.01	17.9	2.28	1.76	17.1	57.3
g4	0.10	86.9	0.00	5.73	165	0.00	134	0.02	18.0	0.00	2.02	18.5	57.3
g5	0.07	84.8	0.00	0.76	169	0.00	136	0.00	39.7	1.02	2.72	20.9	76.9
g6	0.07	141	0.00	111	229	0.00	198	0.00	79.8	0.00	29.47	29.3	126.7
g7	0.37	16.3	0.00	306	32.0	0.00	38.7	0.06	7.83	0.00	3.09	6.21	23.4
g8	0.29	14.3	0.00	35.5	29.9	0.00	35.5	0.02	16.2	0.11	3.38	6.44	25.1
g9	0.10	3.66	0.15	1.19	71.6	0.00	227	0.06	12.9	0.55	4.50	14.1	67.5
g10	0.24	18.8	0.00	49.5	9.97	0.00	101	0.00	18.5	0.00	2.09	7.92	38.7
g11	0.28	4.94	0.00	0.00	182	0.00	146	0.05	20.4	2.59	2.06	13.3	70.6
l1	0.16	3.15	0.00	0.07	4.32	0.00	57.9	0.01	5.42	0.00	0.86	3.24	7.49
l2	0.16	3.30	0.00	1.66	4.57	0.00	55.8	0.00	5.33	0.00	0.84	3.29	7.61
l3	0.11	3.27	0.00	0.61	2.33	0.00	93.3	0.01	5.88	0.00	1.19	5.68	14.7
l4	0.17	22.1	0.00	0.39	3.04	0.10	208	0.00	9.21	0.70	24.2	14.1	24.2
l5	0.09	6.24	0.00	0.65	2.97	0.10	86.8	0.01	6.72	0.00	1.16	4.91	11.4
l6	0.18	4.29	0.00	0.80	9.34	0.10	93.0	0.01	8.41	0.00	1.36	6.47	13.0
r1	0.30	5.76	0.00	2.38	26.7	0.30	52.4	0.01	7.15	0.00	2.99	3.41	10.3
r2	0.19	4.82	0.00	0.65	16.4	0.10	73.1	0.01	6.82	0.00	1.92	3.96	11.4
r3	0.64	5.46	0.00	0.43	5.57	0.00	88.1	0.01	7.11	0.00	1.13	4.04	12.1
r4	1.08	20.4	0.00	19.3	37.3	0.50	195	0.01	13.0	0.00	1.96	11.9	42.8
r5	0.19	4.10	0.00	1.08	15.6	0.00	82.6	0.01	6.71	0.00	2.08	4.38	13.4
s1	0.16	6.44	0.00	1.95	34.3	0.00	24.3	0.02	6.56	0.00	1.62	2.92	8.10
s2	0.05	0.98	0.00	0.45	17.2	0.00	64.9	0.02	9.87	0.00	3.32	9.10	30.8
p1	0.61	2.90	0.00	9.46	12.7	0.00	0.00	0.00	2.09	2.07	1.64	0.88	2.95

1148

1149

1150

1151

**Table 3.** The analytical data of stable and radioactive isotopes measured for the water samples in this study.

Sample ID	$\delta D$ (‰)	$\sigma_{\text{‰}}$	$\delta^{18}O$ (‰)	$\sigma_{\text{‰}}$	deuterium excess (d)	Tritium ( $^3H$ ) (TU)
g1	-66.7	0.199	-8.90	0.026	4.50	/
g2	-64.8	0.291	-9.34	0.039	9.93	/
g3	-63.4	0.269	-8.64	0.008	5.66	/
g4	-66.1	0.149	-9.62	0.062	10.9	7.25
g5	-65.5	0.111	-9.80	0.027	13.0	9.98
g6	-68.9	0.287	-10.5	0.039	15.2	22.9
g7	-73.1	0.298	-10.7	0.041	12.2	/
g8	-73.7	0.220	-11.0	0.037	14.5	19.6
g9	-72.5	0.181	-11.0	0.015	15.8	24.3
g10	-74.4	0.201	-11.1	0.026	14.7	18.7
g11	-75.9	0.340	-11.3	0.015	14.2	1.86
l1	-53.1	0.229	-6.55	0.002	-0.704	/
l2	-50.7	0.304	-6.32	0.026	-0.161	/
l3	-42.9	0.239	-4.29	0.034	-8.55	/
l4	-34.2	0.243	0.381	0.040	-37.2	/
l5	-45.1	0.206	-4.99	0.009	-5.16	/
l6	-52.9	0.187	-6.15	0.049	-3.67	/
r1	-66.2	0.118	-10.1	0.015	14.4	/
r2	-65.0	0.148	-9.55	0.012	11.4	/
r3	-73.8	0.315	-11.1	0.021	14.9	/
r4	-85.2	0.244	-11.8	0.005	9.09	/
r5	-75.0	0.195	-10.1	0.003	5.69	/
s1	-70.8	0.074	-10.3	0.007	11.9	/
s2	-72.6	0.281	-10.5	0.046	11.1	/
p1	-47.4	0.374	-7.14	0.017	9.69	/

1152  
1153  
1154  
1155

**Table 4.** The statistical frequency of rainfall events being >20 mm per year during the recent 30 years from 1985 to 2014. The data come from the China Meteorological Data

1156 Sharing Service System.

Station	One time/year	Two times/year	Three times/year	Four times/year	Five times/year	Six times/year	Seven times/year	Mean times/year
Duolun	2	8	8	4	4	3	1	3.4
Xilinhaote	8	5	2	6	3	2	0	2.5

1157  
1158 **Table 5.** The measured contents of tritium in the groundwater samples studied and the calculated ages of these samples.

Sample-ID	Tritium content (T.U.)	Possible ages (years)
g1	not measured	not clear
g2	not measured	not clear
g3	not measured	not clear
g4	7.25	20-40
g5	9.97	13-33
g6	22.9	0-20
g7	not measured	not clear
g8	19.6	0-20
g9	24.3	0-17
g10	18.7	0-22
g11	1.86	40-65

1159  
1160 **Table 6.** Mineral saturation Index (MSI) of the water samples studied.

Sample-ID	Mineral (Formula)	Anhydrite (CaSO <sub>4</sub> )	Aragonite (CaCO <sub>3</sub> )	Calcite (CaCO <sub>3</sub> )	Dolomite (CaMg(CO <sub>3</sub> ) <sub>2</sub> )	Fluorite (CaF <sub>2</sub> )	Gypsum (CaSO <sub>4</sub> :2H <sub>2</sub> O)	Halite (NaCl)	CH <sub>4</sub> (g) (CH <sub>4</sub> )	CO <sub>2</sub> (g) (CO <sub>2</sub> )	H <sub>2</sub> (g) (H <sub>2</sub> )	H <sub>2</sub> O(g) (H <sub>2</sub> O)	NH <sub>3</sub> (g) (NH <sub>3</sub> )	O <sub>2</sub> (g) (O <sub>2</sub> )
g1	SI	-2.76	-1.21	-1.05	-2.5	-2.69	-2.5	-8.48	-58.68	-1.5	-21.44	-2.04	-8.5	-47.28
	Log IAP	-7.1	-9.45	-9.45	-19.11	-13.56	-7.1	-6.95	-61.37	-2.71	-24.5	0	-6.32	-50
	Log KT	-4.34	-8.24	-8.4	-16.61	-10.86	-4.6	1.54	-2.69	-1.2	-3.06	2.04	2.18	-2.72

g2	SI	-2.04	-0.99	-0.83	-2.12	-2.19	-1.79	-8.39	-60.49	-1.76	-21.82	-2.04	-8.51	-46.44
	Log IAP	-6.39	-9.23	-9.23	-18.74	-13.05	-6.39	-6.86	-63.18	-2.97	-24.88	0	-6.33	-49.16
	Log KT	-4.34	-8.24	-8.4	-16.62	-10.86	-4.6	1.54	-2.69	-1.21	-3.06	2.04	2.18	-2.73
g3	SI	-1.77	-1.25	-1.09	-2.62	-2.8	-1.51	-7.38	-60.71	-1.96	-21.76	-1.99	-8.9	-45.9
	Log IAP	-6.11	-9.49	-9.49	-19.29	-13.63	-6.11	-5.84	-63.41	-3.2	-24.83	0	-6.77	-48.65
	Log KT	-4.34	-8.25	-8.4	-16.66	-10.83	-4.6	1.54	-2.71	-1.23	-3.07	1.99	2.14	-2.74
g4	SI	-1.72	-1.43	-1.27	-2.92	-2.94	-1.47	-7.35	-59.85	-1.88	-21.48	-1.92		-45.59
	Log IAP	-6.06	-9.69	-9.69	-19.64	-13.73	-6.06	-5.8	-62.58	-3.15	-24.56	0		-48.35
	Log KT	-4.34	-8.26	-8.41	-16.72	-10.8	-4.59	1.55	-2.73	-1.27	-3.08	1.92		-2.77
g5	SI	-1.6	-1.74	-1.59	-3.66	-3.09	-1.35	-7.02	-57.1	-1.73	-20.92	-1.99	-9.68	-47.62
	Log IAP	-5.94	-9.99	-9.99	-20.32	-13.93	-5.94	-5.48	-59.81	-2.96	-23.99	0	-7.54	-50.36
	Log KT	-4.34	-8.25	-8.4	-16.66	-10.83	-4.6	1.54	-2.71	-1.23	-3.07	1.99	2.14	-2.74
g6	SI	-1.39	-1.67	-1.52	-3.54	-3.01	-1.13	-6.53	-55.63	-1.45	-20.52	-1.91		-47.4
	Log IAP	-5.73	-9.93	-9.93	-20.27	-13.8	-5.73	-4.98	-58.36	-2.73	-23.6	0		-50.16
	Log KT	-4.34	-8.26	-8.41	-16.73	-10.79	-4.59	1.55	-2.73	-1.27	-3.08	1.91		-2.77
g7	SI	-2.79	-2.45	-2.29	-5.1	-2.12	-2.54	-8.44	-59.68	-2.43	-21.42	-2.01		-46.93
	Log IAP	-7.13	-10.69	-10.69	-21.74	-12.97	-7.13	-6.91	-62.38	-3.65	-24.49	0		-49.66
	Log KT	-4.34	-8.24	-8.4	-16.64	-10.85	-4.6	1.54	-2.7	-1.22	-3.07	2.01		-2.73
g8	SI	-2.65	-2.11	-1.95	-4.43	-2.19	-2.4	-8.15	-61.48	-2.6	-21.84	-2.02	-10.23	-46.21
	Log IAP	-6.99	-10.35	-10.35	-21.06	-13.04	-6.99	-6.61	-64.18	-3.82	-24.9	0	-8.07	-48.94
	Log KT	-4.34	-8.24	-8.4	-16.63	-10.85	-4.6	1.54	-2.7	-1.22	-3.06	2.02	2.17	-2.73
g9	SI	-1.96	-1.14	-0.98	-2.58	-2.77	-1.7	-8.85	-59.22	-1.67	-21.48	-2	-9.68	-46.66
	Log IAP	-6.3	-9.38	-9.38	-19.23	-13.6	-6.3	-7.31	-61.92	-2.9	-24.55	0	-7.53	-49.39
	Log KT	-4.34	-8.24	-8.4	-16.65	-10.84	-4.6	1.54	-2.7	-1.23	-3.07	2	2.15	-2.74
g10	SI	-2.99	-1.63	-1.47	-3.51	-2.24	-2.73	-7.98	-60.04	-2	-21.5	-1.92		-45.59
	Log IAP	-7.32	-9.88	-9.88	-20.23	-13.04	-7.32	-6.44	-62.77	-3.27	-24.58	0		-48.35
	Log KT	-4.34	-8.25	-8.41	-16.72	-10.8	-4.59	1.55	-2.73	-1.27	-3.08	1.92		-2.76
g11	SI	-1.59	-1.01	-0.86	-2.34	-1.92	-1.33	-8.54	-61.8	-2.04	-21.98	-1.96	-8.69	-45.12
	Log IAP	-5.92	-9.26	-9.26	-19.02	-12.74	-5.92	-6.99	-64.51	-3.29	-25.05	0	-6.57	-47.87
	Log KT	-4.34	-8.25	-8.41	-16.69	-10.82	-4.59	1.54	-2.72	-1.25	-3.07	1.96	2.12	-2.75
l1	SI	-3.95	0.37	0.52	0.92	-5.34	-3.7	-9.28	-85.36	-4.77	-26.88	-1.73		-32.25
	Log IAP	-8.29	-7.92	-7.92	-15.97	-16.04	-8.29	-7.72	-88.15	-6.14	-29.99	0		-35.08

	Log KT	-4.34	-8.29	-8.44	-16.9	-10.7	-4.58	1.56	-2.79	-1.37	-3.11	1.73	-2.83	
l2	SI	-3.9	0.18	0.33	0.58	-3.36	-3.66	-9.27	-83.39	-4.49	-26.36	-1.65	-32.33	
	Log IAP	-8.24	-8.12	-8.12	-16.38	-14.02	-8.24	-7.7	-86.2	-5.89	-29.49	0	-35.18	
	Log KT	-4.34	-8.3	-8.45	-16.96	-10.66	-4.58	1.57	-2.81	-1.4	-3.13	1.65	-2.85	
l3	SI	-3.92	-1.1	-0.95	-2.03	-3.4	-3.69	-9.24	-67.05	-2.47	-22.76	-1.64	-39.32	
	Log IAP	-8.27	-9.4	-9.4	-19	-14.06	-8.27	-7.67	-69.87	-3.88	-25.89	0	-42.18	
	Log KT	-4.34	-8.31	-8.45	-16.98	-10.66	-4.58	1.57	-2.82	-1.41	-3.13	1.64	-2.86	
l4	SI	-3.7	-0.07	0.07	0.2	-2.9	-3.46	-8.24	-71.14	-2.6	-23.74	-1.63	-7.72	-37.26
	Log IAP	-8.04	-8.38	-8.38	-16.78	-13.55	-8.04	-6.67	-73.96	-4.01	-26.87	0	-5.86	-40.11
	Log KT	-4.35	-8.31	-8.46	-16.98	-10.65	-4.58	1.57	-2.82	-1.41	-3.13	1.63	1.86	-2.86
l5	SI	-3.92	-0.36	-0.21	-0.51	-3.69	-3.68	-8.9	-74.69	-3.32	-24.46	-1.64	-35.96	
	Log IAP	-8.26	-8.67	-8.67	-17.48	-14.34	-8.26	-7.33	-77.51	-4.73	-27.59	0	-38.81	
	Log KT	-4.34	-8.31	-8.45	-16.97	-10.66	-4.58	1.57	-2.82	-1.41	-3.13	1.64	-2.86	
l6	SI	-3.39	-0.32	-0.16	-0.49	-2.91	-3.13	-8.95	-74.42	-3.47	-24.7	-1.9	-38.88	
	Log IAP	-7.72	-8.58	-8.58	-17.23	-13.7	-7.72	-7.4	-77.16	-4.74	-27.79	0	-41.66	
	Log KT	-4.34	-8.26	-8.41	-16.74	-10.79	-4.59	1.55	-2.74	-1.28	-3.09	1.9	-2.77	
r1	SI	-3.01	-1.57	-1.43	-3.05	-2.69	-2.77	-8.91	-66.73	-2.65	-22.62	-1.63	-39.46	
	Log IAP	-7.36	-9.88	-9.88	-20.03	-13.35	-7.36	-7.34	-69.55	-4.06	-25.75	0	-42.32	
	Log KT	-4.35	-8.31	-8.46	-16.99	-10.65	-4.58	1.57	-2.82	-1.41	-3.13	1.63	-2.86	
r2	SI	-3.18	-1.09	-0.94	-2.14	-2.97	-2.94	-9	-69.01	-2.88	-23.34	-1.78	-40.05	
	Log IAP	-7.52	-9.37	-9.37	-18.98	-13.7	-7.52	-7.44	-71.79	-4.22	-26.44	0	-42.86	
	Log KT	-4.34	-8.28	-8.43	-16.85	-10.73	-4.58	1.56	-2.77	-1.34	-3.1	1.78	-2.81	
r3	SI	-3.62	-1.12	-0.97	-2.3	-1.8	-3.36	-8.91	-67.72	-2.78	-23.24	-1.93	-42.26	
	Log IAP	-7.95	-9.38	-9.38	-19.01	-12.61	-7.95	-7.36	-70.44	-4.04	-26.32	0	-45.02	
	Log KT	-4.34	-8.25	-8.41	-16.71	-10.8	-4.59	1.55	-2.72	-1.26	-3.08	1.93	-2.76	
r4	SI	-2.41	0.06	0.21	0	-0.93	-2.15	-8.11	-70.67	-2.78	-23.94	-1.9	-40.48	
	Log IAP	-6.74	-8.2	-8.2	-16.73	-11.72	-6.75	-6.56	-73.4	-4.06	-27.02	0	-43.25	
	Log KT	-4.34	-8.26	-8.41	-16.74	-10.79	-4.59	1.55	-2.73	-1.28	-3.08	1.9	-2.77	
r5	SI	-3.15	-0.8	-0.65	-1.61	-2.88	-2.89	-9.07	-70.47	-3.03	-23.74	-1.84	-39.99	
	Log IAP	-7.48	-9.07	-9.07	-18.4	-13.63	-7.48	-7.52	-73.23	-4.34	-26.84	0	-42.78	
	Log KT	-4.33	-8.27	-8.42	-16.8	-10.75	-4.59	1.55	-2.76	-1.31	-3.1	1.84	-2.79	
s1	SI	-2.99	-2.83	-2.68	-5.51	-3.34	-2.76	-8.9	-61.12	-2.44	-21.26	-1.62	-42.08	

	Log IAP	-7.34	-11.14	-11.14	-22.5	-13.99	-7.34	-7.33	-63.95	-3.86	-24.39	0	-44.94	
	Log KT	-4.35	-8.31	-8.46	-16.99	-10.65	-4.58	1.57	-2.83	-1.42	-3.13	1.62	-2.86	
	SI	-2.8	-0.89	-0.74	-1.73	-3.79	-2.56	-9.55	-67.85	-2.72	-22.94	-1.67	-39.38	
s2	Log IAP	-7.14	-9.19	-9.19	-18.68	-14.46	-7.14	-7.98	-70.66	-4.12	-26.06	0	-42.23	
	Log KT	-4.34	-8.3	-8.45	-16.95	-10.67	-4.58	1.57	-2.81	-1.39	-3.12	1.67	-2.85	
	SI	-3.81				-2.59	-3.57	-9.73			-17.22	-1.64	-10.5	-50.4
p1	Log IAP	-8.15				-13.25	-8.15	-8.16			-20.35	0	-8.63	-53.26
	Log KT	-4.34				-10.66	-4.58	1.57			-3.13	1.64	1.87	-2.86

1161  
1162